

algebra is the unique determination of the mixing angle  $\theta$  and the equality of the  $\rho$  and  $\omega$  masses. We are able to get a fit to experiment with only two independent parameters, which may be taken as  $m_\rho$  and  $m_{K^*}$ . The good agreement with experiment strongly indicates that the schemes are basically correct. Further refinement is possible by adding terms that break  $U(3)$  into  $SU(3) \otimes U(1)$ . For example, such a model is considered by Brown, Munczek, and Singer.<sup>14</sup> Our analysis shows that

<sup>14</sup>L. M. Brown, H. Munczek, and P. Singer, Phys. Rev. Letters **21**, 707 (1968).

such a term is of lower order in symmetry breaking than in  $SU(3)$  breaking.

### ACKNOWLEDGMENTS

The authors have benefited from discussions with Professor Sakurai, who drew attention to Kimel's work, and with Professor Brown and Professor Munczek. One of the authors (N.G.D.) is indebted to the Aspen Center for Physics for hospitality during the stay when this work was completed.

## Pion-Nucleon and Kaon-Nucleon Scattering in the Veneziano Model\*

EDMOND L. BERGER† AND GEOFFREY C. FOX

*Lawrence Radiation Laboratory, University of California, Berkeley, California 94720*

(Received 14 July 1969)

We present a comprehensive phenomenological examination of the Veneziano ansatz for pion-nucleon and kaon-nucleon processes. Using invariant amplitudes constructed as sums of beta-function terms, we attempt to fit simultaneously all the relevant high- and low-energy scattering data as well as the elastic widths of baryon resonances. We discuss a useful technique for ensuring that the theoretical amplitudes will possess the observed spin-parity structure of the physical spectrum of baryon states. Our main conclusions are the following: (a) Sizable subsidiary terms are required. (b) The predicted duality relation between the  $s$ -channel (baryon) and the  $t$ -channel (meson) Regge poles is not supported quantitatively. (c) Using the polynomial form for residue functions suggested by the model, we have performed detailed fits to all  $\pi N$  backward data and elastic widths. The model fails to provide an adequate extrapolation from the scattering data to the widths of the  $\Delta_\delta(1238)$  and its recurrences; acceptable agreement is found for the other trajectories. Moreover, the residues of the  $\pi N$  trajectories are in marked disagreement with exchange degeneracy. (d) Within a factor of 2 in amplitude, the model reproduces available  $KN$  charge-exchange data from threshold to the highest energy. (e) A Pomeranchuk trajectory with normal slope ( $\alpha_{P'} \approx 1 \text{ GeV}^{-2}$ ) is consistent with both the Veneziano model and all data. (f) The model does not provide any natural resolution of the difficulties inherent in classical Regge-pole model fits, and thus supports the view that Regge cuts are important.

### INTRODUCTION

THE proposal by Veneziano<sup>1</sup> of an elegant beta-function representation for the hadronic scattering amplitude has opened a new chapter in theoretical investigations of strong-interaction phenomena.<sup>2</sup> In a simple closed form, the amplitude is analytic, crossing-symmetric, and has Regge behavior at high energies. Moreover, in a straightforward fashion, it can be expanded as a sum of zero-total-width resonance-pole terms, thus exhibiting a form of duality<sup>3</sup> by quantitatively associating asymptotic behavior to low-energy

resonance structure in one simple function. In addition, research has revealed an interesting relationship of the representation to partially conserved axial-vector current (PCAC) requirements for processes involving pions.<sup>4,5</sup>

From the phenomenological point of view, the Veneziano representation provides several attractive possibilities. It relates the parametrization of the residue structure of a Regge pole to the trajectory itself, removing the erstwhile freedom of an arbitrary multiplicative form factor in the momentum transfer  $t$ . Also, assuming that a given physical process can be represented by the sum of a small number of beta-function terms, the representation provides a strong quantitative connection between forward ( $t \cong 0$ ) and backward ( $u \cong 0$ ) scattering at high energy—features of the data which, dominated by distinct Regge-pole

\* Work supported in part by the U. S. Atomic Energy Commission.

† Faculty Fellow, on leave from Dartmouth College, Hanover, N. H. 03755.

<sup>1</sup>G. Veneziano, Nuovo Cimento **57A**, 190 (1968).

<sup>2</sup>See, e.g., J. A. Shapiro, Phys. Rev. **179**, 1345 (1969), and, for further references, G. Veneziano, in Proceedings of The Coral Gables Conference, 1969 (unpublished); S. Fubini, Comments Nucl. Particle Phys. **3**, 22 (1969); S. Weinberg, *ibid.* **3**, 28 (1969).

<sup>3</sup>R. Dolen, D. Horn, and C. Schmid, Phys. Rev. **166**, 1768 (1968); C. Schmid, Phys. Rev. Letters **20**, 689 (1968).

<sup>4</sup>C. Lovelace, Phys. Letters **28B**, 264 (1968).

<sup>5</sup>M. Ademollo, G. Veneziano, and S. Weinberg, Phys. Rev. Letters **22**, 83 (1969).

exchanges, have until now seemed uncorrelated. Furthermore, the extension of the beta-function representation from the quasi-two-body scattering domain<sup>1,2,4,5</sup> to multiparticle processes promises, among other things, an understanding of interference effects at the locus of intersecting resonance bands in Dalitz plots.<sup>4</sup> This last feature requires for its implementation, of course, some procedure for overcoming the unitarity-violating zero-width aspect of the model. These phenomenological consequences of the model are largely untested as yet.

In this paper we present a critical discussion of meson-baryon scattering within the framework of the Veneziano model.<sup>6</sup> Because pion-nucleon and kaon-nucleon scattering are perhaps the best studied hadronic processes, both theoretically and phenomenologically, it should be instructive to examine in detail the extent to which the model increases our understanding of these processes. Our aim is to indicate in a comprehensive fashion both the strong points and the limitations of the Veneziano beta-function parametrization for these processes.

Very recently, enthusiasm has been generated for the point of view which holds that the Veneziano form is to be regarded as a Born approximation.<sup>7</sup> Presumably this means that "higher-order" terms would be important in achieving agreement with nature; for example, a "unitarized" version is suggested by Mandelstam to eliminate the parity doubling which occurs in his quark-substrate model even for meson trajectories. The methods for obtaining the higher-order terms and/or unitarity corrections are as yet ill defined and are likely to be involved. In our investigation, we sought to represent meson-baryon scattering simply as a sum of beta functions, and our conclusions are limited to that viewpoint.<sup>8</sup>

Whereas there are certain general aspects of the Veneziano-type model which are helpful in gaining a unified qualitative picture of strong-interaction phenomena, our conclusions on the quantitative side are somewhat pessimistic. Detailed empirical knowledge of meson-baryon scattering is far more sophisticated than the capabilities of the model. To be sure, it is very possibly true that a finite set of resonance widths and a finite number of differential cross-section points can be fitted using a similarly finite number of beta-function

terms. However, the more terms one is forced to employ, the smaller is the predictive—or even the unifying—content of the model. In particular, many features of the data enable one to demonstrate the existence of sizable subsidiary<sup>9</sup> terms in the Veneziano expansion. Moreover, we find it impossible to achieve a compelling representation which properly relates even the magnitudes of the leading-trajectory baryon-resonance widths with the sizes of the forward and backward differential cross sections.

Outside the realm of precise fits to data, however, some useful features emerge. First, there is the relation between the asymptotic  $t$ -channel Regge-pole parameters and the qualitative behavior of the  $s$ -channel resonances of the intermediate-energy range. We have in mind, for example, the crossover effect; this is discussed in Secs. II A and III. Second, the Veneziano representation yields a new method for quantitatively estimating the nonasymptotic corrections to the Regge formalism. This could be useful for determining how good a fit one should demand from a high-energy approximation. Finally, as has been pointed out by Virasoro and Amann,<sup>6</sup> it suggests a possibly useful parametrization of the variation of baryon widths as a function of their mass.

In Sec. I, after establishing notation, we focus upon those technical features of the Veneziano formula that are relevant to a reasonable description of meson-baryon scattering. These include signature, parity doubling, PCAC, positivity, and the absence of ghosts. After these theoretical points, we review in Sec. II the experimental picture of meson-baryon scattering which the Veneziano expansion should reproduce. We examine several aspects of Regge-pole-theory fits to forward elastic scattering data, including exchange degeneracy and the crossover effects, and also study the nature of the Pomeranchuk trajectory. For pion-nucleon forward elastic data, we present a good fit to existing data using  $P'$ ,  $\rho$ , and Pomeranchuk pole trajectories, all with normal slope [i.e., near  $1.0 (\text{GeV}/c)^{-2}$ ]. The value for the scale constant  $s_0 \simeq 1/\alpha' \simeq 1$  suggested by the Veneziano formula is consistent with the forward data.

Apart from this treatment of the high-energy forward elastic data, in Sec. II we also discuss the zeros in the scattering amplitude at specific values of  $t$  and  $u$  required in order to obtain the correct spin-parity structure of the baryon resonance spectrum. From the Veneziano expansion we subsequently extract a parametrization for the residue functions of the various baryon trajectories. In general, the model suggests that

<sup>6</sup> Previous studies of meson-baryon scattering include the papers on pion-nucleon scattering by M. Virasoro, Phys. Rev. **184**, 1621 (1969); K. Igi, Phys. Letters **28B**, 330 (1968); Y. Hara, Phys. Rev. **182**, 1906 (1969); R. Amann, Nuovo Cimento Letters **2**, 87 (1969); University of Chicago Report No. EFI 69-27 (unpublished); and those on kaon-nucleon scattering by K. Igi and J. Storrow, Nuovo Cimento **62A**, 972 (1969); T. Inami, *ibid.* **63A**, 987 (1969); K. Pretzl and K. Igi, *ibid.* **63A**, 609 (1969); O. Miyamura considered  $\pi N \rightarrow \eta N$  in Tohoku Report No. Tu/69/41 (unpublished).

<sup>7</sup> S. Mandelstam, Phys. Rev. **184**, 1625 (1969); K. Kikkawa, B. Sakita, and M. A. Virasoro, *ibid.* **184**, 1956 (1969).

<sup>8</sup> We also do not consider the triple-product representation suggested by M. A. Virasoro [Phys. Rev. **177**, 2309 (1969)] nor the parametrization of S. Mandelstam [*ibid.* **183**, 1374 (1969)].

<sup>9</sup> By "subsidiary" we mean either terms which do not contribute to leading order asymptotically in one or more channels or those which do not contribute to the residue of the lowest-lying physical state on a given trajectory. We use the word "daughter" to denote any state in a given resonance tower whose spin  $J$  is less than that of the leading member. The term "exotic" denotes a meson state whose quantum numbers cannot be generated via the quark model as ( $\bar{q}q$ ); an exotic baryon is one for which ( $qqq$ ) structure is not possible.

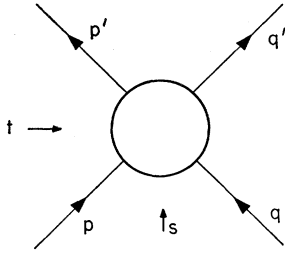


FIG. 1. Scattering diagram for meson-baryon scattering;  $s = (p+q)^2$ ,  $t = (p'-p)^2$ ,  $u = (p'-q)^2$ , where  $p$  ( $p'$ ) and  $q$  ( $q'$ ) are the four-vectors of the initial (final) baryon and meson, respectively.

the reduced residue is a polynomial in  $s^{1/2}$ . We determine the corresponding residues from the published data on elastic widths, and present curves showing this empirical variation with mass. We believe that plots of this type will also prove useful in other reactions for summarizing the data and predicting the elastic widths of undiscovered resonances.

In Sec. II D, we give results of a comprehensive fit to all high-energy backward  $\pi N$  scattering data. We employ the polynomial form for residues, suggested by the Veneziano model, constraining them as much as possible to reproduce the elastic widths of physical states along the trajectories. Because it specifies the residue structure of secondary trajectories, such as the  $N_\gamma$ , the Veneziano approach allows us to go further than previous fits to backward data.

Some explicit beta-function representations for meson-baryon scattering are presented in Sec. III, and there we analyze the extent to which they realize the desiderata given in Secs. I and II. We concentrate on the kaon-nucleon process, and compare several Veneziano-type parametrizations with both scattering data and resonance widths. One exciting feature not present in traditional Regge fits is the possibility of representing  $KN$  scattering data from threshold to infinity with the same functional form.

In the final section, we summarize our conclusions.

The reader interested primarily in new phenomenological results is directed to Secs. II A, II D, and III.

## I. NOTATION AND TECHNICAL ASPECTS OF VENEZIANO REPRESENTATION

In this section we define our notation, discuss the choice of an appropriate set of amplitudes, and give a general expansion for these amplitudes in terms of Veneziano beta-function terms. Securing the appropriate asymptotic behavior and spin structure of the amplitudes imposes certain restrictions on the terms in the expansions. Further limitations and relationships between terms arise from incorporating into the representation general properties of meson-baryon scattering such as signature for trajectories, positivity of resonance widths, and absence of ghosts.

### A. Notation

The kinematics of meson-baryon scattering are relegated to Appendix A. With reference to Fig. 1, we point out that the  $s$  and  $u$  channels are meson-baryon channels, whereas the  $t$ -channel is a meson-meson channel. The description of pseudoscalar-meson and spin- $\frac{1}{2}$  baryon scattering requires  $2T$  independent amplitudes, where  $T$  is the total number of distinct (conserved) values of total isospin. In Sec. I B we will elaborate somewhat on the alternative choices, but for definiteness here we consider the standard invariant amplitudes  $A^{(I)}(s,t,u)$  and  $B^{(I)}(s,t,u)$ , which are free of kinematical singularities. The superscript  $(I)$  is an isospin index. In the particular case of pion-nucleon scattering, we may use the amplitudes  $A^{(\pm)}(s,t,u)$  and  $B^{(\pm)}(s,t,u)$ , which have the properties

$$A^{(\pm)}(s,t,u) = \pm A^{(\pm)}(u,t,s), \quad (1)$$

$$B^{(\pm)}(s,t,u) = \mp B^{(\pm)}(u,t,s), \quad (2)$$

and where the  $+$  ( $-$ ) functions have pure isospin  $I=0$  ( $1$ ) in the  $t$  channel.

If we adopt, as have other researchers, the view that a Veneziano-type representation should be established for the  $A$  and  $B$  functions, then we have, in general, expansions of the form

$$A^{(I)}(s,t,u) = \left\{ \sum_{l,m,n,B,M} C_A^{(I)}(l,m,n,B,M) \frac{\Gamma(l-\alpha_M(t))\Gamma(m-\bar{\alpha}_B(s))}{\Gamma(n-\alpha_M(t)-\bar{\alpha}_B(s))} + \sum_{g,h,i,B_1,B_2} D_A^{(I)}(g,h,i,B_1,B_2) \right. \\ \left. \times \frac{\Gamma(g-\bar{\alpha}_{B_1}(s))\Gamma(h-\bar{\alpha}_{B_2}(u))}{\Gamma(i-\bar{\alpha}_{B_1}(s)-\bar{\alpha}_{B_2}(u))} + \sum_{p,q,r,B,M} E_A^{(I)}(p,q,r,B,M) \frac{\Gamma(p-\alpha_M(t))\Gamma(q-\bar{\alpha}_B(u))}{\Gamma(r-\alpha_M(t)-\bar{\alpha}_B(u))} \right\}, \quad (3)$$

where  $\alpha_M(t)$  denotes a particular meson trajectory and  $\bar{\alpha}_B = \alpha_B - \frac{1}{2}$ , with  $\alpha_B$  being a baryon trajectory function. Similar expansions are appropriate for  $B^{(I)}(s,t,u)$ . The sums run independently over all meson trajectories  $M$  and over all baryon trajectories  $B$ ,  $B_1$ , and  $B_2$  appropriate to the process being considered, as well as over all integer values of  $l$ ,  $m$ ,  $n$ ,  $g$ ,  $h$ ,  $i$ ,  $p$ ,  $q$ , and  $r$ .

Restrictions upon and/or relationships between the constants  $C_A^{(I)}$ ,  $C_B^{(I)}$ ,  $D_A^{(I)}$ ,  $D_B^{(I)}$ ,  $E_A^{(I)}$ , and  $E_B^{(I)}$  arise from imposing certain physical requirements, such as the following:

(a) No states with exotic quantum numbers,<sup>9</sup> as, for instance,  $B=0$ ,  $I=2$  and  $B=1$ ,  $S=1$ .

(b) Absence of states with unphysical spin values; this restricts the values of the integers  $l$  through  $r$ , as discussed in Sec. I C.

(c) Appropriate spin-parity structure at the baryon resonance positions [ $\bar{\alpha}_B(s)=k$ , where  $k$  is an integer] and at the meson pole values [ $\alpha_M(t)=k$ ].

(d) Appropriate isospin structure at the baryon and meson resonance positions.

(e) Signature properties.

The requirements (c)–(e) are in practice applied only for the leading trajectories. Specifically, (d) establishes algebraic relations between the coefficients for the different isospin values,  $I \neq J$ , within the sets  $\{C_A, C_A^{(J)}\}$ ,  $\{D_A^{(I)}, D_A^{(J)}\}$ , and  $\{E_A^{(I)}, E_A^{(J)}\}$ . Secondly, (e) relates the constants  $C$ ,  $D$ , and  $E$ , in pairs, for each isospin  $I$ . Finally, (c) connects the two spin amplitudes  $A$  and  $B$ , whereas all other requirements apply to  $A$  and  $B$  separately.

The situation is much simpler in certain meson-baryon reactions where entire summations can be eliminated. For example, in kaon-nucleon scattering, because the  $K^+p$  system has no known prominent resonances, we want no terms involving  $\alpha_B(u)$  (let the  $s$  channel correspond to  $\bar{K}N$  scattering); therefore only the terms of the first summation in Eq. (3) survive. On the other hand, consider  $\pi^-\Sigma^+ \rightarrow \pi^+\Sigma^-$ ; since no  $I=2$  mesons are prominent, the first and third summations in Eq. (3) are eliminated, *a priori*.

In pion-nucleon scattering, the symmetry property given in Eqs. (1) and (2) can be directly employed to relate the constants of the third summation of Eq. (3) to those in the first, and also to prescribe structure within the second summation.

Later in this paper, when we discuss the spin-parity structure of the baryon states, it will prove convenient to use terms such as

$$(c_1 l + c_2 s + c_3) \frac{\Gamma(l' - \alpha_M(t)) \Gamma(m' - \bar{\alpha}_B(s))}{\Gamma(n' - \alpha_M(t) - \bar{\alpha}_B(s))}, \quad (4)$$

with  $c_1$ ,  $c_2$ , and  $c_3$  constants. This form is not quite that of a typical term in Eq. (3), but, assuming linear trajectories, we can always rewrite it as a particular linear combination of terms within a given summation on the right-hand side of Eq. (3). A similar statement, of course, applies to  $(s, u)$ -type terms.

The reader not familiar with the methods for extracting asymptotic behaviors and pole residues from Eq. (3) is referred to earlier literature. We now state our reasons for working with the invariant amplitudes  $A$  and  $B$ , rather than with some other set.

### B. Choice of Amplitudes

Besides having the convenient crossing properties listed in Eqs. (1) and (2), the invariant amplitudes

$A^{(l)}(s, t)$  and  $B^{(l)}(s, t)$  have simple asymptotic behavior, as  $s \rightarrow \infty$ ,

$$\begin{aligned} A &\sim s^{\alpha_M} && \text{at fixed } t \\ &\sim s^{\bar{\alpha}_B} && \text{at fixed } u, \\ B &\sim s^{\alpha_M-1} && \text{at fixed } t \\ &\sim s^{\bar{\alpha}_B} && \text{at fixed } u. \end{aligned} \quad (5)$$

Other properties one would like to establish include positivity of pole residues, parity, and, more generally, the proper  $t$  dependence of the amplitude demanded by the observed spin-parity structure of the  $s$ -channel resonances. All of these are simply described only in terms of partial-wave amplitudes, and there is no full amplitude which allows even a vaguely complete treatment.

One might like to use the  $t$ -channel nonflip amplitude

$$A' = A + \frac{s-u}{4M(1-t/4M^2)} B,$$

whose imaginary part in the forward direction is  $\text{Im}A' = p_{\text{lab}} \sigma_{\text{tot}}$  and so is positive. Although this has good crossing properties, the kinematic singularity at  $t=4M^2$  would appear to be intolerable in the Veneziano approach which exploits analyticity in all three channels. Similarly,  $A + (s-u)B/4M$  reduces to  $A'$  at  $t=0$ , but complicates the statement of Regge behavior at fixed  $u$ . Finally, the  $s$ -channel nonflip amplitude  $A + E_{\text{lab}}(s)B$  would allow quite a nice discussion of positivity but does not have good  $s \leftrightarrow u$  crossing. This difficulty with crossing is not important for writing terms that have only  $s$ - and  $t$ -channel poles, for these can be easily symmetrized by writing  $s \leftrightarrow u$  terms for the crossed amplitude (both in spin and isospin space); e.g., one writes  $(s, t)$  terms for  $A + E_{\text{lab}}(s)B$  and  $\pi^- p$  elastic scattering, then adds  $(s, u)$  terms for  $A + E_{\text{lab}}(u)B$  for  $\pi^+ p$  scattering. The difficulty arises in the treatment of beta-function terms containing both  $s$ - and  $u$ -channel poles.

Finding no sufficiently significant advantage in any of these alternative choices of amplitudes, we present the remainder of this discussion largely in terms of the traditional  $A$  and  $B$  functions.

### C. Structure of Veneziano Formula for $A$ and $B$

The expansion of the functions  $A^{(l)}(s, t, u)$  and  $B^{(l)}(s, t, u)$  was given in Eq. (3). In this section, we will specialize to pion-nucleon scattering for definiteness and will elaborate somewhat on the properties of individual terms in the expansions. As noted, the desired amplitudes are expanded in a series of the form

$$\frac{\Gamma(m - \bar{\alpha}_B(s)) \Gamma(l - \alpha_M(t))}{\Gamma(n - \bar{\alpha}_B(s) - \alpha_M(t))}, \quad (6)$$

TABLE I. Lowest values of the integers  $m$ ,  $n$ , and  $l$  for the typical term given in expression (6) of the text. Here,  $B-M$  signifies that the term in question contributes asymptotically to leading order in both the  $s$  and the  $t$  channels (i.e., as  $s^{\alpha_M(t)}$  in  $A$  and as  $s^{\alpha_M-1}$  in  $B$  when  $s \rightarrow \infty$  at fixed  $t$ , and as  $t^{\alpha_B}$  in either  $A$  or  $B$  when  $t \rightarrow \infty$  at fixed  $s$ ). The type  $(B-1)-M$  is asymptotic at fixed  $t$ ,  $s \rightarrow \infty$ , but down by  $1/t$  for fixed  $s$ ,  $t \rightarrow \infty$ . The other terms of these types are found by incrementing the listed  $m$ ,  $n$ , and  $l$  by the same integer. All terms of the  $(s,t)$  variety vanish exponentially for  $s \rightarrow \infty$  at fixed  $u$ . The  $(u,t)$  terms are handled similarly and, for  $\pi N$  scattering, prescribed from these  $(s,t)$  terms by crossing symmetry, Eqs. (1) and (2).

Type	$(s,t)$ terms			
	Baryon $m$	Meson $l$	$n$	
$B-M$	0	1	1	$B$ amplitude
$(B-1)-M$	1	1	2	
$B-(M-1)$	0	2	2	
$B-M$	1	1	1	$A$ amplitude
$(B-1)-M$	2	1	2	
$B-(M-1)$	0	1	1	

and similar terms with  $s$  replaced by  $u$ , and

$$\frac{\Gamma(m - \bar{\alpha}_{B1}(s))\Gamma(l - \bar{\alpha}_{B2}(u))}{\Gamma(n - \bar{\alpha}_{B1}(s) - \bar{\alpha}_{B2}(u))}, \quad (7)$$

where  $m$ ,  $n$ , and  $l$  are integers and  $\bar{\alpha}_B = \alpha_B - \frac{1}{2}$ . For the baryon trajectories  $B$ , we can take  $N$ ,  $\Delta$ , or  $N_{\gamma}$ , and for the mesons  $M$ , we have the exchange-degenerate  $P'$  and  $\rho$  trajectories. Whereas this exchange degeneracy ( $\alpha_\rho = \alpha_{P'}$ ) is not necessary if one considers only  $\pi N$ , it is enforced by factorization and the absence of resonances in  $\pi^+\pi^+$  and  $\Sigma^+\pi^+$  elastic scattering. In particular, we cannot allow a multiplicative fixed pole for the  $\rho$  so that, like the  $P'$ , its residue function has a zero at  $\alpha_\rho = 0$  in both  $A$  and  $B$ . This restricts  $l$  in (6) to be  $\geq 1$ . There are no restrictions on the possible combinations of trajectories in a single term. Moreover, as far as pion-nucleon scattering itself is concerned, the Pomeranchuk trajectory (with any slope) may be treated on an equal footing with the  $\rho$  and  $P'$  trajectories and thus included as a possible candidate for  $\alpha_M(t)$  in expression (6). However, in the  $SU(3)$ -related kaon-nucleon process, treating the Pomeranchuk in this manner, without an exchange-degenerate partner, would lead to the prediction of exotic resonances<sup>9</sup> in the  $K^+p$  system.<sup>10</sup> (The elastic widths of these exotic states are fairly narrow, however, as we note in Sec. III E.)

In Tables I and II, for the  $(s,t)$  and  $(s,u)$  terms, respectively, we record the nature of the asymptotic behavior associated with various sets of integers  $(l,m,n)$ . We do this for only those terms which contribute asymptotically to leading order in at least one channel. In order to satisfy the limitations given in expression (5) (and similar ones appropriate when  $u \rightarrow \infty$ ),  $n \geq m$  and  $n \geq l$  in all terms; moreover, for the  $(s,t)$  and  $(u,t)$

<sup>10</sup> Similar inclusion of the Pomeranchuk in  $\pi\pi$  scattering leads to predicted resonances with isospin 2 as discussed in D. Y. Wong, Phys. Rev. **181**, 1900 (1969).

terms in  $B(s,t,u)$ , it is further necessary to have  $n \geq m+1$ . These conditions are also required (but not sufficient) in assuring that the spin associated with a particular pole be no greater than that of the appropriate resonant state; to guarantee polynomial residues,  $m+l \geq n$ .

We note, in passing, that the absence of a physical state at  $\alpha_\Delta(s) = \frac{1}{2}$  does not prevent our using  $m=0$  in (6) and (7) when dealing with that trajectory. Upon taking the appropriate linear combination of (6) and (7) required to obtain the correct signature, we will see that the residue at  $\alpha_\Delta(s) = \frac{1}{2}$  is zero. Notice, however, that the term with  $m=0$  couples nonasymptotically as  $s \rightarrow \infty$  for  $t$  fixed in the  $A$  amplitude. However, only that  $m=0$  term provides a large constant term in the  $\Delta_\delta$  residue function; we elaborate on the importance of this in Sec. II C. For the  $SU(3)$ -symmetric kaon-nucleon situation, there must be exchange degeneracy (and thus no signature properties) for the baryon trajectories if exotic  $KN$  resonances are to be avoided. Thus, the absence of a  $J^P = \frac{1}{2}^- Y_{11}^*$  requires  $m \geq 1$  for the  $SU(3)$ -symmetric trajectory of  $\Delta_\delta$ . Similar arguments in  $\pi N \rightarrow K\Sigma$  imply  $m \geq 1$  for the  $\Delta_\delta$  itself.

Beyond the restrictions of appropriate asymptotic behavior and resonance angular-momentum properties alluded to above, the other elementary constraints on the selection of terms in Eqs. (3), (6), and (7) include crossing symmetry, signature, positivity of resonance widths, parity doubling, and isospin [or, more generally,  $SU(3)$  structure]. It is possible to guarantee these simply only for the leading trajectories in the representation. We will now comment upon some technical questions associated with these desirable properties.

#### D. Signature

Obtaining signature for trajectories in the Veneziano model is by no means natural. Both Igi and Virasoro,<sup>6</sup> however, chose to impose signature in a manner which strongly coupled the over-all contributions of the various baryon trajectories. Specifically, in their solutions, a term of the form

$$c \frac{\Gamma(l - \bar{\alpha}_{B1}(s))\Gamma(l - \bar{\alpha}_{B2}(u))}{\Gamma(l - \bar{\alpha}_{B1}(s) - \bar{\alpha}_{B2}(u))}, \quad (8)$$

which contributes in leading order both as  $s \rightarrow \infty$  at fixed  $u$  and as  $u \rightarrow \infty$  at fixed  $s$ , served to generate the signature properties for both baryon trajectories  $\alpha_{B1}$  and  $\alpha_{B2}$ . Therefore, the multiplicative coupling strength constant  $c$  enters into the definition of the residues of both trajectories and thus, for example, would tend to associate the pion-nucleon coupling constant  $g^2/4\pi$  to  $\Gamma_\Delta$ , the elastic width of the 1238 resonance, in too restrictive a fashion. The asymptotic  $N$  and  $\Delta$  exchange amplitudes are also constrained to be of similar magnitude in this type of solution. A more realistic and less restrictive solution necessarily involves some terms

which contribute to nonleading order in at least one channel. As will be established in detail in Sec. II, these subsidiary terms are also strongly suggested by other features of the low-energy resonance structure.

### E. Parity Doubling

A naive Veneziano formula for meson-baryon scattering generates parity-doubled trajectories. This is a general feature of all theoretical models that enforce analyticity at  $s=0$ . If we cunningly adjust the constants multiplying the subsidiary terms in Eq. (3), we may abolish these parity-doubled states. This is possible for the leading trajectories, but not for the lower-lying trajectories, if one wishes to retain Regge asymptotic behavior.

The partial waves of definite parity are given by (let  $l=J-\frac{1}{2}$ )

$$a_{\tau P+}^J = \frac{1}{4} \int_{-1}^{+1} dz [(P_{l+1}+P_l)(f_1+f_2) - (P_l-P_{l+1})(f_1-f_2)], \quad (9)$$

$$a_{\tau P-}^J = \frac{1}{4} \int_{-1}^{+1} dz [(P_{l+1}+P_l)(f_1+f_2) + (P_l-P_{l+1})(f_1-f_2)]. \quad (10)$$

Now, near  $t=0$ ,

$$P_l - P_{l+1} \sim 1 - z \alpha t/s, \quad (11)$$

$$P_l + P_{l+1} \sim 2. \quad (12)$$

Moreover,

$$\frac{8\pi s^{1/2}}{2M} (f_1+f_2) = A + E_{lab} B \sim s^{\alpha M(0)}, \quad (13)$$

$$\frac{8\pi s^{1/2}}{2M} (f_1-f_2) = \frac{EA}{M} + \omega B \sim s^{\alpha M(0)+1/2}. \quad (14)$$

Thus, since the integrals are presumably dominated by the forward peak, the  $f_1+f_2$  term dominates, whence  $a_{\tau P+}^J \sim a_{\tau P-}^J$ . It follows that it is impossible not to have some parity doubling, and so one can only consider removing the doubling for the leading trajectories, with  $l > s^{1/2}$ , which eventually decouple from the cross section. However, even this modest aim is not easy, and, in practice, one puts zeros into the residue functions by hand at the positions of the unwanted resonances.

### F. Positivity

(1) A remarkable feature of the Veneziano form for  $\pi\pi$  scattering was that it gave positive widths for essentially all resonances, if a reasonable intercept for the  $\rho$ -meson trajectory was employed.<sup>11</sup> One might expect a similar situation in meson-baryon scattering.

<sup>11</sup> Positivity in  $\pi\pi$  scattering has been studied by J. Shapiro (Ref. 2); F. Wagner, Nuovo Cimento **63A**, 393 (1969); R. Oehme, Nuovo Cimento Letters **1**, 420 (1969); J. Yellin, University of California Lawrence Radiation Laboratory Report No. UCRL-18637 (unpublished).

TABLE II. Asymptotic properties of the  $(s,u)$  terms, expression (7) of the text, for the lowest values of  $m$ ,  $n$ , and  $l$ . These have the same structure for  $A(s,l,u)$  and  $B(s,l,u)$ . Here,  $B-B$  signifies that the term contributes asymptotically to leading order both as  $s \rightarrow \infty$  at fixed  $u$  and as  $u \rightarrow \infty$  at fixed  $s$ , e.g., as  $s^{\alpha_B(u)}$  as  $s \rightarrow \infty$ , for fixed  $u$ . The type  $B-(B-1)$  is asymptotic at fixed  $s$ ,  $u \rightarrow \infty$ , but down by  $1/s$  for fixed  $u$ ,  $s \rightarrow \infty$ . For  $(s,u)$ -type terms, fixed- $l$  limits are exponentially vanishing. Other terms with the same asymptotic properties as those listed are found by incrementing the listed  $m$ ,  $l$ , and  $n$  by the same integer.

Type	$m(s)$	$(s,u)$ terms $l(u)$	$n$
$B-B$	0	0	0
$B-(B-1)$	0	1	1

However, one even runs into trouble for the leading trajectory in  $\pi N$ , whereas this was quite trivial in the  $\pi\pi$  case. The width of a resonance of spin  $j$  and mass  $M_R$  on the leading trajectory is

$$\Gamma_{M_R} = \frac{R_i}{4\pi(M_R)^2} q^{2i} 4^{j-1/2} \frac{\Gamma(j+\frac{1}{2})\Gamma(j+\frac{3}{2})}{\Gamma(2j+2)}, \quad (15)$$

where

$$\begin{aligned} i &= 1 & \text{for } \tau P = -1 \\ &= 2 & \text{for } \tau P = +1, \end{aligned}$$

and the leading trajectory residue is

$$R_i = \lim_{s \rightarrow M_R^2} [(M_R^2 - s) 8\pi s^{1/2} f_i / t^{j-1/2}]. \quad (16)$$

It is evidently convenient to treat both parities together, however, and to use, say,  $\tilde{f}_1 = A + (s^{1/2} - M)B$ . One considers then the poles for both positive and negative values of  $s^{1/2}$ . In this approach, positivity of  $\Gamma_{M_R}$  implies that the residue must be positive (negative) for  $s^{1/2}$  positive (negative). Therefore, because the residues of the poles in  $A$  and  $B$  are functions of  $s$  and not  $s^{1/2}$ , we deduce that at a given pole the leading power of  $s$  in the residue for  $A$  must be no higher than for  $B$ . This requirement is not trivial because, in constructing the functions  $A$  and  $B$ , the simplest choice for the  $N_\alpha$  trajectory is to make  $B$ 's residue contribution a constant, whereas  $A$  must be at least linear in  $s$ , if the parity-partner state to the nucleon is to be abolished. We will illustrate this further with examples in Secs. II C and III.

The situation is further complicated by the fact that in nature, parity partners are evidently extinguished, at least for the lower-lying recurrences.

(2) In order to gain further insight into the matter of guaranteeing positivity for all baryon resonance states, we review the  $\pi\pi$  situation more fully.<sup>11</sup> It is possible to present a simple, if nonrigorous, argument leading to an inequality which guarantees that all but a finite number of states will have positive widths. One begins with a single  $(s,t)$  Veneziano-type form, e.g.,

$$\frac{\Gamma(m-\alpha_1(s))\Gamma(l-\alpha_2(t))}{\Gamma(n-\alpha_1(s)-\alpha_2(t))}. \quad (17)$$

At the pole position  $\alpha_1(s) = m'$ , the residue is

$$\frac{(-1)^{m+n-l} \Gamma(N+y)}{\Gamma(m'-m+1) \Gamma(y)}, \quad (18)$$

where

$$y = \alpha_2(t) - l + 1$$

and

$$N = m' + l - n.$$

The modulus of this function is symmetric about  $y = -\frac{1}{2}(N-1)$ . To avoid having a backward peak whose magnitude is as large as that of the forward peak (albeit with oscillating sign, as one moves up through the successive  $s$ -channel resonances), the last zero of (18), for  $y < 0$ , must fall very near or outside the physical-region boundary ( $u \sim 0$ ). This implies that

$$\alpha_1(0) + \alpha_2(0) + \Sigma \gtrsim n, \quad (19)$$

where  $\Sigma$  is the sum of the squares of the external masses.

In  $\pi\pi$  scattering,  $\Sigma \sim 0$  and  $n \geq 1$  gives  $\alpha_p(0) \gtrsim 0.5$ . In  $\pi N$  scattering, the application of Eq. (19) is beclouded. We really should use  $f_1$  and  $f_2$  not  $A$  or  $B$ , to start considering positivity, and even then necessary conditions are difficult to find. Moreover, we should employ  $SU(3)$  symmetry to find reactions with exotic channels so as to be able to apply Eq. (19) to  $(s, t)$  and  $(s, u)$  terms separately.

We may continue to use Eq. (19) as a guide, remembering to use  $\alpha_i = \alpha_B - \frac{1}{2}$  for baryons. Then the inequality is less stringent than in  $\pi\pi$ , because  $\Sigma \sim 1.80$  not 0.08. However, one can draw the general conclusion that for high-lying baryon trajectories such as  $\Delta_8$ , we can expect many Veneziano-type terms, whereas for the lower-lying  $N_7$  we are restricted to fewer terms in Eq. (3).

### G. PCAC

Ademollo *et al.*<sup>5</sup> have made the interesting observation that the PCAC condition plus the beta-function representation imply the (approximately valid) quantization relations  $\alpha_\Delta(0) - \alpha_N(0) = 0.5$  and  $\alpha_\Delta'(0) = \alpha_N'(0)$ . The PCAC condition in, say,  $\pi N$  or  $\pi\Sigma$  scattering, may be stated as  $A'(s=M^2, t=0, \mu^2=0) = 0$ , where  $M$  is the mass of the external baryon and  $\mu$  is the mass of the external meson. (See Sec. I B for a definition of  $A'$ .) Take, for simplicity,  $\pi N$  elastic scattering and treat only the  $s$ - $t$  terms. (The neglect of  $s$ - $u$  terms may be justified by considering  $\pi^- \Sigma^+ \rightarrow \pi^- \Sigma^+$ .) Then the quantization relation ensures that the  $\Delta$  contribution vanishes in the PCAC limit if we take for  $A$  either of the forms

$$\frac{\Gamma(1-\bar{\alpha}_\Delta)\Gamma(1-\bar{\alpha}_\rho)}{\Gamma(1-\bar{\alpha}_\Delta-\alpha_\rho)} \quad \text{or} \quad \frac{\Gamma(-\bar{\alpha}_\Delta)\Gamma(1-\alpha_\rho)}{\Gamma(1-\bar{\alpha}_\Delta-\alpha_\rho)};$$

these will be seen in Sec. III to be reasonable as first guesses. Unfortunately, there remain terms involving

the nucleon trajectory. The simplest form of these is

$$A = a_N \frac{\Gamma(1-\bar{\alpha}_N)\Gamma(1-\alpha_\rho)}{\Gamma(1-\bar{\alpha}_N-\alpha_\rho)}$$

and

$$B = b_N \frac{\Gamma(-\bar{\alpha}_N)\Gamma(1-\alpha_\rho)}{\Gamma(1-\bar{\alpha}_N-\alpha_\rho)}.$$

Then, if  $\mu^2 = 0$ , the amplitude

$$Z = A + [(s-M^2)/2M]B,$$

which is  $A'$  at  $t=0$ , takes the form

$$\left( a_N - \frac{b_N}{2M\alpha_N'(0)} \right) \frac{\Gamma(1-\bar{\alpha}_N)\Gamma(1-\alpha_\rho)}{\Gamma(1-\bar{\alpha}_N-\alpha_\rho)}.$$

Choosing  $a_N = b_N/2M\alpha'$  achieves the PCAC result, but at the cost of decoupling the nucleon trajectory entirely from this amplitude. This violates both positivity ( $Z$  must be positive at  $t=0$ ) and the desired isospin structure of the high-energy behavior in  $A'$ . On the other hand, as we shall see in Sec. II B, the ratio  $Z(t=0)/B(t=0)$  is rather small [ $\sim 0.1$  for the  $D13(1520)$ ], and so indeed  $a_N \sim b_N/2M\alpha'$  to 10%. This does not seem quite good enough; perhaps one should enforce the PCAC result  $a_N = b_N/2M\alpha'$  exactly, and then add small terms to  $Z$  of the form

$$Z = (z_1 s + z_2 t + z_3) \frac{\Gamma(1-\bar{\alpha}_N)\Gamma(1-\alpha_\rho)}{\Gamma(2-\bar{\alpha}_N-\alpha_\rho)},$$

where  $z_1$ ,  $z_2$ , and  $z_3$  are arranged so as to obtain the PCAC vanishing along with a more satisfactory value of  $Z$  at  $t=0$  for the higher recurrences of the nucleon. It is curious that whereas in  $\pi\pi$  scattering, positivity and PCAC seem to be correlated, a similarly naive beta-function choice in  $\pi N$  scattering only achieves PCAC at the cost of violating positivity.

## II. EMPIRICAL KNOWLEDGE OF MESON-BARYON SCATTERING

To ascertain which particular linear combination of beta-function terms should be written for  $A^{(\pm)}(s, t, u)$  and  $B^{(\pm)}(s, t, u)$ , we must first abstract from the data on  $\pi N$  and  $KN$  scattering a certain salient structure for these amplitudes, as a function of  $s$  and  $t$  separately. We may then hope to build that structure into our choice of terms. There are several noteworthy features associated with particular values of  $t$ . In Sec. II A we focus upon the forward elastic scattering region in  $\pi N$  and  $KN$  processes. We stress the conclusions drawn from present Regge-pole-theory fits both as to the relative magnitudes of the various exchanges and as to the structure in  $t$  of their residue functions. In the process of our investigation, we refitted existing data and, as a by-product, obtained a good fit to  $\pi p$  elastic

data using a normal-slope Pomeranchuk trajectory. The remaining subsections deal with various aspects of the baryon spectrum. We first discuss and tabulate the zeros of the amplitudes at certain values of  $t$  and  $u$  required in order to obtain the correct spin-parity structure of the  $s$ -channel resonances. The correspondence of the positions of these zeros with analogous structure in differential cross sections is emphasized. Next, from the general form of the Veneziano expansion, we extract a formal parametrization for both the elastic widths of the resonances on parent baryon trajectories and the backward elastic scattering data. This leads to the definition of a reduced residue function based on the model. From the data we extract the empirical values of the residue function and quantitatively examine in the last subsection the adequacy of the Veneziano-model parametrization of these baryon residues.

#### A. Properties of $A(s,t,u)$ and $B(s,t,u)$ Following from High-Energy Forward Scattering Data

In this section we present a review of the Regge-pole description of  $\pi N$  and  $KN$  forward elastic scattering and examine critically the status of various features of the model fits. We take the usual model of  $P$ ,  $P'$ ,  $\omega$ ,  $\rho$ , and  $A_2$  exchange, with the last four trajectories having intercept  $\alpha(0) = 0.4 \rightarrow 0.65$  and slope  $\alpha'(0) \approx 1$ . In the exchange-degenerate limit described by the Veneziano formula, these four poles have a common intercept and slope. For definiteness, suppose the high-energy limit of the amplitudes  $A'$  and  $B$  is

$$\begin{aligned} A^{(i)}(s,t) &= a_c^{(i)}(t) \eta^{(i)}(t) s^{\alpha^{(i)}(t)}, \\ B^{(i)}(s,t) &= b_c^{(i)}(t) \eta^{(i)}(t) s^{\alpha^{(i)}-1}, \end{aligned} \quad (20)$$

where  $\eta^{(i)}$  is the signature factor, given by

$$\eta^{(i)} = (1 + \tau^{(i)} e^{-i\pi\alpha^{(i)}}) / \sin\pi\alpha^{(i)},$$

and  $(i)$  labels the contribution of a given pole. The functions  $a_c^{(i)}(t)$  and  $b_c^{(i)}(t)$  are classical Regge-pole-model residues whose structure is given in Sec. III A 1.

We have placed the scale factors  $s_0 = 1$  as suggested by the Veneziano formula when a trajectory has slope 1. In this regard, it is certainly interesting to note that all experimental data which call for a slope  $\alpha'(0) \approx 1$  indeed have a  $t$  dependence consistent with the scale factor  $s_0 \approx 1$ .<sup>12</sup> For general slope  $\alpha'$ , the Veneziano formula predicts  $s_0 = 1/\alpha'$ ; but this value is certainly not consistent with those data indicative of a trajectory slope much less than 1. In particular, if one wishes to incorporate the Pomeranchuk trajectory into a Veneziano form, as suggested by Wong,<sup>10</sup> the experimental  $t$  dependence necessitates a trajectory slope of approximately unity. In this section, we will consider both cases—one in which the Pomeranchuk trajectory has a

universal slope near 1 and the other in which it has a very small slope.

#### 1. Structure in $t$ of Residues

For both cases, independent of the the Pomeranchuk-trajectory properties, the data suggest a residue zero at  $t = -0.2$   $(\text{GeV}/c)^2$  in those nonflip amplitudes  $A'$  associated with  $\rho$ ,  $\omega$ , and  $A_2$  quantum numbers [i.e., the corresponding  $a_c^{(i)}(t)$  are proportional to  $t+0.2$ ]. The supporting evidence is the crossover feature in the  $\pi p$ ,  $Kp$ , and  $p p$  elastic differential momentum-transfer distributions.<sup>13</sup> In addition, a residue zero in the  $\rho$  quantum-number flip amplitude  $B$  at the point  $\alpha_\rho \approx 0$ ,  $t \approx -0.6$   $(\text{GeV}/c)^2$  is prescribed by  $\pi N$  charge-exchange data.<sup>13</sup> The  $P'$  and  $A_2$  residue functions for both  $A'$  and  $B$  must contain zeros at  $\alpha_{P'} = 0$  and  $\alpha_{A_2} = 0$ , respectively, to eliminate ghosts at those positions.

We now invoke the concept of exchange degeneracy and conclude that (with  $\alpha_{P'} = \alpha_\rho = \alpha_{A_2} = \alpha_\omega$ ) both  $A'$  and  $B$  should possess the residue zero at  $\alpha = 0$  for each  $t$ -channel quantum number. In classical language, this corresponds to the Regge poles choosing nonsense at  $\alpha = 0$ . This  $\alpha$  factor is, indeed, generated automatically by the Veneziano approach, which suggests

$$\begin{aligned} a_c^{(i)}(t) &= \pi a'(t) / \Gamma(\alpha), \\ b_c^{(i)}(t) &= \pi b(t) / \Gamma(\alpha), \end{aligned} \quad (21)$$

with  $a'(t)$  and  $b(t)$  nonsingular.

The zero in  $A'$  at  $t \approx -0.2$   $(\text{GeV}/c)^2$  is more controversial. We consider first associating it with the residue of each Regge pole. Via exchange degeneracy, the observed  $\omega$  zero at  $t \approx -0.2$   $(\text{GeV}/c)^2$  suggests a similar one in the  $P'$  amplitude. This provides the appealing possibility that the Pomeranchuk trajectory can have universal slope of approximately 1. The sign change in the  $P'$ -Pomeranchukon interference term at  $t \approx -0.2$   $(\text{GeV}/c)^2$  will yield the observed lack of shrinkage in  $\pi p$  scattering. In Fig. 2(a), we demonstrate the fit achieved to  $\pi p$  forward elastic scattering in this fashion. The details of this fit are relegated to Appendix B; for comparison, we present a standard<sup>14</sup> low-slope Pomeranchukon fit in Fig. 2(b). Moreover, it is also attractive for duality reasons to associate the  $t \approx -0.2$   $(\text{GeV}/c)^2$  residue zero with the contributions of these poles. As emphasized by Dolen, Horn, and Schmid<sup>3</sup> and by Dikmen,<sup>15</sup> the contributions of the prominent  $s$ -channel resonances in  $\pi p$  and  $Kp$  scattering vanish at  $t \approx -0.2$   $(\text{GeV}/c)^2$  in the nonflip amplitude  $A'$  and at  $t \approx -0.6$

<sup>13</sup> Typical Regge-pole fits incorporating the crossover effect are given in Reg. 14 for  $\pi N$  and  $N N$  scattering and in G. V. Dass, C. Michael, and R. J. N. Phillips [Nucl. Phys. **B9**, 549 (1969)] for the  $KN$  process. The effect is also considered using finite-energy sum rules for  $\rho$  exchange by Dolen *et al.* (Ref. 3) and for  $\omega$  and  $A_2$  exchanges by C. Michael and G. Dass, Phys. Rev. **175**, 1774 (1968), and references therein.

<sup>14</sup> W. Rarita, R. J. Riddell, C. B. Chiu, and R. J. N. Phillips, Phys. Rev. **165**, 1615 (1968).

<sup>15</sup> F. N. Dikmen, Phys. Rev. Letters **22**, 622 (1969).

<sup>12</sup> See, e.g., Igi, Igi and Storrow, Inami, and Igi and Pretzl (Ref. 6).



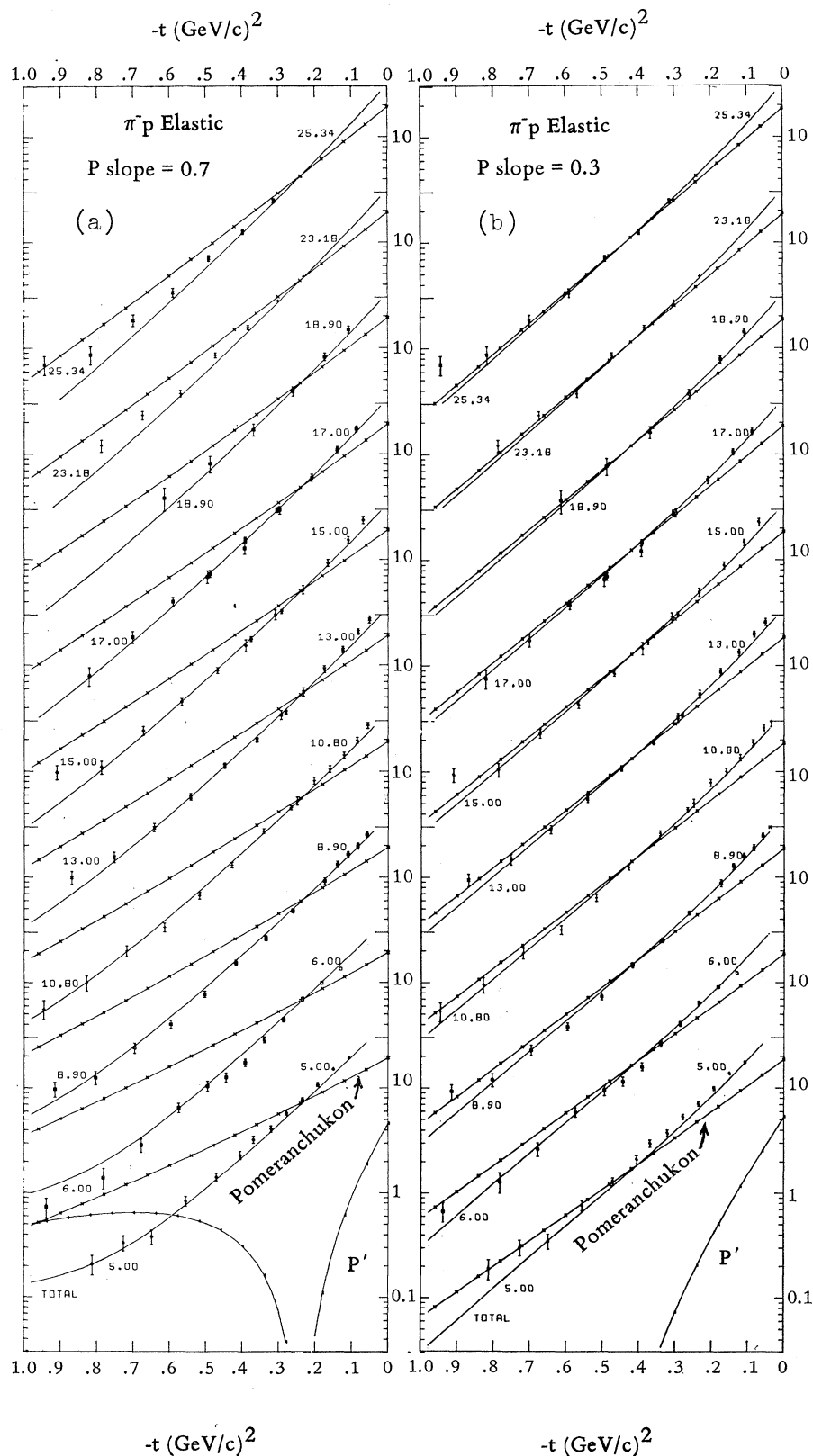


FIG. 2. Fits to  $\pi^-p$  elastic  $d\sigma/dt$  data, described in Appendix B. The data points for neighboring energy values are separated from each other by one decade. The total ( $P+P'+\rho+\rho'$ ) contribution is presented as an unadorned solid line and that of the  $P$  alone as a solid line with 'x's. At the lowest energy, the  $P'$  trajectory contribution is given in order to show how its residue zero moves as the  $P$  slope is altered. In (a) the  $P$  has slope 0.7 and in (b) slope 0.3 ( $\text{GeV}/c$ )<sup>-2</sup>.

$(\text{GeV}/c)^2$  in the flip amplitude  $B$  (to be described in Sec. II B). According to reasoning similar to that of Harari, therefore, the contributions of the  $t$ -channel Regge poles, except for the Pomeranchukon, should have the same zeros.<sup>16</sup>

Unfortunately, however, the above scheme is clearly inconsistent with factorization. From the residue zero in  $A'$  at  $t \simeq -0.2$   $(\text{GeV}/c)^2$ , one derives a square-root zero associated with all vertices  $K\bar{K}M$ ,  $\pi\pi M$ , and  $p\bar{p}M$ , where  $M$  is the Regge pole exchanged. This in turn implies an unobserved residue zero in the spin-flip  $B$  amplitude also at  $t \simeq -0.2$   $(\text{GeV}/c)^2$ . Furthermore, the requirement of exchange degeneracy itself forces an unobserved zero in the  $\rho$  and  $\omega$  residue functions in  $A'$  at  $\alpha=0$ ,  $t \simeq -0.6$   $(\text{GeV}/c)^2$ .<sup>17</sup>

To get around these difficulties, one must add additional  $t$ -channel effects besides the Regge poles listed above. There are two ways to do this, and the different methods suggest quite different  $t$ -channel structure for Veneziano representations of  $KN$  and  $\pi N$  scattering. The first method is illustrated in Fig. 3(a). If we continue to associate zeros at  $t \simeq -0.2$   $(\text{GeV}/c)^2$  with the Regge-pole residues, as above, then some secondary trajectory or cut mechanism must serve to cancel the  $t \simeq -0.6$   $(\text{GeV}/c)^2$  zero from  $A'$ . This way out has the feature of retaining duality of leading  $t$ -channel Regge poles with leading  $s$ -channel resonances, and presumably the effect required could be quantitatively small.<sup>18</sup> To avoid the factorization-induced zero in  $B$  at  $t \simeq -0.2$   $(\text{GeV}/c)^2$ , one must conclude that it is inappropriate to impose factorization on nonunitary solutions, such as those of the Veneziano type. We will say more about this later.

The second method for curing the difficulties requires disassociating the  $t \simeq -0.2$  zero from a single Regge-pole residue altogether. It is illustrated in Fig. 3(b). The leading Regge pole is presumed to have only the one zero at  $\alpha=0$  in  $A'$ . A secondary trajectory or cut<sup>19</sup> having the same quantum numbers interferes with the leading pole, and the zero of the effective amplitude is moved to  $t \simeq -0.2$   $(\text{GeV}/c)^2$ . This remedy preserves factorization of pole residues but disagrees with the duality picture given above. However, it may be that the duality argument was too simple. Inasmuch as it is only the leading baryon resonances whose contributions vanish at  $t \simeq -0.2$   $(\text{GeV}/c)^2$ , one may imagine that if the contributions of the entire degenerate Veneziano-model tower of baryon resonances were included, then

<sup>16</sup> H. Harari, Phys. Rev. Letters **20**, 1395 (1968).

<sup>17</sup> It is interesting to note that the crossover effect is largest in  $p\bar{p}$  scattering. Baryon-baryon scattering is also known to violate the simplest duality picture with no exotic resonances. These effects are possibly connected.

<sup>18</sup> Notice that the leading  $s$ -channel resonances do have zeros in both  $A$  and  $B$  near  $t \simeq -0.6$   $(\text{GeV}/c)^2$ , but the small difference in the exact positions often suffices to move the zero in  $A'$  to a somewhat higher  $|t|$  value. See also the discussions in Secs. II B and III E.

<sup>19</sup> See the review article by C. B. Chiu, Rev. Mod. Phys. **41**, 640 (1969).

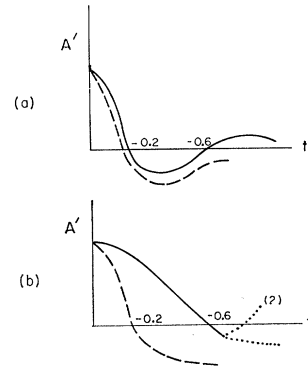


FIG. 3. Two possible “Born” Regge-pole structures in the amplitude  $A'$  (solid line), with the dashed line representing the effective result after secondary-trajectory or cut contributions have been included so as to obtain agreement with nature. Situation (a) is favored by duality and (b) by factorization. Two possibilities exist for the (b) case at larger  $t$ ; the second zero is suggested by the spin-parity structure of  $s$ -channel resonances.

the duality zero would be moved out to  $t \simeq -0.6$   $(\text{GeV}/c)^2$ . An altered form of duality between resonances and Regge poles could thus be restored, although the asymmetry between  $A'$  and  $B$  seems inelegant. Moreover, if we define “background” to be “experiment” minus the contributions of leading trajectories, we see that this background would not have the Pomeranchuk quantum numbers, as conjectured by Harari.<sup>16</sup>

The discussion of the above few paragraphs pertained to a view of data in which the Pomeranchuk trajectory has a near-normal slope of approximately unity. The standard fit of Rarita *et al.*<sup>14</sup> concluded that a smaller slope  $0 \leq \alpha_{P'} \leq 0.3$  is preferred. This alternative allows—indeed, somewhat prefers—the  $P'$  trajectory to vanish at larger  $|t|$ .

For instance, Barger and Phillips<sup>20</sup> have suggested an extra zero at  $t \sim -0.6$   $(\text{GeV}/c)^2$ . Thus, in the model in which the  $P$  has normal slope,  $A'$  for the  $P'$  has residue zeros at  $t \approx -0.2$  and  $-0.6$   $(\text{GeV}/c)^2$ ; the models in which  $P$  has a small slope lead to a rough coincidence of the two zeros at  $t \approx -0.6$   $(\text{GeV}/c)^2$ . This version is now not (obviously) inconsistent with factorization for the  $P'$ , but, nevertheless, the low-slope Pomeranchukon model does not cure the  $t \approx -0.2$   $(\text{GeV}/c)^2$  factorization difficulties connected with the other quantum numbers.

## 2. Numerical Values of Residues at $t=0$

We now turn to a discussion of the numerical values of the residues which we should try to reproduce with our Veneziano parametrization. Having discussed the  $t$  variation above, we need consider only the values at  $t=0$ . One may also hope that the effects of cuts will be at their smallest there. The values of  $a'$  may be deter-

<sup>20</sup> V. Barger and R. J. N. Phillips, Phys. Rev. Letters **20**, 564 (1968).

TABLE III. Values of the coefficients  $\sigma^{(i)}$  from the optical-theorem expression appropriate to the various elastic amplitudes; with  $s$  in  $\text{GeV}^2$ ,  $\sigma_{\text{tot}}$  in millibarns is given by  $-0.3893\pi \sum_i \sigma^{(i)} \tau^{(i)} \times [s^{\alpha(i)-1}]/\Gamma(\alpha(i))$ . The index  $(i)$  labels the Regge poles  $P$ ,  $P'$ ,  $\omega$ ,  $\rho$ , and  $A_2$ ;  $\tau^{(i)}$  denotes the signature, and  $\alpha(i)$  is the trajectory intercept at  $t=0$ . In meson-baryon scattering,  $\sigma^{(i)}=2M a'^{(i)}$  at  $t=0$ . [See Eq. (21) of the text for the definition of  $a'$ .] In Tables III(A)–III(C), the intercepts of the last four poles were fixed to be equal, and only the coefficients  $\sigma^{(i)}$  were varied. The quantities in Table III (D) were obtained by allowing the intercepts to vary also. The  $\chi^2$  on the four fits was 298, 231, 242, and 198, respectively, on 231 data points. Data on  $\sigma_{\text{tot}}$  and on the ratio  $\text{Re}/\text{Im}$  of the  $t=0$  amplitude were used.<sup>a</sup> The  $\rho$  and  $A_2$  couplings to  $N\bar{N}$  are not listed because they are very poorly determined. The  $\pi\pi$  couplings for  $P$  and  $P'$  have been determined by factorization arguments. Table III (E) presents the value of the ratio  $b/a'$  at  $t=0$ , where  $b$  and  $a'$  are defined in Eq. (20) of the text.

Pole	Intercept	$\sigma^{(i)}$			
		$\pi^-p \rightarrow \pi^-p$	$K^-p \rightarrow K^-p$	$p\bar{p} \rightarrow p\bar{p}$	$\pi^+\pi^- \rightarrow \pi^+\pi^-$
(A)					
$P$	0.99	-19.4	-15.4	-33.3	-11.3
$P'$	0.4	-33.3	-14.8	-75.2	-14.7
$\omega$	0.4	0.0	21.3	65.4	0.0
$\rho$	0.4	10.1	6.2	...	...
$A_2$	0.4	0.0	-4.4	...	0.0
(B)					
$P$	1.0	-17.2	-14.1	-30.1	-9.77
$P'$	0.5	-28.9	-12.5	-54.8	-15.2
$\omega$	0.5	0.0	12.8	39.4	0.0
$\rho$	0.5	6.1	3.7	...	...
$A_2$	0.5	0.0	-2.6	...	0.0
(C)					
$P$	1.0	-14.9	-12.7	-27.1	-8.1
$P'$	0.6	-25.6	-10.5	-41.2	-16.0
$\omega$	0.6	0.0	8.0	24.0	0.0
$\rho$	0.6	3.9	2.3	...	...
$A_2$	0.6	0.0	-1.7	...	0.0
(D)					
$P$	1.01	-15.2	-12.7	-26.0	-8.9
$P'$	0.59	-25.9	-12.2	-52.9	-12.7
$\omega$	0.43	0.0	17.7	55.4	0.0
$\rho$	0.59	4.1	2.4	...	...
$A_2$	0.40	0.0	-4.5	...	0.0
	Pole			$b/a'$	
(E)					
	$P, P',$ or $\omega$			$0.0 \leftrightarrow 3.0$	
	$A_2$ or $\rho$			$15.0 \leftrightarrow 30.0$	

<sup>a</sup> A. Citron *et al.*, Phys. Rev. **144**, 1101 (1966); W. Galbraith *et al.*, *ibid.* **138**, B913 (1965); K. J. Foley *et al.*, Phys. Rev. Letters **19**, 193 (1967); **19**, 622(E) (1967); **19**, 330 (1967); **19**, 857 (1967); A. N. Diddens *et al.*, Phys. Rev. **132**, 2721 (1963); D. V. Bugg *et al.*, *ibid.* **146**, 980 (1966); G. Bellettini *et al.*, Phys. Letters **14**, 164 (1965); **19**, 705 (1966); M. N. Kriesler *et al.*, Phys. Rev. Letters **20**, 468 (1968).

mined best from data on  $\sigma_{\text{tot}}$ ,<sup>21</sup> and the errors estimated from varying the intercepts over the range  $\alpha(0)=0.4-0.6$ . The values of  $b$  for  $\rho$  and  $A_2$  exchange are determined from fits to  $\pi N$  and  $KN$  charge-exchange data, which are dominated by the  $B$  amplitude; errors may be estimated from varying the parametrization of  $a'$  and from the effect of different methods of achieving the nonzero polarization in  $\pi N$  charge exchange. The values of  $b$  for the  $P'$  and  $\omega$  are essentially undetermined by

<sup>21</sup> V. Barger, in *Proceedings of the Topical Conference on High-Energy Collisions of Hadrons*, CERN, Geneva, 1968 (Scientific Information Service, Geneva, 1968).

the high-energy fits and are known only through the use of finite-energy sum rules (FESR).<sup>13,22</sup>

We list numerical values in Table III for the  $\pi N$  and  $KN$  couplings, with our estimates of the errors. Our isospin conventions are given in Appendix A.

We note, in passing, that the reduced residue of the Pomeranchukon is not particularly different from that of the  $P'$ . There is also no explanation of the fact that the ratio  $a'/\nu b$  for the  $P$  and  $P'$  is such that there is little or no  $\pi N$  polarization from their interference. These would not seem to be properties of two objects which the low-slope (or fixed-pole/cut)  $P$  models claim to be quite different entities.

### 3. Theoretical Interpretation

To summarize Sec. II A 1, we claim that there is already disagreement between theory and experiment and that a specific model, like the Veneziano form, can only make things worse. In any case, one must put a zero in the  $P'$ ,  $\omega$ ,  $A_2$ , and  $\rho$  residues in  $A$  and  $B$  at  $\alpha=0$ . We then have the two possibilities given below.

(a) *Model of Fig. 3(a)*. Here we arrange the values of  $A$  and  $B$ , for each pole, so that when  $A'$  is formed, the zero at  $t \approx -0.2$  ( $\text{GeV}/c$ )<sup>2</sup> will be generated. This, as described in Sec. II A 1, is superficially consistent with the  $s$ -channel resonances. The unobserved zero at  $-0.6$  ( $\text{GeV}/c$ )<sup>2</sup> in  $A'$  for  $\rho$  and  $\omega$  is deemed to be filled in by cuts. Similarly, the factorization crisis predicted by this model—a double zero at  $-0.2$  in  $p\bar{p}$  and  $\bar{p}p$  scattering rather than the desired single one—is cynically swept aside by not considering baryon-baryon reactions. Again, it may simply be that one should not try to enforce factorization in the narrow-resonance approximation, which violates explicit unitarity. This may be an important conclusion both for the problem of constructing Veneziano forms for more general amplitudes and also for dynamical attempts to generate the Regge poles associated by duality with the  $s$ -channel resonances. Finally, we note that Mandelstam's quark model<sup>7</sup> generates extra trajectories of the same intercept as the customary  $\rho$ ,  $\omega$ ,  $A_2$ , and  $P'$ , and it may be that these explain the lack of factorization observed for  $t \leq 0$ . We consider this extra-trajectory model in Sec. III but find it unattractive.

Having constructed the above solution, we can now allow exotic resonances, as does Wong,<sup>10</sup> and add the Pomeranchukon with slope  $\sim 1.0$ . One amusing possibility is that there is a limit in which the Pomeranchukon is exchange-degenerate with a trajectory of the  $\omega$  quantum numbers (perhaps one of the extra trajectories mentioned above in connection with factorization breakdown) and that unitarity forces  $\alpha_P(0)$  up to 1, breaking the exchange degeneracy.

<sup>22</sup> V. Barger and R. J. N. Phillips, Phys. Letters **26B**, 730 (1968); F. J. Gilman, H. Harari, and Y. Zarmi, Phys. Rev. Letters **21**, 323 (1968); H. Harari and Y. Zarmi, Weizmann Report, 1969 (unpublished).

TABLE IV. Positions of the zeros in the amplitudes  $A$ ,  $B$ , and  $A'$  prescribed by the angular functions associated with the various resonant states. All values are in units of  $(\text{GeV}/c)^2$ . (A) gives the values of  $t$  at the zero positions in  $\pi N$  elastic scattering; (B) gives the same for  $K N$  elastic scattering; (C) gives the values of  $u$  at the zero positions in  $\pi N$  elastic scattering.

	$A$			$B$			$A'$				
	(A)										
$P_{33}(1236)$	-0.44	...	...	2.31	...	...	4.73	-0.11	...	...	
$D_{15}(1680)$	-0.56	-1.65	...	2.69	-0.66	...	4.34	-0.28	-1.0	...	
$F_{37}(1950)$	-0.52	-1.45	-2.63	2.88	-0.63	-1.6	4.16	-0.26	-1.11	-1.93	
$F_{35}(1910)$	-0.6	-1.48	...	...	-0.52	-1.39	...	-0.2	-0.94	-1.71	
$N(938)$	...	...	...	...	...	...	0.04	...	...	...	
$D_{13}(1518)$	-0.44	...	...	-0.4	...	...	-0.17	-0.64	...	...	
$F_{15}(1688)$	-0.4	-0.99	...	-0.35	-0.94	...	-0.14	-0.64	-1.16	...	
$G_{17}(2190)$	-0.61	-1.7	-2.69	-0.51	-1.53	-2.58	-0.2	-0.98	-2.06	-2.92	
	(B)										
$P_{13}(1385)$	-0.38	...	...	2.37	...	...	4.67	0.06	...	...	
$D_{15}(1765)$	-0.45	-1.53	...	2.72	-0.51	...	4.32	-0.22	-0.79	...	
$F_{17}(2030)$	-0.48	-1.33	-2.54	2.89	-0.58	-1.45	4.15	-0.23	-1.0	-1.76	
$\Lambda(1116)$	...	...	...	...	...	...	0.36	...	...	...	
$D_{03}(1520)$	-0.12	...	...	-0.12	...	...	-0.05	-0.18	...	...	
$F_{05}(1815)$	-0.35	-0.87	...	-0.31	-0.84	...	-0.13	-0.57	-1.03	...	
$G_{07}(2100)$	-0.43	-1.2	-1.91	-0.37	-1.1	-1.85	-0.15	-0.71	-1.48	-2.09	
	(C)										
$P_{33}(1236)$	0.71	...	...	...	...	-2.0	0.38	...	...	-4.46	
$D_{15}(1680)$	0.64	-0.45	...	-0.35	...	-3.7	0.01	-0.73	...	-5.35	
$F_{37}(1950)$	0.66	-0.52	-1.44	-0.37	-1.33	-4.84	-0.04	-0.85	-1.71	-6.13	
$F_{35}(1910)$	...	-0.26	-1.14	-0.35	-1.22	...	-0.02	-0.8	-1.53	...	
$N(938)$	...	...	...	...	...	...	0.88	...	...	...	
$D_{13}(1518)$	-0.06	...	...	-0.09	...	...	0.14	-0.33	...	...	
$F_{15}(1688)$	-0.07	-0.66	...	-0.11	-0.7	...	0.1	-0.42	-0.92	...	
$G_{17}(2190)$	-0.31	-1.3	-2.39	-0.42	-1.47	-2.48	-0.08	-0.94	-2.01	-2.8	

(b) *Model of Fig. 3(b)*. Here, one would not try to associate the  $t \approx -0.2$   $(\text{GeV}/c)^2$  zero with Regge poles. We remember that it is only the higher-spin members of a baryon tower that have this zero. Then, cuts (absorption effects) will tend to suppress the lower partial waves, leaving the higher partial waves, and hence the  $-0.2$  zero, more pronounced in the real world than in the Veneziano limit. We will find in Sec. III that most simple series of beta functions correspond to this possibility and not to (a). As we can see from the values of  $a'/\nu b$  in Table III, if  $a$  and  $b$  are constant in  $t$  (as is true in the simplest Veneziano parametrization), then only for the  $\rho$  and  $A_2$  will the very small ratio  $a'/\nu b$  lead to the  $-0.2$  zero: here, coming from the  $4M^2-t$  factor in the definition of  $a'$ ,

$$a' = a + 2Mb/(4M^2 - t).$$

Any correspondence between the crossover zero and the  $s$ -channel resonances is reduced to the level of an accident: The resonances have a zero at  $t \approx -0.2$   $(\text{GeV}/c)^2$  in  $A + \nu B/2M$  ( $= A'$  at  $t=0$ ) whose asymptotic limit  $a + b/2M$  would have no zero for constant  $a$  and  $b$ .

## B. Baryon Spectrum and $t$ Dependence of $A$ and $B$ at Resonance Pole

Perhaps owing to our more detailed knowledge from phase shifts, the baryon spectrum appears to be more complicated than that of the mesons. We must consider both the internal symmetry ( $SU_2$  or  $SU_3$ ) and the spin-parity structure of these resonances.

### 1. Exchange Degeneracy—Internal Symmetry

Many authors have considered the consequences of exchange degeneracy.<sup>23</sup> In  $\bar{K}N$  scattering, there is a rather exact degeneracy between the  $I=0$   $SU_3$  partners of the  $N$  and the  $N_\gamma$ , and between the  $I=1$   $SU_3$  partners of the  $\Delta$  and the  $D_{15}$  ("parity partner of the nucleon's first recurrence"). Such a degeneracy is, of course, a minimum prerequisite for the successful application of the Veneziano form to  $\bar{K}N$  scattering, but also suggests that we should treat the  $N/N_\gamma$  and the  $\Delta/D_{15}$  pairs of trajectories symmetrically in other  $SU_3$ -related reactions (such as  $\pi N$  scattering itself) where the mass degeneracy is not apparent. Similarly,  $\pi\Sigma$  scattering

<sup>23</sup> C. Schmid, Nuovo Cimento Letters 1, 165 (1969).

TABLE V. Values of the contributions at  $t=0$  to the amplitudes  $A$ ,  $B$ , and  $A'$  of the same resonances listed in Table IV. The normalization is arbitrarily adjusted such that  $\alpha_L^J = +1$  (or  $-1$  if the state is below threshold);  $\alpha_L^J$  is defined in Eq. (A5): (A)  $\pi N$  elastic scattering; (B)  $KN$  elastic scattering.

	$A$	$B$	$A'$
(A)			
$P_{33}(1236)$	177	-429	33
$D_{15}(1680)$	275	-204	67
$F_{37}(1950)$	468	-238	104
$F_{35}(1910)$	-358	309	76
$N(938)$	0	+1210	-13
$D_{13}(1518)$	-226	358	41
$F_{15}(1688)$	-400	448	68
$G_{17}(2190)$	-551	322	117
(B)			
$P_{13}(1385)$	305	-808	-37
$D_{15}(1765)$	352	-265	71
$F_{17}(2030)$	529	-263	109
$\Lambda(1116)$	-24	+132	-15
$D_{03}(1520)$	-728	1218	41
$F_{05}(1815)$	-509	503	73
$G_{07}(2100)$	-662	442	113

contains two channels  $\pi^- \Sigma^+ \rightarrow \pi^- \Sigma^+$  and  $\pi^- \Sigma^+ \rightarrow \pi^+ \Sigma^-$ , which have only  $s$ - $t$  and  $s$ - $u$  terms, respectively. Here, exchange degeneracy is required in the Veneziano approach, but in nature it does not appear to be quite as precise as in  $\bar{K}N$  scattering.

## 2. Spin-Parity Structure

As emphasized by Harari<sup>24</sup> and by Mandelstam,<sup>7</sup> the nonrelativistic quark model appears to predict the observed states very well. The  $S$  wave ( $56, 0^+$ ), the  $P$  wave ( $70, 1^-$ ), and  $D$  wave ( $56, 2^+$ ) are evident. Furthermore, there is a radial excitation, another ( $56, 0^+$ ). Unfortunately, such a structure is manifestly inconsistent with any simple model that incorporates analyticity at  $u=0$ : MacDowell symmetry predicts unobserved parity-doubled states for the leading trajectory. Similarly, the theoretical and experimental structure of the daughters will be in disagreement. We do not know of any fundamental solution to this problem, but will instead adopt a phenomenological approach.

Dolen, Horn, and Schmid<sup>8</sup> emphasized the correlation between the zeros of the  $t$ -channel Regge-pole residues and those of the  $s$ -channel resonance contributions. In Table IV, for some of the low-lying resonances in  $\pi N$  and  $KN$  scattering, we give the  $t$  and  $u$  positions of the zeros of  $A$ ,  $A'$ , and  $B$ . We observe that all three show interesting systematic effects. The  $\Delta$  trajectory has zeros in  $A$  at  $t \sim -0.6, -1.6, \dots$ , and in  $B$  at  $t \sim 2.5,$

$-0.6, -1.6, \dots$ . The  $D_{15}$  has a similar zero structure, supporting its classification as exchange-degenerate with the  $\Delta$ . The zeros for  $t < 0$  can be obtained from the  $\Gamma^{-1}(+\alpha_\rho) = 0$  factor in the Veneziano form, whereas the  $t \sim 2.5$  zero in  $B$ , crucial in ensuring, as experimentally observed, that the  $\Delta$  have no daughter, must be explicitly put in by hand, i.e., by writing

$$\frac{\Gamma(l' - \alpha_\rho(t)) \Gamma(m - \bar{\alpha}_\Delta(s))}{\Gamma(m' - \alpha_\rho(t) - \bar{\alpha}_\Delta(s))} (t - 2.5).$$

The nucleon and  $N_\gamma$  contributions seem consistent with just the zeros from  $[\Gamma(\alpha_\rho)]^{-1}$ . One may investigate the zero structure in various  $SU_3$ -related reactions to see if they change according to the precise value of the intercept of the  $t$ -channel pole. In  $\pi N \rightarrow K\Lambda$  (or  $\rightarrow K\Sigma$ ), for instance, the zero at  $t \sim -0.6$  moves to  $\sim -0.4$ , which correlates with a break in the high-energy cross section at this value and suggests a value of  $\alpha_{K^*}(0) \simeq 0.4$  [ $K^*(890)$  or  $K^*(1400)$ ].

The approximate matching of the zeros of the Veneziano form and those of the experimentally prominent resonances eliminates unobserved daughters of large width. However, one still must ensure that  $A$  and  $B$  (and hence  $A'$ ) have the right relative magnitude. We thus list in Table V the relative values of  $A$ ,  $B$ , and  $A'$  at  $t=0$  for our resonances. We note that  $A'$  is often much smaller than  $A$  or  $B$ , and this goes hand in hand with the celebrated "crossover" zero in  $A'$  near  $t \sim -0.2$ , discussed in the previous section. The over-all magnitude (i.e., width) of the resonance is best handled by the plots in Sec. II C.

Finally, we remark on the systematics of the  $u$  zeros which are useful for constructing  $s$ - $u$  terms. The  $\Delta$  family has, in  $B$ , one scurrilous zero at a  $u$  value corresponding to the  $t \sim 2.5$  zero, in addition to the regular family at  $u \sim -0.4, -1.4, \dots$ . The latter are presumably associated with some linear combination of zeros from  $\Gamma^{-1}(+\bar{\alpha}_N)$ ,  $\Gamma^{-1}(+\bar{\alpha}_{N_\gamma})$ , and  $\Gamma^{-1}(-1 + \bar{\alpha}_\Delta)$ . The existence of more than one  $u$ -channel trajectory clearly complicates the problem. The  $\Delta$  family in  $A$  has the same  $u \sim -0.4, -1.4$  series, plus another single zero at  $u \sim 0.7$ , approximately the nucleon position. The association of this zero with the nucleon is supported by a similar analysis of  $\pi\Sigma$  elastic scattering, where the corresponding zero becomes  $u \sim 1.2 \sim m_{\Sigma, \Lambda}^2$ . Such a correlation implies a particular relation between the  $SU_3$  mass splitting of the external and internal particles.

The nucleon family has the same structure in  $A$  and  $B$ , with a rough zero sequence  $u \sim -0.2, -1.2, \dots$ .

## C. General Expression for Baryon Residue Functions

In this section we present the general parametrization for the elastic widths of resonances on the parent baryon trajectories and for the backward-angle differential cross section, as prescribed by the Veneziano-model expansion of the amplitudes. The parametrization is the product of

<sup>24</sup> H. Harari, in *Proceedings of the Fourteenth International Conference on High-Energy Physics, Vienna, 1968* (CERN, Geneva, 1968), p. 195.

an essentially kinematical factor times an energy-dependent polynomial controlled by the constants which multiply the various beta-function terms in the Veneziano expansions (3). Less complete but similar discussions were given previously by Amann<sup>6</sup> and Virasoro.<sup>6</sup> We then treat the experimental data in analogous fashion; after dividing empirical resonance widths by the above-mentioned kinematical factor, we present the resulting reduced widths as a function of resonance mass. The energy dependence of this reduced residue function, coupled with information on the residue culled from backward-scattering data, should enable one to judge how many terms are required in the polynomial, and thus to estimate the complexity required in a Veneziano parametrization of meson-baryon scattering.

We begin by extracting from Eq. (3) only those terms which contribute to the widths of resonances on the general baryon parent trajectory  $\alpha_B(u)$ ; the required terms are those from the second summation with  $g=i$  and those from the third with  $p=r$ . We note that this set of terms also supplies the leading Regge behavior  $s^{\alpha_B(u)-1/2}$  for large  $s$  at fixed  $u$ . Denoting this part of the amplitude  $A^{(l)}$ , we have

$$A^{(l)} = \sum_{q=0,1,2,\dots} \left\{ \sum_{M;p \geq q} E_A^{(l)}(p,q,M) \frac{\Gamma(p-\alpha_M(t))\Gamma(q-\bar{\alpha}_B(u))}{\Gamma(p-\alpha_M(t)-\bar{\alpha}_B(u))} + \sum_{B1;g \geq q} D_A^{(l)}(g,q,B1) \times \frac{\Gamma(g-\bar{\alpha}_{B1}(s))\Gamma(g-\bar{\alpha}_B(u))}{\Gamma(g-\bar{\alpha}_{B1}(s)-\bar{\alpha}_B(u))} \right\}. \quad (22)$$

For convenience in what follows, we define

$$\mathcal{Q}_{qt}^{(l)} = (-1)^q \sum_{M;p \geq q} E_A^{(l)}(p,q,M), \quad (23)$$

$$\mathcal{Q}_{qs}^{(l)} = (-1)^q \sum_{B1;g \geq q} D_A^{(l)}(g,q,B1). \quad (24)$$

Similar quantities  $\mathcal{B}_{qt}^{(l)}$  and  $\mathcal{B}_{qs}^{(l)}$  are understood as appropriate for the  $B^{(l)}(s,t,u)$  amplitudes. We remind the reader that the second summation in Eq. (22) vanishes for kaon-nucleon scattering, whereas, in pion-nucleon scattering, signature is obtained by imposing  $\mathcal{Q}_{qt}^{(l)} = \tau \mathcal{Q}_{qs}^{(l)}$ , where  $\tau = +1$  for  $N_\alpha$  and  $\tau = -1$  for  $N_\gamma$  and  $\Delta_\delta$ .

In the limit  $\bar{\alpha}_B(u) \rightarrow k = J - \frac{1}{2}$ , where  $J$  is the total spin of the resonance, we again retain only terms contributing to widths of resonances on the parent trajectory and, after setting

$$(bt)^k \sim (2q_{c.m.}{}^2 z b)^k \sim (4q_{c.m.}{}^2 b)^k \frac{[\Gamma(k+1)]^2}{\Gamma(2k+1)} P_k(z),$$

we derive

$$A^{(l)} \sim \frac{b^{J-3/2} (4q_{c.m.}{}^2)^{J-1/2} \Gamma(J+\frac{1}{2})}{(M_J^2 - u) \Gamma(2J)} P_{J-1/2}(z) \times \sum_{q \leq J-1/2} c_{qJ} [\mathcal{Q}_{qt}^{(l)} + (-1)^{J-1/2} \mathcal{Q}_{qs}^{(l)}], \quad (25)$$

where

$$c_{qJ} = 1, \quad q=0 \\ = 0, \quad q > J - \frac{1}{2} \\ = \prod_{i=1}^q (J + \frac{1}{2} - i), \quad 1 \leq q \leq J - \frac{1}{2} \quad (26)$$

and  $b$  denotes the slope of the trajectory,  $\alpha_B(u) = \alpha_B(0) + bu$ . Note that one may express  $c_{qJ}$  in terms of  $M_J$ , using  $J = \alpha_B(0) + bM_J^2$ .

After employing the formulas of Appendix A, one obtains the elastic widths of the two parity states at a given  $J$ :

$$\Gamma_{J\pm}^{(l)} = \pm (E_u \pm M) K(J) \gamma^{(l)}(\pm M_J), \quad (27)$$

where the essentially kinematic factor is given by

$$K(J) = \frac{(4b)^{J-3/2} \Gamma(J+\frac{3}{2})}{\pi M_J^2 \Gamma(2J+2)} q_{c.m.}{}^{2J} \quad (28)$$

and

$$\gamma^{(l)}(M_J) = \sum_{q \leq J-1/2} c_{qJ} \times \{ -(M_J - M) [\mathcal{B}_{qt}^{(l)} + (-1)^{J-1/2} \mathcal{B}_{qs}^{(l)}] [\mathcal{Q}_{qt}^{(l)} + (-1)^{J-1/2} \mathcal{Q}_{qs}^{(l)}] \}. \quad (29)$$

In Eq. (27), the  $+$  ( $-$ ) sign is appropriate for states with  $\tau P = -1$  ( $+1$ ), where  $P$  is the parity of the state,  $P = -(-1)^L$ .

For pion-nucleon scattering, employing Eq. (A14), one derives  $A_u^{(+)} = 2A_u^{(-)}$  at the  $I = \frac{3}{2}$  resonance poles and  $A_u^{(+)} = -A_u^{(-)}$  at the  $I = \frac{1}{2}$  resonance poles. Therefore, combining these results with the signature requirement, one reduces Eq. (29) to

$$\gamma^{(l)}(M_J) = 3(-1)^{J+1/2} [1 + \tau(-1)^{J-1/2}] \times \sum_{q \leq J-1/2} c_{qJ} [\mathcal{Q}_{qt}^{(-)} - (M_J - M) \mathcal{B}_{qt}^{(-)}]. \quad (30)$$

For kaon-nucleon scattering, the absence of  $(s,u)$  terms in the Veneziano expansion leads to the reduction

$$\gamma^{(l)}(M_J) = \sum_q c_{qJ} [\mathcal{Q}_{qt}^{(l)} - (M_J - M) \mathcal{B}_{qt}^{(l)}]. \quad (31)$$

The constants  $\mathcal{Q}$  and  $\mathcal{B}$  in these equations are obviously different for each trajectory considered; however, if one wishes to fit simultaneously the resonance widths of all trajectories in  $\pi N$  scattering, say, then definite constraints exist between the sets  $(\mathcal{Q}, \mathcal{B})$  for the different

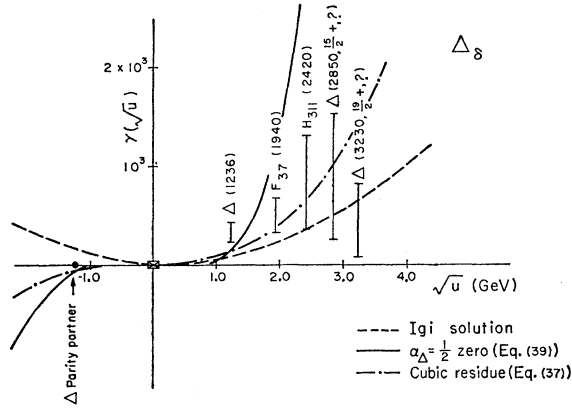


FIG. 4. Reduced residue function for the  $\Delta_8$  trajectory in  $\pi N$  scattering. The quantity is defined in Eqs. (27) and (30) of the text. The bracketed empirical values were extracted from listed elastic widths (Ref. 25); the brackets show the spread determined by varying the trajectory slope from 0.9 to 1.0  $\text{GeV}^{-2}$  and the resonance position from  $M_R + \frac{1}{4}\Gamma_{\text{tot}}$  to  $M_R - \frac{1}{4}\Gamma_{\text{tot}}$ , where  $M_R$  and  $\Gamma_{\text{tot}}$  are the tabulated (Ref. 25) resonance mass and total widths, respectively. The  $\times$  at  $u^{1/2}=0$  denotes the value obtained from  $\pi^-p$  backward elastic scattering fits (Ref. 27). The dashed curve was obtained using Igi's parametrization (Ref. 6) of  $\pi N$  scattering based upon the Veneziano model. The dot-dashed curve (cubic) and the solid curve ( $\alpha_\Delta = \frac{1}{2}$  zero) result from the parametrizations discussed in Sec. II D of the text, Eqs. (37) and (39), respectively.

trajectories, as can be seen by examining the connection between Eqs. (3) and (22).

Some elementary deductions based on these expressions relate to the positivity of widths. Because  $\gamma^{(l)}(M_J)$  and  $-\gamma^{(l)}(-M_J)$  are proportional to the elastic widths of the two parity states, respectively, at a given  $J$ , and because, in the definition of  $\gamma$ ,  $c_{qJ} \sim J^q \sim M_J^{2q}$  for large  $J$ , it is evident that to enforce positivity for both parity states, then  $\mathcal{B}_{qt} \neq 0$  if  $\mathcal{A}_{qt} \neq 0$ . Indeed,  $\mathcal{B}_{qt}$  must grow approximately as fast as  $\mathcal{A}_{qt}/M_J$ . The absence of

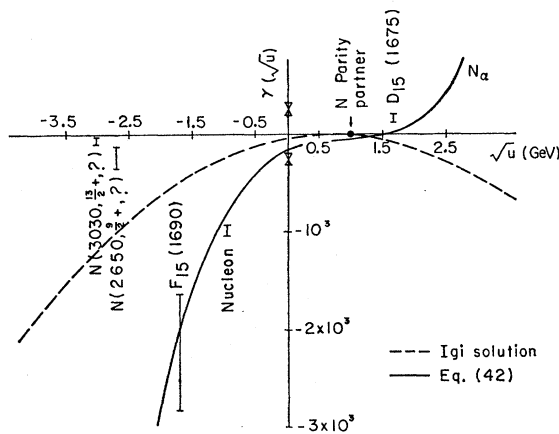


FIG. 5. Reduced residue function for the  $N_\alpha$  trajectory in  $\pi N$  scattering. The description in the caption for Fig. 4 applies here also. Two backward-scattering data points appear, reflecting the sign uncertainty of the fits in Ref. 27. The dashed curve was computed from Igi's parameters (Ref. 6); note that the parity-partner states in his solution ( $u^{1/2} > 0$ ) will have negative elastic widths. The solid curve displays the fit obtained in this paper, as discussed in Sec. II D.

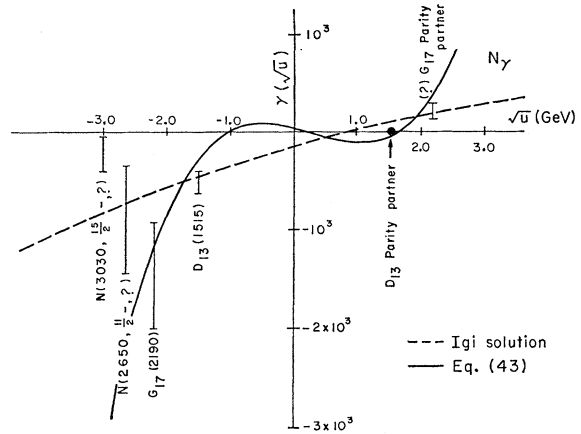


FIG. 6. Reduced residue function for the  $N_\gamma$  trajectory. For the purposes of this plot, the unobserved parity-partner states of the  $G_{17}$  and  $D_{13}$  were assigned elastic widths equal to those of the observed  $\tau P = +1$  states. The meaning of the curves is the same as for Fig. 5; see the caption of Fig. 4 for the definition of the brackets.

parity doubling for the nucleon is assured by setting  $\mathcal{A}_{0t}^{(-)} = 0$  in Eq. (30) for that trajectory. To rigorously eliminate parity doubling of the first states on the  $\Delta_8$  and  $N_\gamma$  trajectories, one must impose the linear relationships

$$\sum_{q=0}^1 \mathcal{A}_{qt}^{(-)} = -(M_\Delta + M) \sum_{q=0}^1 \mathcal{B}_{qt}^{(-)}$$

and

$$\sum_{q=0}^1 \mathcal{A}_{qt}^{(-)} = (M_{D_{13}} - M) \sum_{q=0}^1 \mathcal{B}_{qt}^{(-)},$$

respectively; however, the kinematical factor  $E_u - M$  in Eq. (27) naturally makes the elastic widths of all parity-partner states of the  $\Delta_8$  trajectory small. In fact, the elastic width of the  $\Delta(1238)$  parity partner tends to be two orders of magnitude smaller than that of the  $\Delta$  itself, and so one may elect to relax rigorous elimination for that trajectory. A similar argument applies to the  $\Delta$ 's  $SU(3)$  partner  $Y_1^*$  in kaon-nucleon scattering. This kinematic suppression may not be relevant, for we judge that the Veneziano expression should be constructed so as to fit the invariant amplitudes and not the partial-wave amplitudes. It is these latter which are most subject to the possibly large unitarity effects not present in the model.

The experimental widths of the known baryon trajectories should provide a means for estimating the number of terms required in the summations of Eqs. (29)–(31). We have therefore computed the empirical values for  $\gamma^{(l)}(M_J)$  by inserting the known values<sup>25</sup> of  $\Gamma_{el}$  for the left-hand side of Eq. (27). These are shown for the  $N$ ,  $\Delta$ ,  $\Lambda$ , and  $\Sigma$  trajectories in Figs. 4–9. In obtaining the plotted values, we allowed the value of the empirical resonance mass<sup>25</sup> to vary from  $M_J - \frac{1}{4}\Gamma_{\text{tot}}$

<sup>25</sup> Particle Data Group, Rev. Mod. Phys. 41, 109 (1969).

to  $M_J + \frac{1}{2}\Gamma_{tot}$  and the trajectory slope  $b$ , to run over the range  $0.9 \leq b \leq 1.0$ ; this explains the brackets shown in the figures.

Both parity states, where available, are given on the same graph. We note the absence of candidates for parity-doubled status with the  $\Delta_8$  resonances. We suggest that this absence of parity doubling, generally, may well be a unitarity effect, especially strong for states near threshold; higher along the trajectory, the MacDowell-symmetry analyticity constraint should reassert itself, and parity doubling would be restored.

The graphs indicate no dramatic structure in  $\gamma(u^{1/2})$  but certainly allow considerable flexibility in possible parametrizations. It appears that the sums in Eqs. (30) and (31) can safely be terminated after two or three terms. The systematic structure of the plots for the  $N_\alpha$  and  $N_\gamma$  trajectories and, to a lesser extent, that for the  $\Delta$  trajectory residue suggest that the experimentally determined elastic widths for the high-spin objects on these trajectories could be too small by as much an error as a factor of 4. In this connection, it is significant to recall that, in general, the determinations for elastic widths obtained from backward-scattering data are significantly larger than those derived from the forward data.<sup>26</sup>

Backward-scattering ( $u=0$ ) data points are also given in the figures because the differential cross sections for  $s \rightarrow \infty$  at fixed  $u$  are also determined by the same function,  $\gamma$ . Indeed, as  $s \rightarrow \infty$  for fixed  $u$ , Eq. (22) becomes [with  $c_{q\alpha}$  given by (26) after replacement of  $J$  by  $\alpha$ ]

$$A_B^{(I)} \rightarrow \frac{\pi (bs)^{\alpha_B - 1/2}}{\cos \pi \alpha_B(u) \Gamma(\alpha_B(u) + \frac{1}{2})} \times \sum_q c_{q\alpha} [\alpha_{qt}^{(I)} + i e^{-i\pi \alpha_B} \alpha_{qs}^{(I)}]. \quad (32)$$

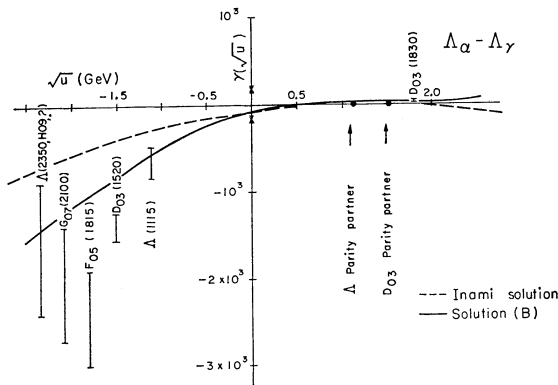


FIG. 7. Reduced residue function for the  $\Lambda_\alpha$ - $\Lambda_\gamma$  exchange-degenerate trajectory pair. The bracketed quantities are defined in the caption to Fig. 4. The backward datum point (X) comes from Ref. 48;  $g_{\Lambda KN}^2/4\pi$  was taken to be  $14 \pm 3$ . The dashed curve was computed using the solution given by Inami (Ref. 6), and the solid curve using the parameters of our solution (II), given in Sec. III D.

<sup>26</sup> See the detailed data-card listings in Ref. 25 for the various determinations of the widths of the baryon states.

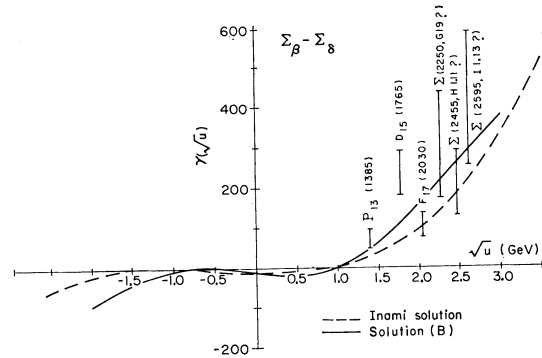


FIG. 8. Reduced residue function for the  $\Sigma_8$ - $\Sigma_8$  exchange-degenerate trajectory pair. The bracketed quantities are defined in the caption to Fig. 4. Parity-partner states of the same elastic width as the corresponding observed states ( $u^{1/2} > 0$ ) would have values of  $\gamma(u^{1/2}) < -10^3$ . The bracketed values for the  $P_{13}(1385)$  were found from  $SU_3$  applied to the  $\Delta(1238)$ . As discussed in the text, the backward datum point is too uncertain to be placed on the graph. The curves have the same meaning as those in Fig. 7.

In the pion-nucleon situation, upon forming  $\tilde{f}(u^{1/2})$  and employing isospin and signature relations, one derives

$$\tilde{f}^{(I)}(u^{1/2}) = \frac{\pi(1+i\tau e^{-i\pi\alpha_B})(bs)^{\alpha_B-1/2}}{2 \cos \pi \alpha_B(u) \Gamma(\alpha_B + \frac{1}{2})} \gamma^{(I)}(u^{1/2}), \quad (33)$$

where

$$\gamma^{(I)}(u^{1/2}) = 3(-1)^{I+1/2} \times 2 \sum_q c_{q\alpha} [\alpha_{qt}^{(-)} - (u^{1/2} - M) \alpha_{qt}^{(-)}]. \quad (34)$$

The isospin index  $I$  is the total isospin in the exchange ( $u$ ) channel. The similarity to Eq. (30) is obvious and shows how the reduced residue function parametrizes both the widths of resonance spectrum and the backward-scattering region in a uniform fashion.

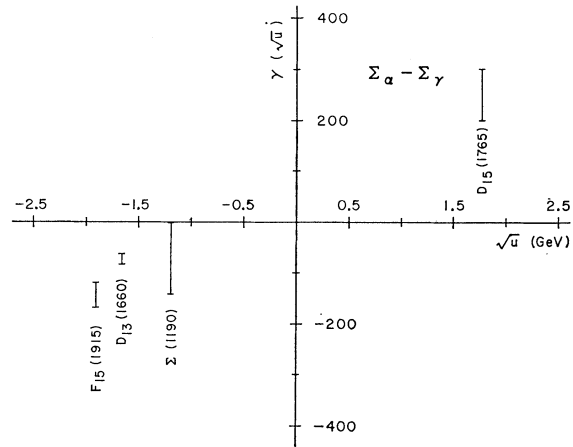


FIG. 9. Reduced residue function for the  $\Sigma_\alpha$ - $\Sigma_\gamma$  exchange-degenerate trajectory pair. The bracketed quantities are defined in the caption to Fig. 4. The data come from Ref. 25 and from Armenteros *et al.* [Phys. Letters **28B**, 521 (1969)];  $g_{\Sigma KN}^2/4\pi$  was taken to lie between 0 and 3.



For purposes of comparison, we point out that in their phenomenological fits, Barger and Cline<sup>27</sup> have retained only the factor  $(\alpha_B + \frac{1}{2})(\alpha_B + \frac{3}{2})$  from  $\Gamma^{-1}(\alpha + \frac{1}{2})$  and used a parametrization

$$\gamma^{(t)}(u^{1/2}) = \beta(1 + \delta u^{1/2})(1/s_0)^{\alpha_B - 1/2},$$

with  $\beta$  and  $\delta$  constants. Similarly restricting the  $\gamma(u^{1/2})$  of Eq. (34) to terms at most linear in  $u^{1/2}$  for all trajectories (i.e.,  $q < 1$  in the sum) has, among other things, the consequences of removing all  $N_\alpha$  terms from  $A(s, t, u)$ , decoupling the  $\Delta_\delta$  and  $N_\gamma$  trajectory terms at  $s \rightarrow \infty$  for fixed  $t$ , and thus forcing  $A$  to have the asymptotically nonleading behavior  $s^{\alpha_M(t)-1}$ . Because all baryon trajectories must couple asymptotically at  $t=0$  (see Sec. II A), a consistent solution thus requires  $q \geq 1$  and, therefore, residue functions at least cubic in  $u^{1/2}$ . The term with  $q=0$  seems strongly demanded at least for the  $\Delta$  trajectory by the nearly linear form of the residue shown in Fig. 4.

The salient features of the parametrization given in Eqs. (33) and (34) are the factor  $\Gamma^{-1}(\alpha_B + \frac{1}{2})$  and the absence of any exponential type of form factor in  $u^{1/2}$ . It is of considerable importance to check whether this latter feature is supportable experimentally because, if correct, it provides the important possibility of extrapolating from the scattering region to distant poles. Except for the well-known dip near  $\alpha_N = -\frac{1}{2}$ , there is little evidence experimentally for the differential cross-section dips predicted by the factor  $\Gamma^{-1}(\alpha_B + \frac{1}{2})$ ; in particular, the absence of the asserted dip near  $\alpha_\Delta = -\frac{3}{2}$  has been the cause of some consternation for standard Regge-pole-theory fits.<sup>27,28</sup> However, it should be noted that all but the  $\alpha_N = -\frac{1}{2}$  dip occur at fairly large values of  $u$ , where secondary-trajectory or cut mechanisms are presumably important.

We have attempted to test whether the Veneziano parametrizations for the resonance widths on a given parent trajectory and for that portion of  $d\sigma/du$  attributable to the trajectory are consistent. This is discussed in the following subsection.

#### D. Pion-Nucleon Backward Scattering and Resonance Widths

In general, the Regge-pole model asserts the intimate connection between the baryon resonances ( $u > 0$ ) and the baryon exchange amplitude in the region of backward scattering ( $u < 0$ ). This connection is established via the trajectory function  $\alpha(u^{1/2})$  and its reduced residue function  $\gamma(u^{1/2})$ . However, classical Regge-model fits to either the backward- or the forward-angle scattering data could never be extrapolated reliably to the poles at  $u$  or  $t > 0$  because of the essentially arbitrary nature of the residue function. The Veneziano model, by specifying both the  $\Gamma^{-1}(\bar{\alpha}+1)$  factor and the scale

factor  $s_0$ , provides a general prescription for pole extrapolation. Hence, it becomes important to test this recipe in those cases where we know both the values of the physical pole residues and the details of the scattering data controlled by the corresponding Regge trajectory. In this section, we examine the success of the Veneziano-model prescription for the  $\Delta$ ,  $N_\alpha$ , and  $N_\gamma$  trajectories in  $\pi N$  scattering. This examination is only a limited test of the model in the sense that the forward-angle data are ignored for the time being, as are the relationships which must exist between the constants appearing in the residue functions for the different baryon trajectories. If reasonable agreement with the baryon residue function aspect is achieved, these other problems could be attacked subsequently.

Restricting ourselves to reduced residue functions with only four parameters, e.g., rewriting Eq. (34) as

$$\gamma(u^{1/2}) = a_R + b_R u^{1/2} + c_R u + d_R u^{3/2}, \quad (35)$$

we find that our best solution in the case of the  $\Delta_\delta$  trajectory yields a  $\Delta(1238)$  width too small by a factor of 2. For the  $N_\alpha$  and  $N_\gamma$  situations, the problem is much less constrained, and we can achieve solutions in agreement with both backward data and baryon resonance widths.

##### 1. $\Delta$ Residue

We begin by discussing the  $\Delta_\delta$  because it is presumably the sole contributor to  $\pi^- p$  backward scattering and because several resonance widths are well determined, as shown in Fig. 4. Many difficulties have been encountered in previous Regge-pole-theory fits<sup>27-30</sup> to  $\pi^- p$  data; these include the anomalously small value of the cross section at  $u=0$ , the absence of a dip near  $\alpha_\Delta = -\frac{3}{2}$ , discussed in the previous section, and the considerable discrepancy with respect to pole extrapolation. To these, we would add another uncertainty: We have extracted an effective trajectory for the available  $\pi^- p$  backward data<sup>31</sup>; this is displayed in Fig. 10. The effective trajectory appears to deviate substantially, for  $u < -0.2$  ( $\text{GeV}/c$ )<sup>2</sup>, from the linear form with slope near unity, expected from drawing a line through the  $\Delta_\delta$  resonance spectrum. Nevertheless, we sought a fit to the  $\pi^- p$  backward elastic data using the full Regge-pole formulation and a  $\Delta_\delta$  trajectory of variable slope. Retaining only data having  $u > -0.75$  ( $\text{GeV}/c$ )<sup>2</sup>, we found that the  $\chi^2$  values did not significantly change as the slope was varied over the range

<sup>29</sup> K. Igi, S. Matsuda, Y. Oyanagi, and H. Sato, Phys. Rev. Letters **21**, 580 (1968).

<sup>30</sup> C. B. Chiu and J. Stack, Phys. Rev. **153**, 1575 (1967).

<sup>31</sup> The data we used are, for  $\pi^\pm p$  backward elastic, C. T. Coffin *et al.*, Phys. Rev. **159**, 1169 (1967); J. Orear *et al.*, *ibid.* **152**, 1162 (1966); S. W. Kormanyos *et al.*, Phys. Rev. Letters **16**, 709 (1966); J. Orear *et al.*, *ibid.* **21**, 389 (1968); W. F. Baker *et al.*, Phys. Letters **28B**, 291 (1968); E. W. Anderson *et al.*, Phys. Rev. Letters **20**, 1529 (1968); for  $\pi^- p \rightarrow \pi^0 n$ , R. C. Chase *et al.*, *ibid.* **22**, 1137 (1969); V. Kistiakowsky *et al.*, *ibid.* **22**, 618 (1969); J. Schneider *et al.*, in *Proceedings of the Fourteenth International Conference on High-Energy Physics, Vienna, 1968* (CERN, Geneva, 1968).

<sup>27</sup> V. Barger and D. Cline, Phys. Rev. **155**, 1792 (1967); Phys. Rev. Letters **19**, 1504 (1967); **21**, 392 (1968); **21**, 1132(E) (1968).

<sup>28</sup> E. Paschos, Phys. Rev. Letters **21**, 1855 (1968).

0.3–1.0 (GeV/c) $^{-2}$ . The  $\Delta_8$  trajectory is evidently poorly specified from the backward data. [We note that the *systematic* errors quoted on the experimental data<sup>31</sup> are rather large. In our analysis, we have allowed for this feature, assuming it to be an effect independent of  $u$ . Because this systematic error feature is as important to the process of obtaining a good fit as is the variation of the  $\Delta$  trajectory slope, we feel that shrinkage (or its absence) in the data is yet to be demonstrated.]

The very small size of the  $\pi^-p$  cross section in the backward direction provides the essential constraint in the problem of finding a suitable  $\gamma_\Delta(u^{1/2})$ . These data in fact require that both  $\gamma_\Delta$  and  $d\gamma_\Delta/d(u^{1/2})$  near  $u=0$  be *two* orders of magnitude smaller than the appropriate pole value,  $\gamma_\Delta(1.238 \text{ GeV})$ . That the derivative must be so small can be appreciated by examining Eq. (A10) near the backward direction for large  $s$ :  $d\sigma/du \propto |A'|^2 + \frac{1}{4} \sin^2\theta |B|^2$ , where  $\theta$  is the direct-channel center-of-mass scattering angle. Because the variation of  $d\sigma/du$  away from  $\cos\theta = -1$  is slight,  $|B|$  cannot be large. However, the contributions of the  $B$  amplitude to  $\gamma(u^{1/2})$ , Eq. (34), enter multiplied by the factor  $u^{1/2} - M$ , and so the magnitude of  $B$  near  $u=0$  is essentially the derivative  $d\gamma_\Delta/du^{1/2}$  there.

In order to proceed, we appropriated a  $\Delta$  trajectory linear in  $u$ , passing through the resonance positions (slope  $\approx 0.9$ ), and sought forms for  $\gamma_\Delta(u^{1/2})$  which would yield sensible agreement with both the backward-angle  $\pi^-p$  data and the reduced residues in the resonance region. Although a residue of the form  $a_\Delta + b_\Delta u^{1/2}$  would seem acceptable from a first glance at Fig. 4, it is ruled out by the considerations of the previous paragraph. Igi used a quadratic form  $a_\Delta + b_\Delta u^{1/2} + c_\Delta u$  for the residue<sup>6</sup>; a curve computed with his parameters is shown on Fig. 4. His width for the  $\Delta(1238)$  is a factor of 4 too small, as he noted, but his fit to the backward  $\pi^-p$  data is most unacceptable ( $\chi^2 \approx 5 \times 10^6$ ), except at  $u=0$ , because of his large  $B$  amplitude. (See also Sec. I D on this point.) A quadratic solution also has the disadvantage of giving negative widths for parity-partner states, as we have noted earlier. We adopted, therefore, a four-parameter form of the type given in Eq. (35) and converged on the following compromise:

$$\alpha_\Delta(u^{1/2}) = -0.02 + 0.9u, \quad (36)$$

$$\gamma_\Delta(u^{1/2}) = 27.3 + 51.7u + (u^{1/2} - M)(27.2 + 34.5u). \quad (37)$$

The  $\Delta(1238)$  elastic width is 53 MeV,  $\approx 45\%$  of its experimental value,<sup>32</sup> and  $\chi^2$  on 82  $\pi^-p$  backward data

<sup>32</sup> The elastic widths have been calculated in this paper by using the narrow-resonance approximation, as indicated in Appendix A. This is possibly a bad idea for the  $\Delta(1238)$ . One should probably reduce the quoted empirical value of 0.120 GeV by about 30% before making comparison with the theory. This factor can be estimated by calculating the integral over the experimental  $I=J=\frac{3}{2}$  discontinuity [A. Donnachie, R. G. Kirsopp, and C. Lovelace, Phys. Letters **26B**, 161 (1968)] from threshold up to, say,  $s = M_\Delta^2 + 1 \text{ GeV}^2$ . This is indeed some 30% lower than the corresponding value from the narrow-resonance approximation. When making comparisons in this paper, we used the 0.120-GeV value.

points<sup>31</sup> is 246. A plot of this function is also given on Fig. 4; the general agreement with the empirical residues is qualitatively not unreasonable, but the  $\chi^2$  for the backward fit seems much too large.

Moreover, from the theoretical point of view, this solution is not particularly appealing because it gives no evidence for a zero at  $\alpha_\Delta = \frac{1}{2}$ . As we remarked in Sec. I C, because there is no observed state at  $J^P = \frac{1}{2}^-$  on the exchange-degenerate  $\Sigma_\beta - \Sigma_8$  trajectory, a Veneziano parametrization for  $KN$  scattering may have terms with the factor  $\Gamma(m - \bar{\alpha}_{Y^*})$  only if  $m \geq 1$ ; consequently the  $Y_1^*$  residue function will contain the factor  $\alpha_{Y^*} - \frac{1}{2}$ . Via  $SU(3)$ -symmetry arguments, therefore, the  $\Delta$  reduced residue might also be expected to have, as a factor, the term  $\alpha_\Delta - \frac{1}{2}$ . Alternatively, the absence of strangeness +1 baryon states implies exchange degeneracy of the  $s$ - and  $t$ -channel exchanges in  $\pi N \rightarrow K\Sigma$ , which suggests more directly, therefore, that the  $\alpha_\Delta - \frac{1}{2}$  factor is appropriate in the  $\Delta$  reduced residue. These arguments provide theoretical support for the *ad hoc* suggestion made by Igi *et al.* that there should be such a wrong-signature nonsense zero.<sup>29</sup>

Without increasing the number of free parameters, we may consider solutions in which the zero at  $\alpha_\Delta = \frac{1}{2}$  is imposed *a priori*. In our best four-parameter fit of this type, we settled upon

$$\alpha_\Delta = 0.09 + 0.9u, \quad (38)$$

$$\gamma_\Delta = (\alpha_\Delta - \frac{1}{2}) [35.2 + 56.0u + (u^{1/2} - M)(29.4 + 35.8u)]. \quad (39)$$

For this case, the  $\chi^2$  on 82  $\pi^-p$  backward data points is 150, and the  $\Delta(1238)$  width is  $\approx 60 \text{ MeV}$ .<sup>32</sup> We also

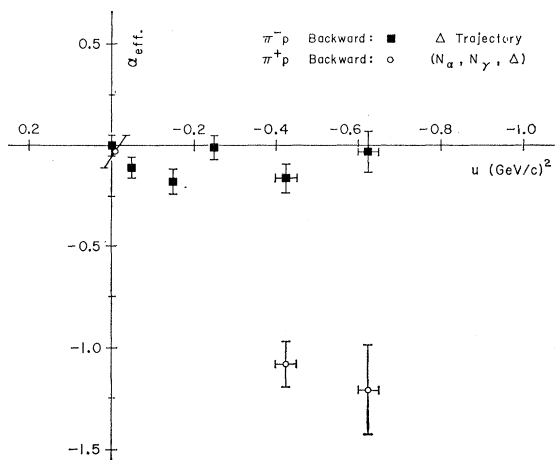


FIG. 10. Values of the effective  $\alpha$  in  $\pi^\pm p$  backward scattering, obtained from fitting  $d\sigma/du$ , at various  $u$  values, to the form  $A(s-t)^{2\alpha_{\text{eff}}-2}$ . The systematic normalization errors on the data were taken into account, as described in Sec. II D. We can only be ashamed of the ridiculously small error bars on  $\alpha_{\text{eff}}$ , which reflect the customary inapplicability of the normal laws of statistics to high-energy data. If, as might be true in  $\pi^-p$  backward scattering, the data are dominated by a single  $u^{1/2}$ -dependent trajectory,  $\alpha_{\text{eff}}$  measures  $\frac{1}{2}[\alpha(u^{1/2}) + \alpha(-u^{1/2})] = \text{Re}\alpha(u^{1/2})$ .

present a plot of this particular residue solution in Fig. 4; although the agreement with the backward data and the  $\Delta(1238)$  width is fairly good, the presence of the  $\alpha_\Delta - \frac{1}{2}$  factor causes the residue to grow too rapidly at large  $|u^{1/2}|$ . It may also be noted that the rather large coefficients of the terms in Eq. (39) proportional to  $u$  and to  $u^{3/2}$  indicate *no* systematic tendency for subsidiary terms in the Veneziano expansion to be small. Moreover, we call attention to the fact that even with the  $\alpha_\Delta = +\frac{1}{2}$  zero factored out, the small value of  $\gamma_\Delta$  at  $u=0$  is achieved through substantial cancellation between the contributions of the  $A$  and  $B$  amplitudes.

Finally, we examined also a six-parameter residue structure, keeping terms up to  $u^{5/2}$  in the  $\Delta$ 's residue parametrization, but releasing the zero at  $\alpha_\Delta = +\frac{1}{2}$ . This fit can lead to an estimate of the size of terms in the  $\Delta$  residue which are nonvanishing at  $\alpha_\Delta = \frac{1}{2}$  and thereby measure to what extent the underlying symmetry discussed above is reflected in the  $\pi N$  situation. The qualitative features of such a solution are very similar to those of the solution given in Eqs. (38) and (39), viz., a reasonably good fit to the backward-scattering data and an elastic width of 80 MeV for the  $\Delta$  are obtained, but at the price of a residue function which produces unreasonably large elastic widths for the higher recurrences along the trajectory.

Some physical arguments may be advanced to explain away these difficulties with the  $\Delta$  residue. We list them and consider each briefly in this paragraph. (1) The small cross section at  $u=0$  may be associated with a vanishing of the residue function near the backward direction<sup>33</sup>; as we noted, our solution, Eq. (36), is indicative of cancellation which reduces the residue from its natural size near  $u=0$ . Absorption effects<sup>34</sup> (in the  $s$  channel) are asserted to be large for such vanishing residue functions and could serve to significantly alter the shape of the differential cross section for  $u < 0$ .<sup>35</sup> (2) A  $\Delta$  trajectory with a substantial term linear in  $u^{1/2}$  has been advanced by Paschos<sup>28</sup> and others. Such a trajectory is not inconsistent with the Veneziano model<sup>36</sup>; we tried it and found, however, that its use does not lead to essential improvement over our preferred solutions, Eqs. (37) and (39). (3) The effects of unitarity (in the  $u$  channel) might be substantial in the

partial wave containing the  $\Delta(1238)$  state, and thus play a great role in determining the  $\Delta$ 's width. It will be recalled that the  $N/D$  model calculations of some years ago, based on unitarity and analyticity, were able to generate the  $\Delta(1238)$  state successfully from crossed-channel nucleon exchange.<sup>37</sup> To estimate this effect in the Veneziano model, we employed the  $K$ -matrix formalism<sup>38</sup> but found that the discontinuity generated by the crossed-channel nucleon state is only 10% of that due to the direct-channel  $\Delta$  pole.

We summarize this study of the  $\Delta$  residue function by pointing out that the Veneziano parametrization does not in fact provide a quantitatively acceptable procedure for extrapolation from the backward-scattering region to the resonance poles on the  $\Delta$  trajectory.<sup>39</sup> Within the Veneziano framework, the best solution involves at least four parameters and yields typical resonance widths a factor of 2 too small. There are two plausible methods for resolving this discrepancy. First, one may conceive that the Veneziano parametrization is simply too naive. In particular, it may be judged that the true residue function should explicitly vanish at all parity-partner locations. However, in this regard, we note that the parity-partner states in our solutions, for mass  $\gtrsim 3.0$  GeV, all have elastic widths less than 30% of the experimentally observed  $\tau P = -1$  states. Second, it may well be that the size of the backward elastic cross section is no true reflection of the  $\Delta$  Regge-pole residue function; we recall our previous comment on the possibility of large absorption corrections.<sup>40</sup>

## 2. $N_\alpha$ - $N_\gamma$ Residues

Achieving agreement with the  $N_\alpha$  and  $N_\gamma$  residue data is much less difficult but also much less constrained. It may be seen from comparing the data points in Figs. 5 and 6 that the  $N_\gamma$ 's residue function is expected to be of similar size to that of the  $N_\alpha$ . Therefore, the contribution of the  $N_\gamma$  to the backward  $\pi N$  data<sup>31</sup> will differ typically from the  $N_\alpha$  only in the intercept [ $\alpha_{N_\alpha}(0) \simeq \alpha_{N_\gamma}(0) + 0.5$ , which strongly favors the  $N_\alpha$ ] and the signature factor (which favors the  $N_\gamma$  near  $u=0$ ). In our various fits to the data, we fixed the  $\Delta$ , using parameters determined from the  $\pi^-p$  fit, and

<sup>33</sup> If the zero in  $\gamma_\Delta(u^{1/2})$  were at  $u=0$ , before absorption effects, this could be interpreted as implying the assignment of Toller quantum number  $M = \frac{3}{2}$  to the  $\Delta$ .

<sup>34</sup> J. D. Jackson, Rev. Mod. Phys. **37**, 484 (1965).

<sup>35</sup> Note that this statement is not inconsistent with the fact that absorption effects are comparatively small for the  $N_\alpha$  trajectory and so leave the prediction of a dip near  $u \approx -0.2$  (GeV/c)<sup>2</sup> unaltered. Only the lowest partial waves are affected by cuts (or absorption corrections). The  $\Delta$  trajectory contribution, with its relatively broad distribution  $d\sigma/du$ , will have much larger low partial waves than the sharply backward-peaked  $N_\alpha$  exchange contribution.

<sup>36</sup> Trajectories of the form  $\bar{\alpha}_B(s) = a + bs + cs^{1/2}$ ,  $c \neq 0$ , may be easily accommodated in the Veneziano framework by simply writing the terms  $\Gamma(m - \bar{\alpha}_B(s))\Gamma(l - \alpha_M(t))/\Gamma(n - \bar{\alpha}_B(s) - \alpha_M(t))$  for the amplitude  $f_1 = A + (s^{1/2} - M)B$ . The desired conditions at the  $s$ - and the  $t$ -channel poles will be satisfied; however, the discussion of the  $(s, u)$  terms is less elegant.

<sup>37</sup> G. F. Chew, Phys. Rev. Letters **9**, 233 (1962).

<sup>38</sup> F. Wagner [Nuovo Cimento **64A**, 189 (1969)] has discussed the  $K$ -matrix method. We remark that a simple Veneziano form for  $\pi N$  scattering already contains the famous relation between the  $N$  and  $\Delta$  couplings following from the static model (Ref. 37). This latter result, in the limit  $M_\Delta = M_N$ , implies that the residues of the  $N$  and  $\Delta$  are equal and opposite in the amplitude  $B^{(\pm)}$ , at  $t=0$ . However, this is guaranteed by making  $B^{(\pm)}$  proportional to  $(s-u)$  [see Eq. (46)], which is indeed the simplest way of ensuring that  $B^{(\pm)}$  is odd under  $s-u$  crossing.

<sup>39</sup> R. Amann (Ref. 6) claimed perfect agreement in pole extrapolation for the  $\Delta$ . However, there is a factor of  $4\pi$  missing from his definition of resonance widths, so that his calculated widths are in fact an order of magnitude too small.

<sup>40</sup> However, a quantitative examination of the effects of absorption is not encouraging in this regard. We thank Chris Quigg (University of California Lawrence Radiation Laboratory) for assistance with this calculation.

varied the residues of the  $N_\alpha$  and  $N_\gamma$  to obtain agreement with the widths of Figs. 5 and 6 and the data on both  $\pi^+p$  elastic and  $\pi^-p$  charge exchange (CEX).<sup>31</sup> We tried three types of fits:

- (i)  $\Delta$  fixed at parameters of Eqs. (36) and (37).
- (ii)  $\Delta$  fixed at parameters of Eqs. (38) and (39).
- (iii) Like (ii) but with an added even-signature  $I_u = \frac{1}{2}$  amplitude, having the same trajectory as the  $\Delta$  and a residue function fixed equal to 0.43 times that of the  $\Delta$  given in Eqs. (38) and (39). This fit is motivated by the exchange degeneracy which occurs in  $\bar{K}N$  scattering between the  $SU_3$  partners of the  $\Delta$  and the  $D_{15}(1680)$ . The constant of proportionality, 0.43, is estimated from Figs. 4 and 5. This type of fit would seem more sensible than (i) and (ii), but rather depressing in that four trajectories allow one far too many parameters with which to fit the backward data.

In fits (i)–(iii), the  $N_\alpha$  is clearly dominant, and the three subsidiary trajectories  $\Delta$ ,  $N_\gamma$ , and  $D_{15}$  contribute about equally. The various experiments<sup>31</sup> on  $\pi N$  CEX backward scattering are not notably consistent with each other. However, they all seem to indicate that there should be destructive interference between the  $I_u = \frac{1}{2}$  and the  $I_u = \frac{3}{2}$  contributions to the CEX reaction. This feature is realized in fit (i), but not in fits (ii) and (iii). The values of  $\gamma(u^{1/2})$  at the resonance positions, given in Figs. 5 and 6, were not an important constraint in the fits; in particular, the  $N_\gamma$  contribution is badly determined.

We can try to limit the freedom in the fits by requiring agreement with the trend of the  $\pi^+p$  polarization data measured near 3 GeV/c.<sup>41</sup> In fits (ii) and (iii), the  $\Delta$ - $N_\alpha$  interference term gives positive polarization, which rises to a maximum of approximately 1 near  $u = -0.1$  (GeV/c)<sup>2</sup> and then vanishes when  $\alpha_N = -0.5$  [at  $u = -0.15$  (GeV/c)<sup>2</sup>]. The  $D_{15}$  addition in fit (iii) produces similar behavior. In fit (i), the  $\Delta$  and  $N_\alpha$  interfere to give polarization of the opposite sign to that of fit (ii). We present the result of a type-(i) fit, for which the experimentally observed<sup>41</sup> positive polarization in  $\pi^+p \rightarrow \pi^+p$  near  $u = 0$  comes from the  $N_\alpha$ - $N_\gamma$  interference term.

The trajectories of the fit are

$$\alpha_{N_\alpha}(u) = -0.34 + 0.88u, \quad (40)$$

$$\alpha_{N_\gamma}(u) = -0.75 + 0.9u. \quad (41)$$

In terms of the four-parameter form given in Eq. (35), the residue functions are

$$\gamma_{N_\alpha}(u^{1/2}) = (104 - 184u) + (u^{1/2} - M)(293 + 106u), \quad (42)$$

$$\gamma_{N_\gamma}(u^{1/2}) = (-131 + 21u) + (u^{1/2} - M)(-170 + 110u). \quad (43)$$

<sup>41</sup> We thank A. Yokosawa (Argonne National Laboratory) for discussions of his preliminary  $\pi^+p$  backward polarization data.

These are plotted in Figs. 5 and 6. We note that the ratio of the reduced residue of the  $N_\gamma$  to that of the  $N_\alpha$  is smaller at  $u = 0$  than it is in the resonance region  $u^{1/2} \sim -1.5$  GeV.

Extracting a reliable parametrization for the subsidiary  $N_\gamma$  and  $D_{15}$  trajectories will require more good data. Specifically, we would suggest differential cross-section and polarization measurements in all charge configurations over a wide range of energies for lab momenta greater than 5 GeV/c. Particularly crucial is the matter of the correct relative normalization between data of different energies.

Our values for the  $N_\gamma$  can be regarded only as representative. Similarly, our skepticism of the fundamental nature of our fit prevents us from plotting any of our predictions for (or fits to) the  $\pi N$  backward data. (We will supply these to any interested reader and discuss them in more detail in a subsequent paper.)

We close this section by underscoring the unfortunate features of our best fit, represented in Eqs. (36), (37), and (40)–(43). In addition to the unproved shrinkage and poor  $\Delta_8$  pole extrapolation in  $\pi^-p$  backward elastic scattering, the fit also indicates a marked violation of even approximate exchange degeneracy. Specifically, the  $\Delta_8$  residue does not have the desired  $\alpha_\Delta = \frac{1}{2}$  zero, and the  $N_\gamma$  residue function bears little resemblance to that of the  $N_\alpha$ .

### III. EXPLICIT VENEZIANO-FUNCTION PARAMETRIZATIONS

In this section, we derive and discuss several explicit Veneziano-type representations for the pion-nucleon and kaon-nucleon processes. We endeavor to incorporate into these parametrizations both the general requirements of appropriate isospin, signature, positivity, and spin-parity content discussed in Sec. I, as well as the more specific structure emphasized in Sec. II.

#### A. $K$ - $N$ Scattering—First Approximation

We begin by treating  $KN$  scattering in the most obvious manner. In this approximation, exotic resonances are presumed absent, and thus we include no strangeness +1 baryon trajectories in our functions. Moreover, for the same reason, the  $t$ -channel meson trajectories are taken in exchange-degenerate pairs as are the  $s$ -channel  $\bar{K}N$  trajectories. We deal, therefore, only with Veneziano terms of the  $(s, t)$  type. This problem is thus considerably more simple than the  $\pi N$  situation (treated in Sec. III F), which demands, in addition,  $(u, t)$ - and then  $(s, u)$ -type terms for signature reasons. In this first approximation, we also do not include the Pomeranchuk trajectory as a possible  $t$ -channel exchange. To do so in  $KN$  scattering, without accepting the price of exotic  $u$ -channel resonances, would require installing the Pomeranchuk trajectory as an exchange-degenerate object; this seems inappropriate. We return to the Pomeranchuk situation in

Sec. III E, where we argue that there is no compelling reason to leave it out of a Veneziano representation; in fact, it can be associated directly with low-lying exotic  $\bar{K}N$  states.<sup>9</sup>

A good solution to  $\bar{K}N$  scattering at this first level was independently obtained by Inami<sup>6</sup>; we will first motivate his result, discuss its properties, and then go on to possible improvements. Our approach begins with the results we established in Sec. II B relating to the  $t$  dependence required of the  $A(s, t, u)$  and  $B(s, t, u)$  functions if appropriate spin and parity is to be secured for the  $s$ -channel resonances. Next, we note that the  $t$  dependence of a single Veneziano form, Eq. (6), near a pole  $\bar{\alpha}_1(s) = m'$  is given by  $\Gamma(l - \alpha_2(t))/\Gamma(n - m' - \alpha_2(t))$ , which has zeros for  $t$  values,  $\alpha_2(t) = l - 1, \dots, n - m'$ . In Table IV, the states on the  $\Lambda_\alpha - \Lambda_\gamma$  trajectory are shown to possess a structure of zeros in both  $A$  and  $B$ , which is roughly consistent with the prediction of a single Veneziano beta-function expression. For the  $\Sigma_\beta - \Sigma_\delta$  pair, a similar statement is true for the  $A$  amplitude, but the  $B$  function requires an additional zero at  $t \approx 2.3(\text{GeV}/c)^2$ .

We are thus led to consider the following representations:

$\Lambda_\alpha - \Lambda_\gamma$   $I = 0$   $\bar{K}N$  amplitude:

$$A_1^{(0)} = \Lambda_{A1} \frac{\Gamma(1 - \bar{\alpha}_\Lambda)\Gamma(1 - \alpha_t)}{\Gamma(1 - \bar{\alpha}_\Lambda - \alpha_t)} + \Lambda_{A2} \frac{\Gamma(-\bar{\alpha}_\Lambda)\Gamma(1 - \alpha_t)}{\Gamma(1 - \bar{\alpha}_\Lambda - \alpha_t)},$$

$$B_1^{(0)} = \Lambda_{B1} \frac{\Gamma(-\bar{\alpha}_\Lambda)\Gamma(1 - \alpha_t)}{\Gamma(1 - \bar{\alpha}_\Lambda - \alpha_t)};$$

$\Sigma_\beta - \Sigma_\delta$   $I = 1$   $\bar{K}N$  amplitude:

$$A_1^{(1)} = \Sigma_{A1} \frac{\Gamma(1 - \bar{\alpha}_\Sigma)\Gamma(1 - \alpha_t)}{\Gamma(1 - \bar{\alpha}_\Sigma - \alpha_t)},$$

$$B_1^{(1)} = \Sigma_{B1}(t_0 - t) \frac{\Gamma(1 - \bar{\alpha}_\Sigma)\Gamma(1 - \alpha_t)}{\Gamma(2 - \bar{\alpha}_\Sigma - \alpha_t)}.$$
(44)

As noted, the isospin indices  $I$  in  $A^{(I)}$  and  $B^{(I)}$  denote the total isospin value in the  $s$ -channel  $\bar{K}N$  system. Crossing relations, which prescribe the  $u$ -channel  $\bar{K}N$  amplitudes in terms of the above, are given in Appendix A. For notational convenience, we write  $\bar{\alpha}_\Lambda = \alpha_\Lambda(s) - \frac{1}{2}$ , where  $\Lambda$  denotes the  $\Lambda_\alpha - \Lambda_\gamma$  exchange-degenerate trajectory;  $\bar{\alpha}_\Sigma = \alpha_\Sigma(s) - \frac{1}{2}$ , where  $\Sigma$  denotes the  $\Sigma_\beta - \Sigma_\delta$  pair; and  $\alpha_t = \alpha_\rho(t) = \alpha_{A_2}(t) = \alpha_\omega(t) = \alpha_{P'}(t)$ . Our omission of the  $\Sigma_\alpha - \Sigma_\gamma$  trajectory from these formulas may be justified by Fig. 9; the residue function has a quite small magnitude when compared with that of  $\Lambda_\alpha - \Lambda_\gamma$  or  $\Sigma_\beta - \Sigma_\delta$ .

We emphasize that Eq. (44) is essentially the simplest one can devise for the  $\bar{K}N$  process in that only two terms of a subsidiary nature<sup>9</sup> appear. The term pro-

portional to  $\Lambda_{A2}$  is subsidiary because it does not contribute in leading order as  $s \rightarrow \infty$  for  $t$  fixed. It is present simply to achieve the precise extermination of the parity partner of the  $J^P = \frac{1}{2}^+ \Lambda(1115)$ ; it is, in fact, small and unimportant. The other subsidiary term is that proportional to  $t_0$  in  $B^{(1)}$ . The  $t_0 - t$  term is indeed a crucial factor in  $B$  because it leads to reversal of the sign of the  $\Sigma_{B1}$  term between large  $t$  [where it is normalized by the  $Y_1^*(\Sigma_\beta - \Sigma_\delta)$  widths] and the  $t = 0$  point, where it contributes asymptotically to known high-energy forward scattering. Terms proportional to  $\Gamma(-\bar{\alpha}_\Sigma)$  are excluded because they would predict an unobserved  $J^P = \frac{1}{2}^-$  state, and no  $\Gamma(-\alpha_t)$  terms appear for similar reasons. We remark, however, that in this solution the reduced residue function for the  $\Lambda$  trajectory is quadratic in  $u^{1/2}$ , and thus positivity cannot be guaranteed for the elastic widths of both parity states on the parent trajectory.<sup>42</sup>

The values of the constants appearing in Eq. (44) may be established in various ways. We will present two different approaches and then go on to a discussion of the properties of the solutions. Inami's approach was guided by the assertion that, in accordance with Nature, certain residues should vanish. He chose to abolish the  $\frac{1}{2}^-$  and  $\frac{3}{2}^+$  states of the  $\Lambda$  trajectory, the  $\frac{3}{2}^-$  state of the  $\Sigma$  trajectory, and the  $\frac{1}{2}^+$  daughter state of the  $\Sigma$  trajectory. This is accomplished essentially by using the  $t_0$  value listed in Table IV and determining the ratios  $\Lambda_{A1}/\Lambda_{B1}$  and  $\Sigma_{A1}/\Sigma_{B1}$  from the values listed in Table V for the  $\frac{3}{2}^-$  and  $\frac{3}{2}^+$  states of the  $\Lambda_\alpha - \Lambda_\gamma$  and  $\Sigma_\beta - \Sigma_\delta$  trajectories, respectively. Inami then fixed his two remaining parameters by adopting the high-energy fitted values of  $A'$  at  $t = 0$  in the two different isospin states (see Table III). We denote his solution (I); in units of  $\hbar = c = 1$  and GeV, it is

$$\begin{aligned} \Lambda_{A1} &= 55.5, & \Lambda_{A2} &= -24.4, & \Lambda_{B1} &= 138.7, \\ \Sigma_{A1} &= -22.4, & \Sigma_{B1} &= -9.8, & t_0 &= 2.3, \\ \bar{\alpha}_\Lambda &= -1.24 + s, & \bar{\alpha}_\Sigma &= -0.9 + s, & \alpha_t &= 0.5 + t \end{aligned}$$

[solution (I)].

In order to illustrate the uncertainty present in even this simplest parametrization, we present a second set of values, denoted solution (I')

$$\begin{aligned} \Lambda_{A1} &= 48.0, & \Lambda_{A2} &= -24.6, & \Lambda_{B1} &= 117.5, \\ \Sigma_{A1} &= -20.7, & \Sigma_{B1} &= -24.2, & t_0 &= 0.62, \\ \bar{\alpha}_\Lambda &= -1.15 + 0.9s, & \bar{\alpha}_\Sigma &= -0.8 + 0.9s, \\ & & \alpha_t &= 0.55 + 0.9t \end{aligned}$$

[solution (I')].

<sup>42</sup> Igi and Storrow (Ref. 6) also proposed a parametrization similar to Inami's, except that they decoupled the  $\Sigma_\beta - \Sigma_\delta$  ( $Y_1^*$ ) trajectory from contributing asymptotically to leading order in the  $B$  amplitude. We have not seen the version in which this error is corrected. In addition, we believe that their definition of resonance widths is wrong for the higher recurrences on the trajectories because it ignores the contributions from the  $A$  amplitude. A similar criticism applied to the widths defined by Igi and Pretzl (Ref. 6).

With this solution, the low-energy daughter<sup>9</sup> states and parity-partner states are not abolished with quite the same religious exactitude as in solution (I). However, according to  $\chi^2$ , a much better over-all fit is achieved to a collection of  $\bar{K}N$  and  $KN$  scattering data as well as to the widths of sundry parent- and daughter-state resonance widths. Before presenting a critique of these solutions, we list the relevant data against which we judged the solutions.

## B. $KN$ Data Set

### 1. Resonance Widths

The empirical elastic widths of states on the parent  $\Lambda_\alpha$ - $\Lambda_7$  and  $\Sigma_\beta$ - $\Sigma_\delta$  trajectories were discussed in Sec. II D and the reduced residue functions were extracted and plotted in Figs. 7 and 8, respectively. We also assumed that elastic widths of daughter<sup>9</sup> states are rather small ( $\lesssim \frac{1}{2}$  the size of the parent widths) but positive. In some cases, widths of such states can in fact be estimated by using the results of  $\pi N$  phase-shift analysis<sup>43</sup> and invoking  $SU(3)$  symmetry. The handling of the daughter states in the model is, in general, a difficult problem because certainly some of the lower-lying embryo resonances in the Veneziano formulation will acquire *total* widths so large that they will never be discerned empirically. Some of the interesting low-lying states predicted by the quark model will be discussed later.

### 2. Forward-Scattering Data

Some of the qualitative features of the high-energy data were discussed in Sec. II A. The data which we employed are explicitly

- (i)  $K^-p \rightarrow \bar{K}^0n$  at 3.5 and 5–12.3 GeV/c,<sup>44</sup>
- (ii)  $K^+n \rightarrow K^0p$  at 0.35–0.81, 0.86–1.36, 2.3 and 3.0 GeV/c.<sup>45</sup>

The  $K^+n$  data are particularly interesting information from the standpoint of a complete test of the model. All of the applications of the model we have so far discussed in this paper have involved comparing data against a quantity extracted from the model via a limiting procedure. This is necessary because of the unitarity-violating zero-width aspect of the model which places resonance poles directly on the real energy axes. However, in the approximation to which we work,

<sup>43</sup> A. Donnachie *et al.* (Ref. 32).

<sup>44</sup> A. D. Brody and L. Lyons, *Nuovo Cimento* **45A**, 1027 (1966); P. Astbury *et al.*, *Phys. Letters* **23**, 396 (1966).

<sup>45</sup> W. Slater *et al.*, *Phys. Rev. Letters* **7**, 378 (1961); A. Hirata *et al.*, University of California Lawrence Radiation Laboratory Report No UCRL-18322 (unpublished); CERN-Brussels-Munich Collaboration, *Phys. Letters* **27B**, 603 (1968); I. Butterworth *et al.*, *Phys. Rev. Letters* **15**, 734 (1965). We wish to thank G. Goldhaber and A. Hirata for supplying us with the results of their latest analysis of data from 0.86 to 1.36 GeV/c. However, our theory is so rough that their preliminary data are sufficient for general conclusions; Fig. 13 displays the preliminary data.

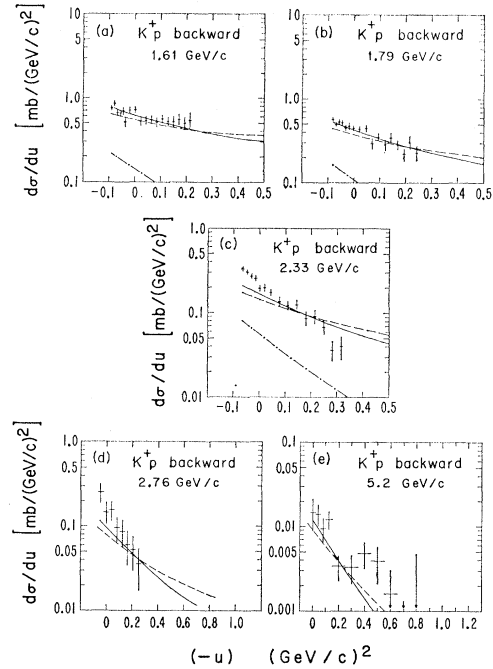


FIG. 11.  $K^+p$  backward scattering (Ref. 46). The dashed curve is solution (I), and the solid curve is solution (II), given in Sec. III D. The dot-dashed line denotes solution (II), but calculated with the usual Regge asymptotic approximation (proportional to  $s^{\alpha-1/2}$ ) in the  $A$  and  $B$  amplitudes (rather than the full Veneziano formula). The data are at lab momenta of (a) 1.61, (b) 1.79, (c) 2.33, (d) 2.76, and (e) 5.2 GeV/c.

there are no  $KN$  resonances and thus no poles in the  $K^+n$  channel above threshold. The full model, without limiting operations, may therefore be used in  $K^+n$  scattering and applied even at quite low energies. The omission of a Pomeranchuk trajectory from our formalism requires that comparison of the Veneziano form be restricted to the CEX process, however.

### 3. $K^+p$ Backward Scattering

The data included are distributions from exposures at 0.99–2.45, 2.76, 3.53, 3.55, 5.2, and 6.9 GeV/c.<sup>46</sup> Actually, we estimate that it is not reliable to use such data below 1.3 GeV/c because the effects of the neglected  $t$ -channel Pomeranchuk trajectory may be important. The statements made in Sec. III B 2 about a complete test of the model apply here also, of course.

### 4. $KN$ Scattering Lengths

We use the values<sup>47</sup> 0 and  $-1.47$  in the  $I_u=0$  and 1  $KN$  states, respectively. There are not very important data, since the  $I_t=0$  combination may be affected quite

<sup>46</sup> A. S. Carroll *et al.*, *Phys. Rev. Letters* **21**, 1282 (1968); G. S. Abrams *et al.*, *ibid.* **21**, 1407 (1968); D. Cline *et al.*, *ibid.* **19**, 675 (1967); J. Banaigs *et al.*, *Nucl. Phys.* **B9**, 640 (1969); W. F. Baker *et al.* (Ref. 31).

<sup>47</sup> S. Goldhaber *et al.*, *Phys. Rev. Letters* **9**, 135 (1962); B. J. Stenger *et al.*, *Phys. Rev.* **134**, B1111 (1964).

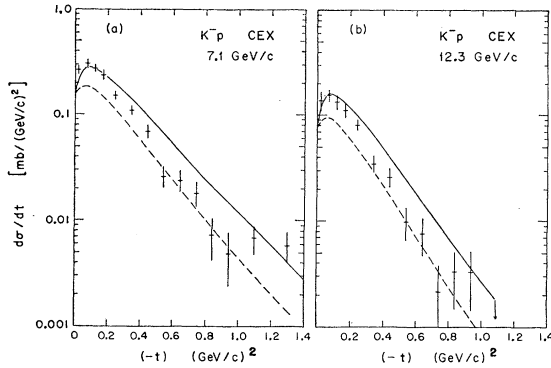


FIG. 12.  $K^-p \rightarrow \bar{K}^0n$  scattering (Ref. 44). The data are at lab momenta of (a) 7.1 and (b) 12.3 GeV/c. The curves are defined in the caption for Fig. 11.

significantly by the Pomernichukon, whereas the  $I_t=1$  part is already implied by the low-energy  $K^+n$  CEX data, 0.35–0.81 (GeV/c)<sup>2</sup>, from which it was in fact extracted.

### C. Critique of Solutions (I) and (I')

Having determined the constants in his parametrization as discussed above, Inami found that his expression (I) produced good agreement with both  $K^-p$  CEX data and  $K^+p$  backward-scattering data, as reproduced in Figs. 11 and 12. In this section, we discuss the significance of these verified predictions and also comment upon the value given by his solution for the elastic widths and scattering lengths.

We begin with the  $K^-p \rightarrow \bar{K}^0n$  result. Given the value of  $A'$ , asymptotically, a good fit to the  $K^-p$  CEX data will be obtained once one specifies, in addition, the approximately correct value for the ratio  $A'/\nu B$  at  $t=0$ . This was done when the correct spin-parity structure of the low-energy spectrum was imposed. We argue below that the success achieved in the fit is therefore not a triumph for the particular Veneziano formulation, but is a practically expected result of a wide class of models which embody a duality of resonances and Regge poles. To make this more quantitative, we first focus on some general features of the duality of resonances and Regge poles, well known from FESR results.<sup>3</sup> Both of the  $s$ -channel trajectories  $\Sigma_\beta\text{-}\Sigma_\delta$  and  $\Lambda_\alpha\text{-}\Lambda_\gamma$  (or, for that matter,  $N_\alpha$ ,  $N_\gamma$ , and  $\Delta$  in the  $\pi N$  situation) are associated with large values of the  $B$  amplitude and a small ratio  $A'/\nu B$ . In Table V, this is shown to be the case for the high-spin members of each resonance tower. Any Veneziano form which does not contain daughter states with huge widths must exhibit this feature, and, indeed, as we noted, the ratio conditions were imposed in each of the  $s$ -channel isospin states when the parameters of solution (I) were derived. The signs of the amplitudes are also such that the  $\Lambda_\alpha\text{-}\Lambda_\gamma$  and the  $\Sigma_\beta\text{-}\Sigma_\delta$  terms interfere constructively in forming the  $B$  amplitude with  $t$ -channel isospin  $I_t=1$  but destructively in  $I_t=0$ . The well-determined high-energy value of  $A'$  at

$t=0$  served to normalize solution (I), and values for  $B(I_t=1)$  and  $B(I_t=0)$  were deduced.

The  $B(I_t=0)$  number is small, owing to the cancellations, but is essentially undetermined experimentally. The major testable prediction is that for  $B(I_t=1)$ , which is supported. However, as this discussion indicates, essentially the same prediction would come from any model imposing duality and normalizing to  $A'$ . The only surprising aspect is that the precise numerical values Inami uses produce uncannily good agreement with the  $t=0$  values of Table III (E).

Upon examining the  $t$  dependences of solutions (I) and (I'), we find that  $A$ ,  $B$ , and  $A'(I_t=0)$  are essentially constant, subject to the expected  $\alpha_t = -n$  zeros, whereas  $A'(I_t=1)$  has the sought-for crossover zero at  $t \approx -0.25$  (GeV/c)<sup>2</sup>. These effects are also expected because, as explained in Sec. II, any roughly constant  $A$  and  $B$  will generate the crossover zero in  $A'(I_t=1)$  but not in  $A'(I_t=0)$ , simply as a consequence of the  $1-t/4M^2$  factor [see Eq. A11] and the appropriate magnitude of  $A'/\nu B$  at  $t=0$ . As noted, this latter quantity is small for the  $I_t=1$  amplitude but of order unity for  $I_t=0$ . The absence of a crossover zero in  $A'$  ( $\omega$  exchange) implies that solutions (I) and (I') will poorly reproduce the empirical value of the difference  $d\sigma/dt(K^+p \text{ elastic}) - d\sigma/dt(K^-p \text{ elastic})$ .

The predictions of solution (I) for the reduced residue functions of the baryon trajectories are given in Figs. 7 and 8. The baryon widths for both (I) and (I') are a factor of 2–3 times too small in comparison with the empirical values.

The fit which Inami achieved to the backward  $K^+p$  scattering data, Fig. 11, is a free prediction and is reasonably good, but this may be a fluke. From Fig. 7, one may note that Inami's value for the  $\Lambda_\alpha\text{-}\Lambda_\gamma$  residue is approximately a factor of 2 smaller than that obtained by Barger<sup>48</sup> from a classical Regge-model fit to the data. The difference can be attributed to the very different size of the  $\Sigma_\beta\text{-}\Sigma_\delta$  contribution between the two cases. In fact, solution (I) gives a value for the  $\Sigma_\beta\text{-}\Sigma_\delta$  residue which is an order of magnitude larger than the value estimated from applying  $SU(3)$  arguments, at fixed  $u$ , to the known  $\Delta \rightarrow \pi N$  coupling at  $u=0$ . Whereas the  $\Sigma$  trajectory was neglected by Barger,<sup>48</sup> it is quite

TABLE VI. Partial-wave analysis of the resonance tower, under the  $F_{17}(2030)$ , for two of the solutions presented for  $KN$  scattering in Sec. III. The kinematic factors have been evaluated at the pole position predicted by the theoretical trajectories. Listed is  $\Gamma_{el}$  (MeV).

$J$	Solution (I)		Solution (II)	
	$\tau P_+$	$\tau P_-$	$\tau P_+$	$\tau P_-$
0.5	15.7	8.9	21.0	52.5
1.5	2.7	8.3	-18.3	-5.9
2.5	-0.3	9.0	5.7	5.0
3.5	0.2	8.9	2.2	29.9

<sup>48</sup> V. Barger, Phys. Rev. **179**, 1371 (1969).

important in the parametrization of solution (I). The resolution of this question awaits reliable high-energy backward-scattering data for  $K^+n \rightarrow K^0p$  or  $K^+n \rightarrow K^+n$ . However, a preliminary answer is possible inasmuch as the full Veneziano formula can be used to study low-energy  $K^+n$  CEX data, which extend to the backward angles. Solution (I) is seen to give much too small a cross section, whereas a phenomenological model, normalized to the backward  $K^+p$  data and using a smaller  $\Sigma$  contribution, is in better agreement with the data. In particular, when we tried to extend our parametrization beyond that of Eq. (44), we found good solutions with a very small  $\Sigma$  contribution at  $u=0$ . However, our best solutions did not exhibit this feature.

We notice from Fig. 13 that the fit to the  $K^+n$  CEX data is generally rather poor. At low energies, the theory predicts more  $S$  wave and less  $P$  wave than is indicated by the data. The presence of the large  $P$ -wave component of the data may be identified with rapid variation of the amplitude produced by the nearby baryon poles. The residues of these poles are too small in both (I) and (I'). In the next section, solutions will be considered whose residues at the nearby poles agree better with experiment, and a larger  $P$ -wave component will be generated.

#### D. Improved Veneziano Parametrization of $KN$

We gain some inkling as to the source of the deficiencies of solution (I) by examining the results of a partial-wave analysis of the various resonance poles. Table VI is a presentation of the widths of the members of the resonance tower associated with the  $F_{17}(2030)$  state of the  $\Sigma_\beta$ - $\Sigma_\delta$  family. The widths are pleasantly positive, except for the  $\frac{5}{2}^+$  state, which has a small negative width. On reflection, this latter feature is curious because the  $\frac{5}{2}^+$  state is the  $SU_3$  partner of the experimentally observed<sup>25</sup>  $F_{35}(1910)$ , which, in turn, is a member of the tower associated with the  $F_{37}(1950)$ , correspondingly the partner of the  $F_{17}(2030)$ . Moreover, these states, parents, and daughters are classified successfully by the quark model<sup>24</sup> in the  $(56, 2^+)$  representation. Both the reasonably large elastic widths in  $\pi N$  [ $\Gamma_{e1}(F_{35})/\Gamma_{e1}(F_{37}) \sim 0.5$ , which, via  $SU(3)$ , implies the same ratio in  $\bar{K}N$ ] and the theoretical association with the quark model suggest that we should seek a solution with reasonable properties for this  $\frac{5}{2}^+$  state. Similar considerations relate the  $\frac{3}{2}^+$  daughter of the  $D_{15}(1770)$  state in  $\bar{K}N$  to the corresponding  $SU(3)$  partners  $D_{15}(1675)$ ,  $D_{13}(1730)$ , and  $D_{33}(1670)$  in  $\pi N$ .

From Tables IV and V may be noted the amusing fact that the  $F_{35}$  destructively interferes with its parent  $F_{37}$  in both the  $A$  and  $B$  amplitudes. This fact would enable one to increase the size of the  $F_{37}$  width without sacrificing the desired high-energy limiting values of  $A$  and  $B$ . In particular, the  $F_{35}+F_{37}$  combination does not necessarily have the effective zero at the canonical  $t=2.3$   $(\text{GeV}/c)^2$  position in the  $B$  amplitude; the addi-

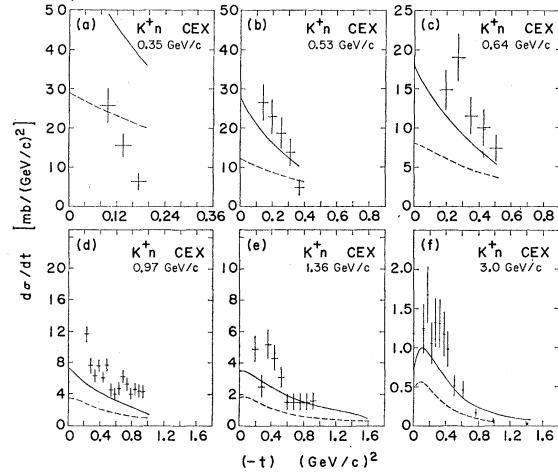


FIG. 13.  $K^+n \rightarrow K^0p$  scattering (Ref. 45). The theoretical curves have not been corrected for any deuterium effects. We have not plotted the experimental points near the forward direction, where such corrections are dominant. The data are at lab momenta of (a) 0.35, (b) 0.53, (c) 0.64, (d) 0.97, (e) 1.36, and (f) 3 GeV/c. Only at 3 GeV have deuterium corrections been applied to the experimental points. The curves are described in the caption for Fig. 11.

tion of the  $F_{35}$  moves it to smaller  $t$ . For this reason, the simple solution (I) is suspect in that the zero at  $t=2.3$   $(\text{GeV}/c)^2$  is present unaltered in the high-energy limit.

We can try similar arguments for states on the  $\Lambda_\alpha$ - $\Lambda_\gamma$  trajectory, but there are no obvious quark daughters for the  $F_{05}(1690)$ . One evident discrepancy in (I) is that the  $\Lambda_\alpha$ - $\Lambda_\gamma$  residue function is quadratic in  $s^{1/2}$ , implying necessarily negative widths for all the parity-partner states above a critical mass value.

Based upon such thoughts, plus some trial and error, from our Pandora's box of possible extra Veneziano forms, we select a few that are particularly helpful. These are in addition to those in Eq. (44):

$\Lambda_\alpha$ - $\Lambda_\gamma$   $\bar{K}N$   $I=0$  amplitude:

$$A^{(0)} = A_1^{(0)} + \Lambda_{A3} \frac{\Gamma(1-\bar{\alpha}_\Lambda)\Gamma(2-\alpha_t)}{\Gamma(2-\bar{\alpha}_\Lambda-\alpha_t)},$$

$$B^{(0)} = B_1^{(0)} + \Lambda_{B2} \frac{\Gamma(1-\bar{\alpha}_\Lambda)\Gamma(2-\alpha_t)}{\Gamma(2-\bar{\alpha}_\Lambda-\alpha_t)} + \Lambda_{B3} \frac{\Gamma(1-\bar{\alpha}_\Lambda)\Gamma(1-\alpha_t)}{\Gamma(2-\bar{\alpha}_\Lambda-\alpha_t)};$$

$\Sigma_\beta$ - $\Sigma_\delta$   $\bar{K}N$   $I=1$  amplitude:

$$A^{(1)} = A_1^{(1)} + \Sigma_{A2} \frac{\Gamma(1-\bar{\alpha}_\Sigma)\Gamma(1-\alpha_t)}{\Gamma(2-\bar{\alpha}_\Sigma-\alpha_t)},$$

$$B^{(1)} = B_1^{(1)} + \Sigma_{B3} \frac{\Gamma(2-\bar{\alpha}_\Sigma)\Gamma(2-\alpha_t)}{\Gamma(3-\bar{\alpha}_\Sigma-\alpha_t)} + \Sigma_{B4} \frac{\Gamma(2-\bar{\alpha}_\Sigma)\Gamma(1-\alpha_t)}{\Gamma(3-\bar{\alpha}_\Sigma-\alpha_t)}. \quad (45)$$



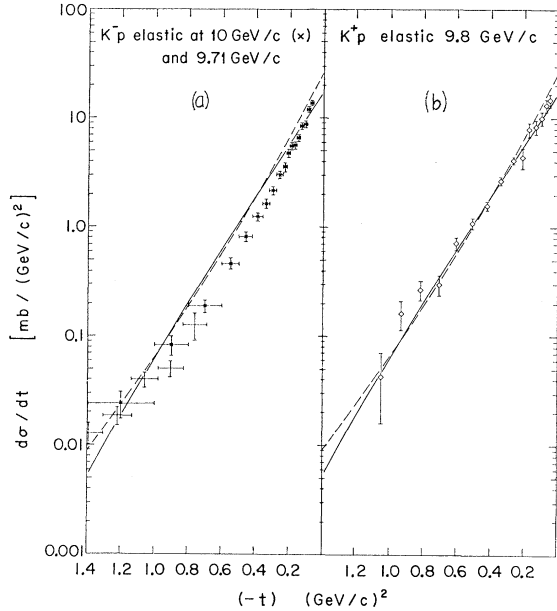


FIG. 14.  $K^\pm p$  elastic scattering (Ref. 51): (a)  $K^-p$  scattering data at 9.71 and 10 GeV/c; (b)  $K^+p$  at 9.8 GeV/c. Both curves give the theoretical predictions for  $K^-p$  (dashed line) and  $K^+p$  (solid line) scattering (at 9.85 GeV/c) obtained from superimposing a Pomeranchukon onto solution (II) as described in Sec. III D.

A computer search was performed to find the set of constants which would best fit the data set given in Sec. III B. These values are

$$\begin{aligned} \Lambda_{A1} &= 68.0, & \Lambda_{A2} &= -35.5, & \Lambda_{A3} &= 61.5, \\ \Lambda_{B1} &= 254.2, & \Lambda_{B2} &= -33.8, & \Lambda_{B3} &= -90.9, \\ \Sigma_{A1} &= -20.2, & \Sigma_{A2} &= -1.1, & \Sigma_{B1} &= -26.6, \\ t_0 &= 0.64, & \Sigma_{B3} &= -3.4, & \Sigma_{B4} &= 3.6 \end{aligned}$$

[solution (II')],

with the same baryon and meson intercepts as in solution (I').

We notice that this solution in the  $\Sigma$  segment is not essentially different from (I'). We have also obtained fits with a larger value of  $\Sigma_{A1}$ . The data on the  $Y_1^*(1385)$  are not sufficiently precise to determine the size of  $\Sigma_{A1}$ , but when we study  $\pi N$  scattering we find that the solution analogous to (I') gives much too small a  $\Delta$  width. A typical fit with a larger  $Y_1^*(1385)$  coupling is

$$\begin{aligned} A_{A1} &= 57.6, & \Lambda_{A2} &= -37.3, & \Lambda_{A3} &= 80.5, \\ \Lambda_{B1} &= 256.9, & \Lambda_{B2} &= -50.2, & \Lambda_{B3} &= -106.7, \\ \Sigma_{A1} &= -45.0 \text{ (fixed)}, & \Sigma_{A2} &= 9.7, & \Sigma_{B1} &= -29.0, \\ t_0 &= 1.52, & \Sigma_{B3} &= -5.9, & \Sigma_{B4} &= 6.6 \end{aligned}$$

[solution (II)].

Solutions (I), (I'), (II), and (II') all yield quite similar values of  $\chi^2$  for the scattering data. In all cases,

the major discrepancy between theory and experiment is the  $K^+n$  CEX data (Fig. 13) at the lowest momentum, 0.35 GeV/c. The computer was unable to reproduce the cancellation<sup>49</sup> necessary to yield a rather small  $S$  wave at low energy. In Fig. 13(a), one may choose between the devil and the deep blue sea. Fits (I) and (I') have too small a  $P$ -wave component, whereas (II) and (II') have a reasonable  $P$ -wave but a disastrously large  $S$ -wave component (too large by a factor of 2 in the amplitude). We tried many alternatives in an attempt to improve the fit. The addition of various beta-function terms to our amplitude, with small multiplicative coefficients, will, in fact, yield agreement with the 0.35-GeV/c data. However, all of our fits which were successful at 0.35 GeV/c fell well below the data curves at higher values of energy.

In Fig. 11, the (I) and (II) fits to the  $K^+p$  backward elastic data are presented. The quantitative agreement between theory and experiment seems to get worse as the energy increases.<sup>50</sup> Figure 12 presents the fits to the  $K^-p$  CEX data which are adequate.

The major difference (and claimed improvement) between (I), (I') and (II), (II') lies in the values of the baryon residue functions, which are typically a factor of 2 larger in the (II) and (II') fits. In Table VI, we give the results of the partial-wave analyses of the  $F_{17}(2030)$  tower. As rumored earlier in this subsection, the residue of the  $F_{15}$  is positive in (II). This happy state of affairs is in fact enjoyed by (I'), (II), and (II') but not, as we said, by (I). In Figs. 7 and 8, we plot the residue functions of the leading baryon trajectories for solutions (I) and (II).

In Fig. 14, the deviations of our Veneziano-model solutions from the elastic scattering data are illustrated. To achieve a fit to elastic data one must, of course, include an appropriate Pomeranchuk-trajectory contribution. We did this simply by parametrizing the Pomeranchuk amplitude as in Eqs. (20) and (21) with  $\alpha_P(t) = 1 + 0.85t$ ,  $a(0) = 2.5$ ,  $b(0) = -10.5$ , and with the only  $t$  dependence of  $a(t)$  and  $b(t)$  specified by inserting a Veneziano-type scale factor  $s_0 = 1/\alpha_{P'}$  into the formulas. The results of the addition of such a

<sup>49</sup> The cancellations are indeed large. For example, the term proportional to  $\Lambda_{B1}$  in Eq. (44) gives a contribution to the  $K^+n$  CEX differential cross section  $d\sigma/dt$ , which is about 20 times larger than the total theoretical curve.

<sup>50</sup> Pretzl and Igi (Ref. 6) attempted a residue analysis of backward  $K^+p$  scattering similar to the one we gave for  $\pi N$  in Sec. II D. However, because the data are rather sparse at high energies, they are forced to use lower-energy data. They claim almost perfect agreement, but several sobering comments are in order. First, we demonstrated in Sec. II D that a good fit is not obtainable in the  $\pi^+p$  situation where the data are much better and where the fit is far more constrained, because only one trajectory contributes. The residue parametrization is also rather naive. It leads to parity-partner states of negative elastic width on the  $\Lambda_\alpha\text{-}\Lambda_\gamma$  trajectory. A parametrization as simple as the one they used in the  $\Sigma_B\text{-}\Sigma_\delta$  case would give poor results for the  $SU(3)$ -related  $\Delta_\beta\text{-}\Delta_\delta$ . Second, the asymptotic approximations they employ give results which differ by a factor of 2 from those obtained by using the full Veneziano formalism at their lowest energy. In Sec. III, we always employed the full form for  $K^+p$  scattering.

Pomeranchuk amplitude to solution (II') are given in the figure; however, the other solutions have very similar features. The difference between the experimental values<sup>51</sup> of  $K^+p$  and  $K^-p$  elastic scattering is clearly not well reproduced. As we have remarked before, such a failure is to be expected of any model which does not possess the crossover zero in the  $A'(t=0)$  amplitude at  $t \simeq -0.2$  (GeV/c)<sup>2</sup>. We should hastily admit that the excellent fit to the 9.8-GeV/c  $K^+p$  data is by no means representative; the high-slope Pomeranchukon yields too much shrinkage.<sup>52</sup>

In conclusion, we may say that the results of fits (II) and (II') are disappointing. We carried out a rather extensive search, adding in turn many different individual beta-function terms, and combinations thereof, to our amplitudes in an effort to find a good over-all fit. Our lack of success suggests to us that there are substantial effects outside the scope of the model. More specifically, for instance, as we noted, fits (I) and (I') exhibited discrepancies, which are typically a factor of 2 in magnitude. In our effort to achieve improvement, we determined solutions (II) and (II'). These two solutions do yield satisfactory agreement with the magnitudes of resonance widths and certain other quantities associated with the form of the amplitude in its high-energy limit. However, they fail to reproduce a (possibly) more subtle effect associated with energy dependence. As we have remarked, the model should fit the  $KN$  data over the whole energy range, from threshold on up; but we were unable to overcome discrepancies in over-all magnitude for the  $K^+n$  CEX data, and in  $t$  variation for the  $K^+p$  backward-scattering data, particularly in the 2.0–3.0-GeV/c region. These features remained qualitatively invariant when we added further Veneziano beta-function terms to the set given in Eq. (45). Our lack of success in fitting the  $K^\pm p$  elastic data (after adding a Pomeranchuk trajectory, and using the Veneziano-model relation  $s_0 = 1/\alpha'$ ) is also indicative of the presence of important effects outside the framework of the model.<sup>52</sup>

## E. General Deductions and Comments

### 1. Nonasymptotic Corrections, Cuts, and Two-Trajectory Solutions

We wish to emphasize a rather alarming general consequence of dealing with the amplitudes  $A$  and  $B$ . It is the nonflip amplitude  $A'$  which is the dominant amplitude in determining experimental cross sections. Not surprisingly, therefore,  $A'$  and  $B$ , not  $A$  and  $B$ , are the amplitudes parametrized in classical Regge-pole-

theory fits. However, as we argued in Sec. II B,  $A$  and  $B$  are the sensible amplitudes from the Veneziano-model viewpoint. Moreover,  $A'$  is essentially the difference between the two functions  $A$  and  $-B$  whose magnitudes are typically five times that of the resultant,  $A'$ . This implies that, in our plebian approach at least, the nonasymptotic terms in  $A'$  will inherit the typical size of the coefficients in  $A$ , not that of the asymptotic coefficient in  $A'$ . For example, if we use the parameters of solution (I), at 5 GeV/c in  $K^-p$  CEX, the effect of employing the correct definition of  $A'$  rather than the asymptotic form  $A' \rightarrow A + sB/[2M(1-t/4M^2)]$  is a reduction of the cross section by some 40% in the forward direction.

Recall, now, that it is  $A'$  which exhibits the most obvious violations of our or any simple Regge model. For this is the infamous amplitude in which the crossover zero does or does not appear and which does not exhibit the  $t \approx -0.6$  (GeV/c)<sup>2</sup> zero in either  $K^-p$ ,  $K^+p$  elastic, or the  $\pi N$  and  $\bar{K}N$  CEX amplitudes. Perhaps the correct, but rather barren, deduction is that the effects of cuts are small near  $t=0$  in  $A$  and  $B$ , but can become very important in the difference,  $A'$ . More quantitatively, we call Sec. II to mind and the suggestion from Mandlestam's model<sup>7</sup> that the leading meson trajectories are doubled.<sup>53</sup> One need only suppose that in the real world, for each  $t$ -channel quantum number,  $A$  and  $B$  have effective intercepts which differ by  $\sim 0.05$  near  $t=0$  in order to generate effects in  $A'$  that simulate the crossover effect over as wide a range of energies as it has so far been experimentally verified. However, we could find no reasonable model that gave this result as well as the correct sign of the polarization in  $\pi N$  CEX.

We would like to stress, as a general comment, that simple Regge theory should only be expected to hold for certain amplitudes in which the duality-associated resonances are large. This may be useful in understanding why simple Regge theory is often an abysmal failure.

### 2. Pomeranchuk Trajectory

As noted before, the Pomeranchukon was not explicitly included as a normal-slope trajectory function in any of the Veneziano-function parametrizations discussed in this section. However, we did notice that it may be associated, via duality, with the mysterious bump in  $KN$  scattering observed by Cool *et al.*<sup>54</sup>; if normalization is established by using the high-energy cross-section data, then the elastic width of the possible resonance, and its recurrences, may be deduced. These values are not unreasonable.

More quantitatively, regarding the  $K^+p$  channel as the  $u$  channel, as usual, we suppose that terms appear

<sup>51</sup> Figure 14 displays only representative data: for  $K^+p$ , K. J. Foley *et al.*, Phys. Rev. Letters **11**, 503 (1963); for  $K^-p$ , Aachen-Berlin-CERN-London (I.C.)-Vienna Collaboration, Phys. Letters **24B**, 434 (1967); J. Orear *et al.*, *ibid.* **28**, 61 (1968).

<sup>52</sup> The shrinkage of the  $K^+p$  elastic data suggests  $\alpha p p' \approx 0.5$  GeV<sup>-2</sup>, but then the relations  $s_0 = 1/\alpha p'$  would not work.

<sup>53</sup> This may also be suggested by the splitting of the  $A_2$  meson.

<sup>54</sup> R. L. Cool *et al.*, Phys. Rev. Letters **17**, 102 (1966); see also the discussion of the  $Z^*$  effects in Ref. 25.

in  $A$  and  $B$  having the form

$$A = a_p \frac{\Gamma(1 - \bar{\alpha}_c(u))\Gamma(1 - \alpha_p(l))}{\Gamma(1 - \bar{\alpha}_c(u) - \alpha_p(l))},$$

$$B = b_p \frac{\Gamma(-\bar{\alpha}_c(u))\Gamma(1 - \alpha_p(l))}{\Gamma(1 - \bar{\alpha}_c(u) - \alpha_p(l))},$$

with  $\alpha_p(l) = 1 + l$ . A complete treatment requires additional terms, of course, in order to achieve signature for the Pomeranchuk trajectory and the elimination of the  $j=0$  daughter state at  $\alpha_p = 1$ . However, because we give this argument for illustrative purposes, we ignore these considerations as well as those relating to possible  $(s, u)$  terms.

The data (Table III) suggest that the real world lies somewhere between the limits  $b_p = 13$ ,  $a_p = 0$  and  $b_p = 7$ ,  $a_p = -3$ . If we take  $\bar{\alpha}_c = -3.6 + u$  so that the bump observed by Cool *et al.* has  $j = \frac{1}{2}$ , then its larger component, the  $\frac{1}{2}^-$  state, has elastic width varying from 90 to 170 MeV, according to the two choices of  $b$ . However, if we take  $\bar{\alpha}_c = -2.6 + u$  and the  $j = \frac{3}{2}^+$  assignment for the bump of Cool *et al.*, then the elastic width varies from 30 to 40 MeV. In this latter case, the daughters of the bump of Cool *et al.* have positive elastic widths of similar size. In either case, the predicted elastic width seems consistent with that suggested by a naive interpretation of the data as a resonance.

In both cases the Pomeranchukon corresponds to a shorter-range force than the  $P'$ , the  $J = \frac{3}{2}$  case being one unit lower in the  $j$  plane and the  $J = \frac{1}{2}$  two units lower than the leading resonances associated with the  $P'$ . Finally, although available  $K^-p$  backward elastic data<sup>46</sup> are at much too low energy for a decisive test, they are consistent with a  $Z^*$ -exchange interpretation.

#### F. Veneziano-Function Parametrizations of Pion-Nucleon Scattering

Our treatment of the pion-nucleon process will be relatively brief because fewer detailed checks on the model are possible in this process than were available in the kaon-nucleon situation. This fact arises from a combination of circumstances. On the one hand, because all channels admit resonance poles, there is much more freedom in the choice of possible beta-function expressions. Secondly, there are effectively less useful data with which to test the model in the pion-nucleon case. This latter handicap is also a result of the fact that there are no  $\pi N$  states with exotic quantum numbers. The unitarity violation inherent in the zero-width model precludes using the model exactly at small values of the energy in any channel, as was possible in the  $K^+n$  CEX process discussed earlier. Effectively, therefore, because we are not incorporating possible unitarization schemes, our tests of the beta-function representations can examine only their high-energy consequences, after limiting procedures have been employed.

The major technical difficulty, but one which we shall be able to sidestep, fortunately, is associated with the  $(s, u)$ -type terms, given in the second summation of Eq. (3). There are at least three baryon trajectories:  $N_\alpha$ ,  $N_\gamma$ , and  $\Delta$ , and four if the  $D_{15}(1680)$  is judged to lie on a distinct trajectory. As a result, even if  $m$ ,  $n$ , and  $l$  are restricted to small values, there is a decidedly large number of possible terms of the form

$$\frac{\Gamma(m - \bar{\alpha}_{B1}(s))\Gamma(l - \bar{\alpha}_{B2}(u))}{\Gamma(n - \bar{\alpha}_{B1}(s) - \bar{\alpha}_{B2}(u))}.$$

For example, if all terms with  $m, n, l = 0$  or  $1$  are allowed [ $m, l \geq n \geq \max(m, l)$ ], subject only to the requirements of crossing symmetry and the restriction that  $m \neq 0$  and  $n \neq 0$  for the  $\Delta$ , then 50 beta-function terms arise. These are then subject to 12 constraints which arise from abolishing the spin- $\frac{1}{2}$  poles<sup>55</sup> of the  $N_\alpha$  and  $N_\gamma$  from the  $A$  amplitude and from guaranteeing appropriate isospin properties in the various channels. Although the results of Sec. II B and the values in Table IV (C) suggest that certain of these terms are dominant, it is clear that 38 parameters is more than the number of data points available for determining them. Furthermore, there is reason to believe that the restriction to terms with  $m, n$ , and  $l \leq 1$  is an implausible simplification. Consider, for instance, the possibly mythical limit<sup>7</sup> in which  $\alpha_B = \alpha_{N_\alpha} = \alpha_{N_\gamma} = \alpha_\Delta - 1$  and imagine that

$$B^{(+)} = c(s-u) \frac{\Gamma(-\bar{\alpha}_B(s))\Gamma(-\bar{\alpha}_B(u))}{\Gamma(-\bar{\alpha}_B(s) - \bar{\alpha}_B(u))}. \quad (46)$$

Upon breaking the degeneracy, we discover terms such as

$$(s-u) \frac{\Gamma(1 - \bar{\alpha}_\Delta(s))\Gamma(1 - \bar{\alpha}_\Delta(u))}{\Gamma(2 - \bar{\alpha}_\Delta(s) - \bar{\alpha}_\Delta(u))}.$$

When these are reexpressed in the form of pure beta-function terms, we obtain terms proportional to  $\Gamma(2 - \bar{\alpha}_\Delta(s))$ , for example, which were ignored in the above count of 50 functions.

The above discussion emphasizes again the great arbitrariness of the Veneziano type of expansion. No strong *a priori* principles exist which could be employed to choose between the various beta-function terms. The only working criterion is that of fitting the available information. Inasmuch as the tests of the model are primarily in the high-energy domain, however, it is possible to avoid altogether writing down explicitly any terms of either the  $(s, u)$  or the  $(u, t)$  types. This simplification arises from exploitation of crossing symmetry and the experimentally observed signature property of the meson and the baryon trajectories.

<sup>55</sup> The values in Table IV (C) suggest that terms like  $\Gamma(-\bar{\alpha}_{N_\gamma}(s))\Gamma(-\bar{\alpha}_N(u))/\Gamma(-\bar{\alpha}_{N_\gamma}(s) - \bar{\alpha}_N(u))$  are important in the amplitudes  $A$  and  $B$ . The  $\bar{\alpha}_N(u) = 0$  pole in  $A$  is then canceled by similar terms with  $\bar{\alpha}_{N_\gamma}(s)$  replaced by  $\bar{\alpha}_\Delta(s) - 1$ , for example.

In particular, let us see explicitly how knowledge of the  $(s, t)$  terms alone is sufficient for generating the baryon residue functions and the high-energy behavior of the amplitude near both  $t=0$  and  $u=0$ . In the limit  $s \rightarrow \infty$  for fixed  $t$ , the contributions of  $(s, u)$  terms vanish exponentially, but

$$\frac{\Gamma(m - \bar{\alpha}_B(s))\Gamma(n - \alpha_M(t))}{\Gamma(l - \bar{\alpha}_B(s) - \alpha_M(t))} \rightarrow (-bs)^{\alpha_M(t) + m - l} \Gamma(n - \alpha_M(t)),$$

where  $b$  is the trajectory's slope. Crossing symmetry requires that for each  $(s, t)$  term, we add (or subtract) an identical term with  $s$  replaced by  $u$ . After doing so, and taking the limit  $s \rightarrow \infty$  at fixed  $t$ , we find that the over-all result is equivalent to multiplying the right-hand side of the above statement by the signature factor  $1 \pm e^{-i\pi\alpha_M}$  for the meson trajectory. Next, consider the situation near  $u=0$  as  $s \rightarrow \infty$ . The  $(s, t)$  terms give an exponentially vanishing contribution, but their required  $(u, t)$  counterparts provide the limit

$$(bs)^{\bar{\alpha}_B(u) + n - l} \Gamma(m - \bar{\alpha}_B(u)).$$

The effect of adding the beta-function terms of the  $(s, u)$  type, required to establish signature along the baryon trajectory, is simply to multiply this limit by the baryon signature factor  $1 \pm e^{-i\pi\bar{\alpha}_B}$ .

In the remainder of this section, therefore, we will write down explicitly only the  $(s, t)$  variety of terms and model our discussion on that given for  $KN$  scattering earlier in this section.

Because we are not concerned in detail with the daughter<sup>9</sup> structure in the model, isospin requirements can be invoked to justify our writing down expansions for the  $A^{(+)}$  and  $B^{(+)}$  amplitudes only. We assert that all terms containing a given  $s$ -channel trajectory must satisfy exactly the isospin restriction demanded by the states on the parent trajectory. For the  $N_\alpha$  and  $N_\gamma$  situations, therefore, for any given beta-function type of term appearing in the expansion for  $A^{(+)}$  (or  $B^{(+)}$ ), there must be an identical term in  $A^{(-)}$  (or  $B^{(-)}$ ). This is true because we want no  $N_\alpha$  or  $N_\gamma$  poles to appear in the  $s$ -channel isospin  $\frac{3}{2}$  amplitude  $A_s^{3/2} = A^{(+)} - A^{(-)}$ . For the  $\Delta$  trajectory case, there are two physically meaningful alternatives:

(a) The  $\Delta$  is a pure  $I = \frac{3}{2}$  state. The relationship  $A_s^{1/2} = A^{(+)} + 2A^{(-)}$  implies that the coefficient of a given beta-function term in  $A^{(-)}$  be equal to  $-0.5$  that in the  $A^{(+)}$  amplitude.

(b) The isospin along the  $\Delta$  trajectory alternates; the odd-signature states have  $I = \frac{3}{2}$ , whereas the even ones have  $I = \frac{1}{2}$ . The first even-signature,  $I = \frac{1}{2}$  state would be the  $D_{15}(1680)$ . The desired isospin relation in this case is  $A^{(-)} \approx -0.24A^{(+)}$ .

By analogy with solutions (I) and (I') given for the kaon-nucleon situation, we considered the

following:

(i) Nucleon terms:

$$A_1^{(+)} = N_{A1}^+ \frac{\Gamma(1 - \bar{\alpha}_N)\Gamma(1 - \alpha_M)}{\Gamma(1 - \bar{\alpha}_N - \alpha_M)},$$

$$B_1^{(+)} = N_{B1}^+ \frac{\Gamma(-\bar{\alpha}_N)\Gamma(1 - \alpha_M)}{\Gamma(1 - \bar{\alpha}_N - \alpha_M)};$$

(ii)  $N_\gamma$  terms:

$$A_1^{(+)} = G_{A1}^+ \frac{\Gamma(1 - \bar{\alpha}_{N_\gamma})\Gamma(1 - \alpha_M)}{\Gamma(1 - \bar{\alpha}_{N_\gamma} - \alpha_M)},$$

$$B_1^{(+)} = G_{B1}^+ \frac{\Gamma(-\bar{\alpha}_{N_\gamma})\Gamma(1 - \alpha_M)}{\Gamma(1 - \bar{\alpha}_{N_\gamma} - \alpha_M)};$$
(47)

(iii)  $\Delta$  terms:

$$A_1^{(+)} = D_{A1}^+ \frac{\Gamma(1 - \bar{\alpha}_\Delta)\Gamma(1 - \alpha_M)}{\Gamma(1 - \bar{\alpha}_\Delta - \alpha_M)},$$

$$B_1^{(+)} = D_{B1}^+(t_0 - t) \frac{\Gamma(1 - \bar{\alpha}_\Delta)\Gamma(1 - \alpha_M)}{\Gamma(2 - \bar{\alpha}_\Delta - \alpha_M)}.$$

The trajectories are

$$\alpha_M = 0.55 + 0.9t, \quad M = P' \text{ or } \rho$$

$$\bar{\alpha}_N = -0.85 + 0.9s,$$

$$\bar{\alpha}_{N_\gamma} = -1.15 + 0.9s,$$

and

$$\bar{\alpha}_\Delta = -0.4 + 0.9s.$$

By fitting to the values of the high-energy forward-scattering amplitudes given in Table III and to the spin-parity structure of the baryon resonances, we found the parameters

$$N_{A1}^+ = 4.5, \quad N_{B1}^+ = 18.7, \quad G_{A1}^+ = 7.1,$$

$$G_{B1}^+ = 11.6, \quad D_{A1}^+ = -15.1, \quad D_{B1}^+ = -7.9,$$

$$t_0 = 1.68 \quad [\text{solution (II 1)}].$$

The corresponding values of  $g^2/4\pi$ ,  $\Gamma_\Delta$ , and  $\Gamma_{N_\gamma}$  are 3.3, 22 MeV, and 24 MeV, respectively. [In computing these numbers, proper account has been taken of the effect of the required  $(s, u)$  terms, which doubles the values computed from  $(s, t)$  terms alone.] These three values are roughly a factor of 4 too small. For solution (II 1), we made the pure isospin- $\frac{3}{2}$  choice for the  $\Delta$ . Parameters determined from an alternating isospin assignment for the  $\Delta$  are

$$N_{A1}^+ = 4.1, \quad N_{B1}^+ = 15.9, \quad G_{A1}^+ = 7.2,$$

$$G_{B1}^+ = 11.5, \quad D_{A1}^+ = -34.8, \quad D_{B1}^+ = -13.1,$$

$$t_0 = 3.2, \quad [\text{solution (II 2)}],$$

with  $g^2/4\pi = 2.8$ ,  $\Gamma_\Delta = 39$  MeV, and  $\Gamma_{N_\gamma} = 24$  MeV.

In determining these two sets of parameters, we did not enforce the values of the baryon residue function near  $u=0$ , known from the analysis of backward-scattering data, as discussed in Sec. II D. It would therefore appear that, regardless of this constraint or of the difficulties associated with  $(s,u)$  terms, one is simply unable to secure quantitative agreement, within the model, between the magnitudes of the baryon resonance widths and the values of the high-energy forward-angle differential cross section. This disagreement is somewhat worse than in the kaon-nucleon problem; solutions (I) and (I') in  $KN$  were determined by methods similar to those used in getting (II 1) and (II 2), but gave widths off typically by a factor of 2.

By introducing additional Veneziano beta-function expressions into the problem, ones which contribute asymptotically to nonleading order at  $t=0$ , one can, of course, achieve magnificent agreement with the baryon resonance widths. However, the paucity of relevant data precludes any check on their significance. We will not report such results here because they are simply examples of curve fitting, even more blatantly so than are solutions (II) and (II') of our  $KN$  investigation.

#### IV. DISCUSSION AND CONCLUSIONS

As a result of the investigation reported here, we can offer several conclusions regarding the strong-interaction dynamics of the kaon-nucleon and pion-nucleon systems. In this concluding section, we present our estimate of the relevance and success of the Veneziano beta-function representation for meson-baryon scattering. We then go on to summarize the phenomenological status of the Pomeranchukon. Finally, we suggest that a realistic scheme for quantitatively fitting experimental data could be based on the asymptotic Regge-pole content of the Veneziano model if one were to include explicitly, in addition, the Regge cuts generated from the poles. The Veneziano model has the distinctly attractive feature, in this regard, of specifying precisely the momentum-transfer structure of the Regge-pole residue, including all nonsense factors. This could resolve a problem which has caused trouble in previous investigations of high-energy reactions: Without an unambiguous definition of the pole residue, it has always been very difficult to distinguish phenomenologically between poles and cuts.

##### A. Estimate of Success of Veneziano Representation

We begin by listing, in the form of questions, our criteria for judging the usefulness of the Veneziano-model representation.

(1) It is possible to write an *a priori* theoretically justifiable and convenient parametrization of the meson-baryon process in terms of the beta-function expansions?

(2) In terms of these general parametrizations, can one reproduce as good fits to empirical high-energy distributions as are achieved in classical Regge-pole theory?

(3) The model contains both the baryon resonance poles and the associated Regge trajectories, and it prescribes a procedure for extrapolating from the region of physical scattering to the values of the resonance-pole residues. Is this feature supported quantitatively in nature?

(4) The model incorporates duality. Therefore, the magnitudes of the widths of the baryon resonances should be determined by the magnitudes of the  $t$ -channel meson-exchange trajectories, and vice versa. Is the quantitative relationship between these values, as specified by the model, in agreement with the empirical situation?

(5) Inasmuch as the model is intended to be applicable over the entire range of values of  $s$ ,  $t$ , and  $u$ , are checks possible either at low energy or as  $s \rightarrow \infty$  for fixed angles, away from  $u=0$  and  $t=0$ , and are these verified in nature?

(6) To what extent is the daughter structure in the model physically meaningful?

These are some of the questions to which we address ourselves; within this framework, we propose the following conclusions.

##### 1. Parametrization of Meson-Baryon Scattering Amplitudes

This first item divides itself into two parts: (a) choice of amplitudes and (b) parametrizations thereof.

(a) We chose to work with the standard invariant amplitudes  $A(s,t,u)$  and  $B(s,t,u)$  because crossing properties can be specified most conveniently in terms of these. However, retaining crossing has its price; as we noted in Sec. I B, the amplitudes  $A$  and  $B$  are not especially natural for expressing the correct spin-parity structure for the resonances or for guaranteeing positivity of their widths. Moreover, the high-energy forward elastic scattering data are best described in terms of the nonflip amplitude  $A'$ , and not in terms of  $A$ . This is significant, as discussed in Sec. III E, because  $A'$  often turns out to be an order of magnitude smaller than either  $A$  or  $B$ .

(b) Other than vague simplicity, we could establish no strong and easily implemented principles for *a priori* limitation of the types or number of beta-function terms in the parametrization of  $A$  and  $B$ . As a working hypothesis, we adopted the approach of starting with a minimum set of terms and then adding subsidiary terms, as necessary, to achieve the various requirements discussed in Secs. I and II.<sup>9</sup> Finally, as a result of our searches and fits to the data, we found no systematic tendency which would indicate that the coefficients of subsidiary terms are small.

##### 2. High-Energy Regge-Pole Fits

Roughly speaking, the Veneziano parametrization, *per se*, does as well as a noncontrived, classical Regge-pole model in fitting the high-energy differential cross-

section data near the forward and backward directions. However, this is true only if we ignore the questions of over-all normalization, which will be addressed in conclusions (3) and (4). The  $t$  dependence of the forward data is consistent with the suggestion from the model of slowly varying residues with the traditional scale factor  $s_0$  equal to  $1/\alpha'$ . Difficulties do arise as a result of unobserved shrinkage (suggesting  $\alpha' \ll 1$ ) and unobserved dips. The latter have been discussed in Sec. II A for the forward-scattering data and in Sec. II D for the backward direction. The most serious fault of the predicted  $t$  dependence of the Veneziano model is its failure to reproduce the crossover zero. However, all of these difficulties are also present in classical Regge-pole phenomenology unless one contrives to insert or to remove nonsense factors, in a purely *ad hoc* manner, and to vary the residue structure arbitrarily. Thus, the Veneziano formalism suggests that the resolution of all these problems lies not in even more complicated pole parametrizations but rather in other explanations, such as Regge cuts.

### 3. Pole Extrapolation

The failure in the case of the  $\Delta$  trajectory is significant, as we discussed in Sec. II D, but the Veneziano model seem to provide an adequate parametrization of the residue functions of the other major baryon trajectories. We found that the residues of the states on the  $N_\alpha$ ,  $\Sigma_\beta$ - $\Sigma_\delta$ , and  $\Lambda_\alpha$ - $\Lambda_\gamma$  trajectories are related well by the model to the corresponding backward-scattering data. Nevertheless, we are not sure that this agreement should be taken seriously because of the failure with the  $\Delta$ , which is the best determined experimentally. On a purely phenomenological level, however, our successful residue parametrizations for the  $N_\alpha$  and  $\Lambda_\alpha$ - $\Lambda_\gamma$  trajectories could be applied usefully to other elastic reactions as well as to multiple-production processes.

Pole extrapolation tests are not meaningful for the meson trajectories because the baryon-baryon-meson residues are essentially unknown.

### 4. Duality

The expression of duality in the model is its most attractive aspect. However, we found that the duality structure of the model agrees with nature only in an order-of-magnitude sense. For example, if in  $\pi N$  scattering one makes the simplest choices of terms and normalizes to the high-energy  $t=0$  data, then the predicted values for  $g^2/4\pi$ , the pion-nucleon coupling constant, and for  $\Gamma_\Delta$ , the elastic width of the  $\Delta(1238)$ , are typically a factor of 4 too small. Stated otherwise, in order to achieve agreement with  $g^2/4\pi$  and  $\Gamma_\Delta$ , one is forced to accept the presence of terms with very large coefficients which contribute asymptotically in non-leading order at  $t=0$ . Because all channels in the  $\pi N$  process contain resonances, no low-energy checks on these nonasymptotic terms are possible. In kaon-

nucleon scattering, good agreement with the baryon resonance widths was obtained at the price of adding such terms. There, a check on their effects at low energy was possible through a study of the  $K^+p$  and  $K^+n$  reactions. As reported in Sec. III D, our examination of the  $K^+n$  CEX reaction indicated only fair agreement at low energies.

### 5. Low-Energy and Fixed-Angle Behavior

Certain low-energy tests of the Veneziano-model amplitude are possible in pion-nucleon scattering, but, for the most part, the full power of the model cannot be realized because of the unitarity conflict. For the reasons already given in Sec. I G, we have no conclusion regarding whether the PCAC condition is consistent with the model. It probably could be made so, but without any attendant consequences. A similar remark applies to the scattering lengths, in that there are not enough additional low-energy checks to render meaningful predictive power from a forced agreement with PCAC and the scattering lengths. It is already too obvious from studying just the high-energy data that a large number of nonasymptotic, subsidiary terms are required.

This fundamental drawback is less damaging in kaon-nucleon scattering. As we noted in Sec. III D, however, too large an  $S$ -wave component is present in the model, and it is not easy to remove it without also removing the necessary  $P$  wave. The scattering lengths in our best solutions are correspondingly a factor of 2 too large. We discussed other aspects of the inconsistency between low- and high-energy fits to the  $KN$  data in Sec. III.

In general, much of the model's potential is unrealized because of the unitarity difficulty associated with zero-total-width resonance poles located on the real energy axes. One conceivable remedy for the  $\pi N$  problem might involve trying to determine the coefficients of the necessary subsidiary terms by fitting the detailed  $\pi N$  phase-shift data. For example, this could be accomplished on a limited basis by equating the integral of the discontinuity of the Veneziano-model amplitude, across the real axis, with the same quantity derived from the phase shifts.

We insert a plea at this point for more good data *at all energies*. Irrespective of the details of the Veneziano model, it is likely to be followed by other models which closely relate high- and low-energy phenomena. Therefore, it would be most advantageous to have much better information on both the isospin and energy dependence of the  $KN$  system. Additional polarization measurements in the elastic and CEX processes would also be most useful in indicating the magnitude of the background contribution in both  $t$ -channel isospin states. The Veneziano model predicts a purely real  $KN$  amplitude in all charge states; the only imaginary part comes from the addition of the  $I_t=0$  Pomeranchukon.

Improved measurements are desirable at both high and low energies.

We have not taken seriously the predictions of our parametrizations for the large- $s$  fixed-angle behavior because the rather accurate  $pp$  data indicates that phenomena in that region are dominated by effects outside the model, such as cuts. In particular, the distribution in momentum transfer for the  $pp$  scattering data exhibits a change of slope at a value of  $t$  which varies in position from  $t = -0.5$  (GeV/c)<sup>2</sup> at  $P_{\text{lab}} = 5.0$  GeV/c to  $t = -1.0$  (GeV/c)<sup>2</sup> at  $P_{\text{lab}} = 19.0$  GeV/c. Any currently accepted Pomeranchuk parametrization, or the Veneziano formalism, in its asymptotic limit,<sup>56</sup> fails to reproduce this experimental feature. It is easy to show that the Pomeranchuk Regge-pole contribution alone falls very far below the data in the intermediate-angle region.<sup>57</sup>

### 6. Daughters and Parity Doubling

We did not make a concerted attempt to take the daughter<sup>9</sup> structure of the model seriously, but some reflections emerge. (a) In pion-nucleon scattering, for example, an almost inevitable consequence of a Veneziano-model parametrization for the amplitudes  $A$  and  $B$  will be the appearance of daughter states generated by the  $\Delta$  trajectory in both the isospin  $I = \frac{1}{2}$  and  $I = \frac{3}{2}$  configurations. Such diseases can, of course, be remedied by the addition of compensatory subsidiary beta-function terms, but the process of correcting for the secondary diseases could go on *ad infinitum*. (b) The daughter trajectories in the pion-nucleon problem will not have definite signature, even though this property may have been enforced for the states along the parent trajectory. (c) For all four solutions to the kaon-nucleon process, (I), (I'), (II), and (II') in Sec. III, we computed the elastic widths of the daughter states up to  $J = \frac{11}{2}$  in all cases, most were positive and of a size similar to those of the parents. This result does not seem unreasonable, but we have not pursued a detailed comparison with experiment. We made comments in Sec. III on the size of daughters expected on the basis of the quark model.

One rather model-independent statement about the leading baryon trajectories is that they will create parity-doubled mass-degenerate states. The elastic widths of the two states in a given pair can differ greatly in the low-mass region, but they grow increasingly independent of parity as the mass is increased along the trajectory. This asymptotic limit is rather slowly realized in solutions (II) and (II') of Sec. III; even at  $J = \frac{11}{2}$ , the wrong parity states of both the

$\Lambda_\alpha$ - $\Lambda_\gamma$  and  $\Sigma_\beta$ - $\Sigma_\delta$  trajectories have roughly  $\frac{1}{4}$  the elastic width of their partners. Nevertheless, this degeneracy should be borne in mind when meson-baryon scattering data are analyzed for the spin-parity structure of resonant states. The daughter states are also, of course, predicted to be parity-doubled. The typical sizes of these effects can be appreciated from a glance at Table VI. We have no practical or helpful suggestions to make to those seeking to untangle the spin-parity structure of such mass-degenerate towers in the experimental data.

### B. Pomeranchukon

We have studied the Pomeranchukon in processes where there are direct-channel resonances, such as  $\pi N$ ,  $\bar{K} N$ , and  $\bar{p} p$  scattering, as well as in those without resonances. Our analysis of  $\pi^\pm p$  scattering showed explicitly that a Pomeranchuk trajectory with high slope ( $\alpha_{P'} \approx 1.0$ ) is consistent with the data. For reactions of the second type, we offer two considerations. (a) In Sec. III, we pointed out that a Pomeranchukon constrained to fulfill the Veneziano-model residue structure and the relation  $s_0 = 1/\alpha'$  cannot reproduce simultaneously both the  $s$  and  $t$  dependence of the data. However, the fits in Fig. 14 strongly suggest that the difficulty is associated with the way the Veneziano model handles the  $P'$  and  $\omega$  quantum-number exchanges. Any simple scheme in which the  $P'$  and  $\omega$  trajectories are exchange-degenerate will predict a zero in the  $\omega$  quantum-number amplitudes at  $\alpha_\omega(t) = 0$ . In nature, the zero is not observed there, but at the cross-over point  $t \approx -0.2$  (GeV/c)<sup>2</sup> in the  $A'$  amplitude. In order to fit the data, we are compelled to include additional poles or cuts; the effects of these would be sufficiently large that it seems likely that a Pomeranchuk trajectory having slope  $\alpha_{P'} \approx 1$  would also be admissible. (b) Our second consideration involves states with exotic quantum numbers. We demonstrated in Sec. III E that the Pomeranchuk trajectory may well be associated via duality with the bump of Cool *et al.*<sup>54</sup> (or  $Z^*$ ) seen in  $KN$  processes. This interpretation indicates that exotic resonances will have values of mass squared roughly 2 GeV<sup>2</sup> greater than that of the lowest nonexotic states and values of spin typically one or two units smaller than those of the nonexotic states of similar mass. We would certainly encourage experimental effort aimed at locating and studying the properties of enhancements which have exotic quantum numbers.<sup>9</sup>

Our arguments are hardly conclusive, and so we can only stress that there is really no compelling evidence for or against the conjecture that the Pomeranchukon is an object essentially different from any other Regge trajectory.<sup>16</sup>

### C. Phenomenological Uses of Veneziano Formula

Perhaps the most striking success we found for the Veneziano model was the agreement, within a factor of

<sup>56</sup> Either the fixed- $t$   $s \rightarrow \infty$  or the fixed-angle  $s \rightarrow \infty$  limit leads to this conclusion.

<sup>57</sup> S. Frautschi and B. Margolis [Nuovo Cimento **56**, 1155 (1968)] have explained these  $pp$  data in terms of multiple-scattering corrections to a Pomeranchukon of slope 1. See also M. Cassandro *et al.*, Rome Report No. LNF-68/74 (unpublished).

2, for the  $K^+n \rightarrow K^0p$  process over the entire range of measured energies. This is illustrated in Fig. 13. We hasten to point out, however, that this agreement was not achieved in the most straightforward manner. Specifically, successful application of the model to data analysis requires, at least, that one construct scattering amplitudes which enforce explicitly the observed spin and isospin structure of the low-energy spectrum. Although this is sometimes equivalent to using a single beta-function term, as has been proposed for  $\pi\pi$  scattering,<sup>2,4</sup> more care is required when the external particles have nonzero spin. Complicated sums of beta-function expressions may be required, in general, with the result that one loses the attractive simplicity of the original Veneziano proposal. Moreover, it is not often easy to visualize in advance what the over-all effects will be when one varies the values of the constant coefficients multiplying the various beta-function terms.

With respect to ensuring the correct spin-parity structure, a very useful technique exists for determination of the desired expansions. As we described in Sec. II B, one first deduces the positions of the zeros in  $t$  and  $u$  required of the invariant amplitudes by the angular functions  $d_{\lambda\mu}^j(\theta)$  associated with observed spin and parity values of the physical spectrum. Subsequently, the Veneziano beta-function expansions may be designed to match this analytic structure at the pole residues. However, the examples we have studied indicate that even this will not guarantee detailed agreement with experiment.<sup>58</sup>

At high energy, the difficulties of the Veneziano model are essentially those which also beset classical Regge-pole models. Nevertheless, an attractive phenomenological feature of the model is that it does offer a reasonably unique definition of the form of the Regge-pole contribution to a given reaction. The Veneziano approach specifies the relation  $s_0 = 1/\alpha'$  and the presence of all the nonsense zeros in the residue function, and it predicts shrinkage characteristic of a universal trajectory slope near unity. This aspect could be exploited in a scheme which attributes the empirical deviations from such a simple Regge-pole description to the effects of cuts and not to complicated residue functions<sup>59</sup> and/or to random trajectory slopes adjusted for nature's whims. With the Regge-pole structure given by the Veneziano formalism, it will be possible to test various models of cuts without the customary ambiguity of the traditional Regge-pole models. Cuts generated from the absorption model<sup>34</sup> using input pole residues similar to those we just described have been studied recently with some encouraging successes.<sup>60</sup>

<sup>58</sup> For an appraisal of detailed beta-function fits to data in the resonance region, see E. L. Berger, in *Proceedings of the Conference on  $\pi\pi$  and  $K\pi$  Scattering* (Argonne National Laboratory, Argonne, Ill., 1969).

<sup>59</sup> G. C. Fox and L. Sertorio, *Phys. Rev.* **176**, 1739 (1968).

<sup>60</sup> See, for example, C. B. Chiu and J. Finkelstein, *Nuovo Cimento* **57A**, 649 (1968); **59A**, 92 (1969); R. C. Arnold and M. L. Blackmon, *Phys. Rev.* **176**, 2082 (1968).

## ACKNOWLEDGMENTS

We have benefited from discussions with Professor Geoffrey Chew and Professor David Jackson. One of us (E. L. B.) is grateful to Geoffrey Chew for warm hospitality and to Dartmouth College for Faculty Fellowship support.

## APPENDIX A: KINEMATICS AND NOTATION

We collect and present in this appendix our explicit definitions of the various amplitude functions used in the text and their relationships to measurable cross sections and resonance widths.

With reference to Fig. 1, we define

$$s = (p+q)^2 = (p'+q')^2, \quad t = (p-p')^2 = (q-q')^2,$$

and

$$u = (p-q')^2 = (p'-q)^2,$$

where  $p$  ( $p'$ ) and  $q$  ( $q'$ ) are the four-momenta of the incident (outgoing) baryon and meson, respectively. The  $S$  matrix is given, with isospin labels suppressed, as

$$S_{f,i} = \delta_{f,i} + i(2\pi)^4 \delta(p'+q'-p-q) T_{f,i}, \quad (\text{A1})$$

with

$$T(p',q'; p,q) = \bar{u}(p') [A + \frac{1}{2}(q+q')B] u(p). \quad (\text{A2})$$

The functions  $A(s,t,u)$  and  $B(s,t,u)$  are free of kinematical singularities; our Dirac spinor amplitudes satisfy  $(\not{p}-M)u(p)=0$  and  $\bar{u}(p)u(p)=2M$ . In this paper,  $M$  denotes the baryon mass and  $\mu$  the meson mass. We define the kinematical quantity

$$E_s = (s+M^2-\mu^2)/2s^{1/2}, \quad (\text{A3})$$

which is the energy of the baryon in the  $s$ -channel center-of-mass system; the corresponding  $E_u$  is obtained from (A3) by replacing  $s$  with  $u$ .

We will also use  $v = \frac{1}{2}(s-u)$  and

$$\omega = (s-M^2+\mu^2)/2s^{1/2}.$$

### 1. Partial-Wave Analysis

The usual  $f_i^s$  functions are

$$f_1^s = [(E_s+M)/8\pi s^{1/2}] [A + (s^{1/2}-M)B] \quad (\text{A4a})$$

and

$$f_2^s = [(E_s-M)/8\pi s^{1/2}] [-A + (s^{1/2}+M)B]. \quad (\text{A4b})$$

In terms of these functions, partial-wave amplitudes associated with a particular total angular momentum  $J$  and parity  $P = -(-1)^L$  are given by

$$a_{L=J\mp 1/2}^J = \frac{1}{2} \int_{-1}^{+1} dz [f_1^s P_L(z) + f_2^s P_{L\pm 1}(z)], \quad (\text{A5})$$

where  $z$  is the cosine of the  $s$ -channel center-of-mass scattering angle, given in terms of  $s$  and  $t$  by

$$z = 1 + t/2q^2, \quad (\text{A6})$$



with

$$q^2 = [s - (M + \mu)^2][s - (M - \mu)^2] / 4s. \quad (\text{A7})$$

Notice that

$$f_1^s(-s^{1/2}) = -f_2^s(s^{1/2})$$

and that

$$\alpha_{L=J+1/2}^J(s^{1/2}) = -\alpha_{L=J-1/2}^J(-s^{1/2}),$$

the usual MacDowell-symmetry statement. In the text, we use

$$\tilde{f}(u^{1/2}) = A - (u^{1/2} - M)B = [8\pi u^{1/2} / (E_u + M)] f_1^u(u^{1/2}).$$

### 2. Resonance Widths

Near a resonance of mass  $M_R$ , total width  $\Gamma$ , and elastic width  $\Gamma_{el}$ ,

$$\alpha^J(s) \rightarrow \frac{\Gamma_{el} M_R / q_R}{M_R^2 - s - i\Gamma M_R}, \quad (\text{A8})$$

where  $q_R$  is obtained upon setting  $s = M_R^2$  in (A7).

In the zero-total-width Veneziano-model approach, the "resonances" occur on the real energy axis, and thus the imaginary term in the denominator of (A8) vanishes. One may, nevertheless, expand the expression, given by the Veneziano representation, for the left-hand side of (A8) and identify the corresponding  $\Gamma_{el}$  expressions as the "elastic widths" of the various pole terms.

### 3. Differential Cross Sections

Several alternative forms may be given for the differential cross sections. It is traditional to use either

$$d\sigma/d\Omega = |f_1^s + f_2^s|^2 + (t/q^2) \operatorname{Re}(f_1^{s*} f_2^s) \quad (\text{A9})$$

or, more commonly in Regge-theory fits,

$$\frac{d\sigma}{dt} = \frac{1}{\pi s q^2} \left( \frac{M}{4} \right)^2 \left[ \left( 1 - \frac{t}{4M^2} \right) |A'|^2 + \frac{t}{4M^2} \left( s - \frac{(M + E_{\text{lab}})^2}{1 - t/4M^2} \right) |B|^2 \right], \quad (\text{A10})$$

where

$$A' = A + \frac{E_{\text{lab}} + t/4M}{1 - t/4M^2} B, \quad (\text{A11})$$

and  $E_{\text{lab}} = (s - M^2 - \mu^2) / 2M$ . In terms of the non-spin-flip amplitude  $A'$ , the total cross section is given by  $\sigma_T(s) = [\operatorname{Im} A'(s, t=0)] / p_{\text{lab}}$ . Because we write a Veneziano representation for  $A$  and  $B$ , it is convenient to use (A10) for backward scattering, also, after replacing  $t$  by  $2M^2 + 2\mu^2 - s - u$ . Note, also, that the coefficient of  $|B|^2$  in (A10) is proportional to  $\sin^2 \theta_s$ , and therefore vanishes for both forward and backward scattering.

For the convenience of those making comparisons between our results and those of Barger and Cline (BC),<sup>27</sup> especially as regards the backward data, we remark here that our reduced residue  $\gamma^{(I)}(u^{1/2})$  given in

Eq. (34) of the text may be expressed in terms of theirs [see their Eq. (15)] by

$$\gamma^{(I)}(u^{1/2}) = 16(1/b s_0)^{\alpha-1/2} \Gamma(\alpha + \frac{5}{2}) \gamma_{\text{BC}}(u^{1/2}), \quad (\text{A12})$$

where  $\gamma_{\text{BC}}$  is, of course, the reduced residue function of Barger and Cline. The quantity  $s_0$  is their scale factor,  $b$  is the trajectory slope,  $\alpha = \alpha(0) + bu$ , and the factor  $\Gamma(\alpha + \frac{5}{2})$  enters because they keep only the  $(\alpha + \frac{1}{2})(\alpha + \frac{3}{2})$  factor from  $[\Gamma(\alpha + \frac{1}{2})]^{-1}$ .

### 4. Isospin Conventions

(a)  $\pi N$  scattering. For pion-nucleon scattering, we express our results in terms of the  $(\pm)$  amplitudes.

In terms of these, the amplitudes in the  $s$  channel for a state of definite isospin  $I$ ,  $A_s^I$  and  $B_s^I$  are

$$A_s^{1/2} = A^{(+)} + 2A^{(-)}, \quad (\text{A13a})$$

$$A_s^{3/2} = A^{(+)} - A^{(-)}. \quad (\text{A13b})$$

For  $\pi^\pm p$  elastic scattering and for  $\pi^- p \rightarrow \pi^0 n$  in the  $s$  channel, we have

$$A_s(\pi^- p \rightarrow \pi^- p) = A^{(+)} + A^{(-)}, \quad (\text{A13c})$$

$$A_s(\pi^+ p \rightarrow \pi^+ p) = A^{(+)} - A^{(-)}, \quad (\text{A13d})$$

$$A_s(\pi^- p \rightarrow \pi^0 n) = -\sqrt{2} A^{(-)}. \quad (\text{A13e})$$

The same algebraic equations hold for  $B_s$  in terms of  $B^{(\pm)}$ . The  $+$  ( $-$ ) amplitude is associated with a state of definite isospin  $I_t = 0$  (1) in the  $t$  channel. For  $u$ -channel scattering, the amplitudes  $A_u^I$  for a state of definite isospin  $I$  are

$$A_u^{1/2} = A^{(+)} - 2A^{(-)}, \quad (\text{A14a})$$

$$A_u^{3/2} = A^{(+)} + A^{(-)}. \quad (\text{A14b})$$

Again, the same algebraic equations hold for  $B_u$  in terms of  $B^{(\pm)}$ . However, in the definition of  $f_1^u$  (or any other  $u$ -channel quantity) the sign of  $B$  is the opposite of that appropriate in the  $s$ -channel amplitude. This is also true in  $KN$  scattering. Explicitly,

$$f_1^u = [(E_u + M) / 8\pi u^{1/2}] [A - (u^{1/2} - M)B]. \quad (\text{A15})$$

This should be contrasted with Eq. (A4a).

In order to make our normalizations and sign-convention statements more explicit, we remark that at the nucleon pole position,

$$B^{(\pm)}(s, t, u) = g^2 \left( \frac{1}{M^2 - s} \mp \frac{1}{M^2 - u} \right). \quad (\text{A16})$$

Because there is no parity partner for the nucleon, our  $A^{(\pm)}(s, t, u)$  amplitudes have no pole at the nucleon position.

(b)  $KN$  scattering. The expressions for the experimental amplitudes in terms of our  $s$ -channel states of

definite isospin are

$$\begin{aligned} A_s(K^-p \rightarrow K^-p) &= \frac{1}{2}(A_s^{(0)} + A_s^{(1)}), \\ A_s(K^-p \rightarrow \bar{K}^0n) &= \frac{1}{2}(-A_s^{(0)} + A_s^{(1)}). \end{aligned} \quad (\text{A17a})$$

In the  $u$  channel,

$$\begin{aligned} A_u(K^+p \rightarrow K^+p) &= A_u^{(1)}, \\ A_u(K^+n \rightarrow K^0p) &= \frac{1}{2}(-A_u^{(0)} + A_u^{(1)}). \end{aligned} \quad (\text{A17b})$$

The  $s$ - $u$  crossing formula is

$$\begin{bmatrix} A_u^{(0)} \\ A_u^{(1)} \end{bmatrix} = \begin{bmatrix} -\frac{1}{2} & \frac{3}{2} \\ \frac{1}{2} & \frac{1}{2} \end{bmatrix} \begin{bmatrix} A_s^{(0)} \\ A_s^{(1)} \end{bmatrix}. \quad (\text{A18})$$

In Table III, the isospin convention is such that

$$A(K^-p \rightarrow K^-p) = A^{P'} + A^\omega + A^\rho + A^{A_2} \quad (\text{A19})$$

normalizes the four  $t$ -channel amplitudes corresponding to the four isospin- $G$ -parity combinations  $(0, +)$ ,  $(0, -)$ ,  $(1, +)$ , and  $(1, -)$ , respectively.

#### APPENDIX B: DESCRIPTION OF FITS DISPLAYED IN FIG. 2

In Fig. 2, two fits to the  $\pi^-p$  elastic differential cross section are presented.<sup>61</sup> The parameters of the fits were actually obtained from a simultaneous minimum  $\chi^2$  fit to all available  $\pi^+p$  and  $\pi^-p$  elastic as well as  $\pi^-p \rightarrow \pi^0n$  data above the lab momentum 5 GeV/ $c$  and in the  $-t$  interval  $0 < |t| < 1$  (GeV/ $c$ )<sup>2</sup>. Data on polarization,  $d\sigma/dt$ ,  $\sigma_{\text{tot}}$ , and  $\text{Re}/\text{Im}$  were used. For both fits, the  $P$ ,  $P'$ ,  $\rho$ , and  $\rho'$  Regge poles were employed, and their residue functions were parametrized staidly, as in the paper of Fox and Sertorio.<sup>59</sup> In the context of  $t$ -channel helicity amplitudes, the residue functions were written as linear functions of  $t$ , permitting, for instance, the  $P'$  residue to develop a zero in the physical region. These are "classical" Regge-pole-model fits: The several trajectory intercepts and residue parameters were varied independently in achieving the best fits.

The distinction between the two fits is basically that in Fig. 2(a) the Pomeranchuk trajectory has slope 0.7, as recommended by Dikmen,<sup>15</sup> whereas in Fig. 2(b) its slope is 0.3, as in Rarita *et al.*<sup>14</sup> As explained in the text, the absence of shrinkage in the data is obtained in (a) through the vanishing of the  $P'$  residue at  $t \approx -0.2$  (GeV/ $c$ )<sup>2</sup>. The  $\chi^2$  for fit (b) is somewhat smaller than than for (a): 400 versus 435 on the 450 elastic scattering points. (These  $\chi^2$  values are actually artificially reduced because the errors on the lower-energy data points were increased<sup>62</sup> in the fit to simulate neglected lower-lying trajectories.)

<sup>61</sup> The data plotted are a selection of those used in the over-all fit. Those at 5 and 6 GeV/ $c$  come from C. F. Coffin *et al.*, Phys. Rev. **159**, 1169 (1967), and the rest from K. J. Foley *et al.*, Phys. Rev. Letters **11**, 425 (1963); **15**, 45 (1965).

<sup>62</sup> Explicitly, the errors from 5 to 9 GeV/ $c$  were increased by a factor 1.75, and from 9 to 12 GeV/ $c$  by 1.25.

We feel that neither fit should be accepted uncritically outside the range  $|t| < 0.5$  (GeV/ $c$ )<sup>2</sup> because like fits do not work successfully in  $p\bar{p}$  scattering for  $-t > 0.5$  (GeV/ $c$ )<sup>2</sup>, over a similar energy range. (See our comment in Sec. IV B.) If, as a consequence, one restricts attention to the smaller  $t$  range [ $|t| < 0.5$  (GeV/ $c$ )<sup>2</sup>], the errors in the determination of the Pomeranchuk-trajectory slope grow; undoubtedly, a slope of 1 is consistent with fit (a) and a slope of 0 with fit (b).

A second note of caution relates to FESR results. The fits given do not reproduce well the FESR results,<sup>3</sup> which have the rather low cutoff  $s^{1/2} = 2.19$  GeV. The discrepancy would disappear, however, if the larger  $t$  values [ $|t| > 0.5$  (GeV/ $c$ )<sup>2</sup>] were neglected.

The outcome of the explicit Veneziano-model fits to  $KN$  scattering, described in Sec. III, also sheds some light on the high-slope Pomeranchukon fit. As will be recalled, in the  $KN$  situation the residue functions for the  $P'$  and  $\omega$  Regge poles did not naturally have the crossover zero. This result tends to support the particular alternative, discussed in Sec. II A, in which the residue of the  $P'$  Regge pole vanishes at  $t \approx -0.6$  (GeV/ $c$ )<sup>2</sup> and in which the zero at  $t \approx -0.2$  (GeV/ $c$ )<sup>2</sup> is achieved only as a result of the mixture of the  $P'$  plus the absorption cuts, which remove the low partial waves. The suggestion is, therefore, that the  $P'$  used in the fits of this appendix is not really a simple pole. However, left unaltered is our basic contention that the  $\pi N$  elastic data admit a good fit with a Pomeranchuk trajectory of high slope.

Dikmen has given fits to  $KN$  and  $p\bar{p}$  scattering using a Pomeranchukon of high slope.<sup>63</sup> His results are difficult to interpret within our framework, however, until a procedure is devised for removing the unobserved zero at  $t \approx -0.6$  (GeV/ $c$ )<sup>2</sup> from the amplitude with the  $\omega$  quantum numbers. See Fig. 14 and Sec. III E on this point.

With respect to the point about removing unobserved zeros from amplitudes, Igi<sup>6</sup> has suggested that the corresponding Veneziano-model prediction of zero cross section in  $\pi N$  CEX at  $t \approx -0.6$  (GeV/ $c$ )<sup>2</sup> will be rendered compatible with the data if nonasymptotic terms are retained. He has in mind employing the terms in his Veneziano expansion which fall like  $s^{-1}$  in comparison with those of the leading Regge pole. However, there is evidence from  $[d\sigma/dt(K^-p \text{ elastic}) - d\sigma/dt(K^+p \text{ elastic})]$ ,  $[d\sigma/dt(p\bar{p} \text{ elastic}) - d\sigma/dt(p\bar{p} \text{ elastic})]$ ,  $d\sigma/dt(\gamma N \rightarrow \pi^0 N)$ , and both the polarization and  $d\sigma/dt$  data on  $\pi^-p \rightarrow \pi^0 n$  that the energy dependence in the dip region does not differ appreciably from that expected of the leading pole.<sup>64</sup>

<sup>63</sup> F. N. Dikmen, Nuovo Cimento Letters **1**, 544 (1969), and private communications.

<sup>64</sup> G. C. Fox, unpublished calculations, and in *Proceedings of the Stony Brook Conference on High-Energy Physics, 1969* (Gordon and Breach, Science Publishers, Inc., New York, 1970).